Targeting Telomerase Overexpression by Synthetic Dosage Lethality

A Thesis Submitted to the
College of Graduate and Postdoctoral Studies
In Partial Fulfillment of the Requirements
For the Degree of Doctor of Philosophy
In the Department of Pharmacy
University of Saskatchewan
Saskatoon

By

Omar Abuhussein

PERMISSION TO USE

In presenting this thesis in partial fulfillment of the requirements for a Postgraduate degree from the University of Saskatchewan, I agree that the Libraries of this University may make it freely available for inspection. I further agree that permission for copying of this thesis/dissertation in any manner, in whole or in part, for scholarly purposes may be granted by the professor or professors who supervised my thesis/dissertation work or, in their absence, by the Head of the Department or the Dean of the College in which my thesis work was done. It is understood that any copying or publication or use of this thesis or parts thereof for financial gain shall not be allowed without my written permission. It is also understood that due recognition shall be given to me and to the University of Saskatchewan in any scholarly use which may be made of any material in my thesis.

Requests for permission to copy or to make other uses of materials in this thesis/dissertation in whole or part should be addressed to:

Dean

College of the Pharmacy and Nutrition

University of Saskatchewan

Saskatoon, Saskatchewan S7N 4L3 Canada

OR

Dean

College of Graduate and Postdoctoral Studies

University of Saskatchewan

116 Thorvaldsen Building, 110 Science Place

Saskatoon, Saskatchewan S7N 5C9 Canada

ABSTRACT

Telomerase reverse transcriptase (hTERT) is upregulated in multiple cancers and accompanied by the evidence suggesting that up-regulation of telomerase expression is linked to tumorigenesis, raised the hypothesis that inhibiting this enzyme is a powerful antitumor strategy. Despite intensive research to seek direct enzyme inhibitors, sufficiently potent and specific small-molecule inhibitor has not been fount yet. This suggests that direct targeting of hTERT might not be an optimal strategy in cancer treatment. Genetic interactions, such as synthetic dosage lethality can overcome these issues and identify targets that is specific only tumor cells that overexpress telomerase.

We used a combination of pooled shRNA and CRISPR screening platforms to comprehensively query the entire human genome and identify hTERT-specific Synthetic dosage lethality (SDL) interactions. Our screens identified several potential SDL genes specific to hTERT in the model cell lines. We prioritized 187 candidate SDL genes using different computational approaches and validate them on one-by-one bases in model cell lines. Subsequent validation of these genes in multiple cancer cell lines in arrayed CRISPR/Cas9-based strategy and several xenograft models identified several potential targets that exhibit specify to hTERT overexpressing tumors. Assessment of telomeres structure followed by telomere activity assay results suggest that the knockout of these target affect the canonical and non-canonical functions of hTERT.

Our results indicated that validated SDL targets may provide a basis for the development of tumor agnostic therapeutic strategies applicable in a wide range of patients, since hTERT is overexpressed in the majority of human malignancies.

ACKNOWLEDGEMENTS

I would like to express my sincere gratitude to my Supervisor Dr. Franco Vizeacoumar for the continuous support of my Ph.D. study and related research, for his motivation, and immense knowledge. His guidance helped me in all the time of research and writing of this thesis. I would like to thank the rest of my thesis committee: Dr. Jian Yang, Dr. Andrew Freywald and Dr. Changiz Taghibiglou for their insightful comments and encouragement.

My sincere thanks also go to Dr. Judy Wong lab (University of British Colombia), for their valuable help in the project and Dr. Sabine Mai lab and Genomic Centre – Cancer Care Manitoba for providing me the opportunity and training in their centre, and who gave access to the laboratory and research facilities.

Table of Contents

List of Tables

List of Figures

List of Abbreviations

ASF1	Anti-Silencing Function 1A Histone Chaperone
ATCC	American Type Culture Collection
ATM	Ataxia-telangiectasia mutated
ATR	Ataxia telangiectasia and Rad3 related
ATRIP	ATR-interacting protein
ATRX	Alpha Thalassemia/Mental Retardation Syndrome X-Linked
BLM	Bloom syndrome RecQ-like helicase
bp	Base pairs
BSA	Bovine serum albumin
BUB1B	Mitotic Checkpoint Serine/Threonine-Protein Kinase BUB1 Beta
CCLE	Cancer cell line encyclopedia
CDC25C	Cell division cycle 25C
CDK	Cyclin dependent kinase
cDNA	Complementary DNA
CHEK1	Checkpoint kinase 1
CHEK2	Checkpoint kinase 2
CIN	Chromosomal instability
CML	Chronic myeloid leukemia
CNA	Copy number alteration
CRISPR	Clustered regularly interspaced short palindromic repeats
DAISY	Data mining synthetic lethality
DAXX	Death Domain Associated Protein
DDR	DNA damage response
DMSO	Dimethyl sulfoxide
EGFR	Epidermal growth factor receptor
Exo1	Exonuclease1
ETS	Transcription Factor
ER	Estrogen receptor
HDR	Homology directed repair
FBS	Fetal bovine serum
Hsp90	Heat shock protein 90
hTERT	Human telomerase reverse transcriptase
IGF2BP2	Insulin-like growth factor 2 mRNA binding protein 2
Indels	Insertions or deletions
ISG15	Interferon Stimulated Gene 15 kDa
MOI	Multiplicity of infection
MRN	Mre11, Rad50, Nibrin complex
MYC	Proto-Oncogene C-Myc
NTC	Non targeting control

P13K	Phosphoinositide 3-kinase
PARP	Poly-ADP-ribose polymerase
PBS	Phosphate buffered saline
PDB	Protein data bank
PDX	Patient-derived xenograft
PLK1	Polo-like kinase 1
POT1	Protection of Telomeres 1
PP2A	Protein phosphatase 2A
qPCR	Quantitative real-time PCR
RAP1	Repressor/activator protein 1
RNP	Ribonucleoprotein
SDL	Synthetic dosage lethality
SDS	Sodium dodecyl sulfate
sgRNA	Single guide RNA
shRNA	Short hairpin RNA
siRNA	Small interfering RNA
SL	Synthetic lethality
TAD	Topologically associating domains
TBS	Tris buffered saline
TBST	Tris buffered saline Tween-20
TCAB1	Telomerase Cajal body protein 1
TCGA	The Cancer Genome Atlas
TERRA	Telomeric repeat-containing RNA
TIN2	TRF1-interacting nuclear factor 2
TRF1	Telomeric repeat-binding factor 1
TRF2	Telomeric repeat-binding factor 2
TERC	Telomerase RNA Component
TERT	Telomerase Reverse Transcriptase
TL	Telomere length
TNKS	Tankyrase
TP53	Tumour protein 53
TPE	Telomere position effect
TPE-OLD	Telomere portion effect over long distance
TPP1	Tripeptidyl Peptidase 1
SNP	Single nucleotide polymorphisms
SCC	Small cell carcinoma

CHAPTER 1: Introduction

Human telomeres contain repetitive hexanucleotide DNA sequence 5'-TTAGGG-3' often termed the canonical telomeric sequence(Moyzis et al., 1988). These repeats form a double strand telomeric DNA. Telomeres are guarded by a six-protein subunit complex known as the shelterin complex. This complex together with telomere protect chromosome end from DNA repair mechanisms(Shay and Wright, 2019).

As cells continue to divide their telomeres continue to shorten until they became too short to protect the ends for chromosomes, end to end fusion start to occur as a result on unprotected end of chromosome(de Lange, 2018). The fused chromosome ends lead to many forms of genome instability. Some cells can escape out of telomere crisis by activation of telomerase which eventually will lead to formation of cancer clone with rearranged genome(Shay and Wright, 2011).

Telomerase is a ribonucleoprotein (RNP) enzyme that is composed of reverse transcriptase (TERT), RNA template(TERC) and accessory proteins(Shay and Wright, 2019). The holoenzyme adds telomeric repeat DNA to chromosome ends preventing progressive telomere shortening(Blackburn and Collins, 2011). During human development, TERT is being silenced in most somatic cells leading to decreased activity of telomerase(Jafri et al., 2016). Therefore, somatic cells will undergo programmed telomere shortening that eventually leads to insufficient chromosome end protection(Muraki et al., 2012). This lack of protection triggers DNA damage response initiating cell proliferation arrest and activation of apoptosis or senescence. While This pathway seems as protective mechanism to suppress tumor growth, this dysfunction can become a driver for genome instability(Shay, 2016).

Since it was discovered, Telomerase constitute a luring target for cancer treatment supported by the fact that telomerase is expressed in most cancer cells and not in normal human somatic cells. Different approaches have taken to suppress telomerase-mediated telomere maintenance. Despite intensive efforts to seek direct enzyme inhibitors by screening thousands of compounds and pursuing hundreds of chemical leads including focused sub-libraries of reverse transcriptase inhibitors, no one has yet found a sufficiently potent and specific small-molecule inhibitor.

To circumvent these concerns, we propose to identify potential therapeutic targets by applying a basic biological concept called synthetic dosage lethality (SDL) where overexpression of a gene is lethal when another mutation or deletion is present. Discovering SDL interactions could reveal new therapeutic targets for cancer treatment in this situation, cancer cells overexpressing hTERT would be killed when the expression of another gene is silenced/inhibited. Importantly, normal cells would be spared as the gene whose expression is silenced, is not essential for its survival.

1.Telomeres: The guardians of genome.

Telomeres were first discovered in 1938 by geneticist Hermann J. Muller working on *Drosophila melanogaster*. He noticed a cap like structure at the end of the chromes which he called them telomere. The word telomere is derived from the Greek nouns *telos* meaning "end" and *meros* meaning "part"(Kheirollahi, 2013). A landmark observation made by geneticist Barbara McClintock that naturally occurring chromosome ends prevent chromosomal instability(Shay and Wright, 2019). In 1960 Hayflick and Moorhead discovered that in culture, cell can divide for a limited time. This built -in mechanism that limit the proliferative capacity of the cells was termed Hayflick limit(Shay and Wright, 2019). They then hypothesized that cells after certain number of

divisions can go through cell senescence. Few years later, DNA replication studies showed incomplete DNA replication of linear chromosome suggesting telomeres are lost with every cell division until they reach the Hayflick limit. The exact sequence of human telomere was unknow until 1988(Shay and Wright, 2019). Further research revealed that chromosomes are capped by complex nucleoprotein that prevent chromosome ends from being recognized as DNA Double stand breaks essential to protect these regions from recombination and degradation(Ferreira and Cooper, 2004).

2. Telomeric DNA

2.1 Telomere structure

Most species contain tracts of repetitive DNA at the tips of linear chromosomes. These tips consist of a simple repeat array in which the repeat unit is generally 5-8 bp in length. However several yeast species have irregular repeats that range from 6 to 26 nucleotides(Podlevsky et al., 2008). Human telomeres are nucleoprotein structures of short tandem repetitive DNA sequence at the ends of linear chromosome(Blackburn, 1991). This repeated sequence TTAGGG is of about 5–10 kb in length sequestered by proteins that interact with the sequence know as shelterin complex(Moyzis et al., 1988). The telomeric DNA forms a double-stranded followed by a termini consist of 25-200 nucleotides of single-stranded DNA referred as 3 G-overhang(Lu et al., 2013). The single strand invades the double stranded telomeric sequence forming a structure knows as T-loop(Griffith et al., 1999). Telomeric DNA is composed of G and C strands because the telomere strand that ends in 3′ is rich in guanosine while the complementary 5′ strand is rich in cytosine. The G-rich sequences, which readily fold into a variety of G-quadruplex structures(Kaulage et al., 2018).

3.1.1 Quadruplex Structures

The first indication to the presence of G-quadruplex structure came from the observation that G-quadruplex stabilizing ligands lead to telomere shortening by impairing telomeric repeat synthesis(Rhodes and Lipps, 2015). Telomeric DNA can fold into compact G-quadruplex structures(Rhodes and Lipps, 2015). G-quadruplexes are four-stranded DNA secondary structures that contains stacked G-tetrad planes of four guanines connected by a network of hydrogen bonding(Williamson et al., 1989). The G enriched strand of telomeric DNA is capable of Hoogsteen base pairing forming planner G quartet structures that stack on each other to from G-quadraplexes(Reddel, 2014). Exitance of this structure at the tend of telomeric DNA was first reported in ciliate *Stylonychia lemnae* using specific antibody against G-quadruplexes(Lipps and Rhodes, 2009) and later has visualized in human telomeres(Biffi et al., 2013).

Based on the initial observations, G-quadruplex structures were hypnotized to possess protective role. Genome wide studies also revealed that are highly enriched at DNaseI hypersensitive sites(Hegyi, 2015). Moreover, their abundance in nucleosome low regions supported this hypothesis. In human, telomeric G-quadruplex structures have been implicated in telomere protection (Lipps and Rhodes, 2009). Clearly the structure is more stable than regular DNA sequences making telomeres more resistant to nucleases than non-G-quadruplex structures(Cao et al., 2006). Telomerase-mediated telomere extension require a free 3′ telomere end in single-stranded form(Burger et al., 2005). G-quadruplex are poor substrates for the telomerase where they preferentially forms at the very 3′ end of telomeres inhibiting telomerase accessibility for telomere extension(Tang et al., 2008). Additionally G-quadruplex structure unwinding by helicases requires more energy than unwinding of duplexes, supporting the role of G-quadruplexes in telomere protection(Liu et al., 2010).

The exitance of these structure at the telomeric end provide additional protection for telomeres from DNA damage responses(Rhodes and Lipps, 2015).

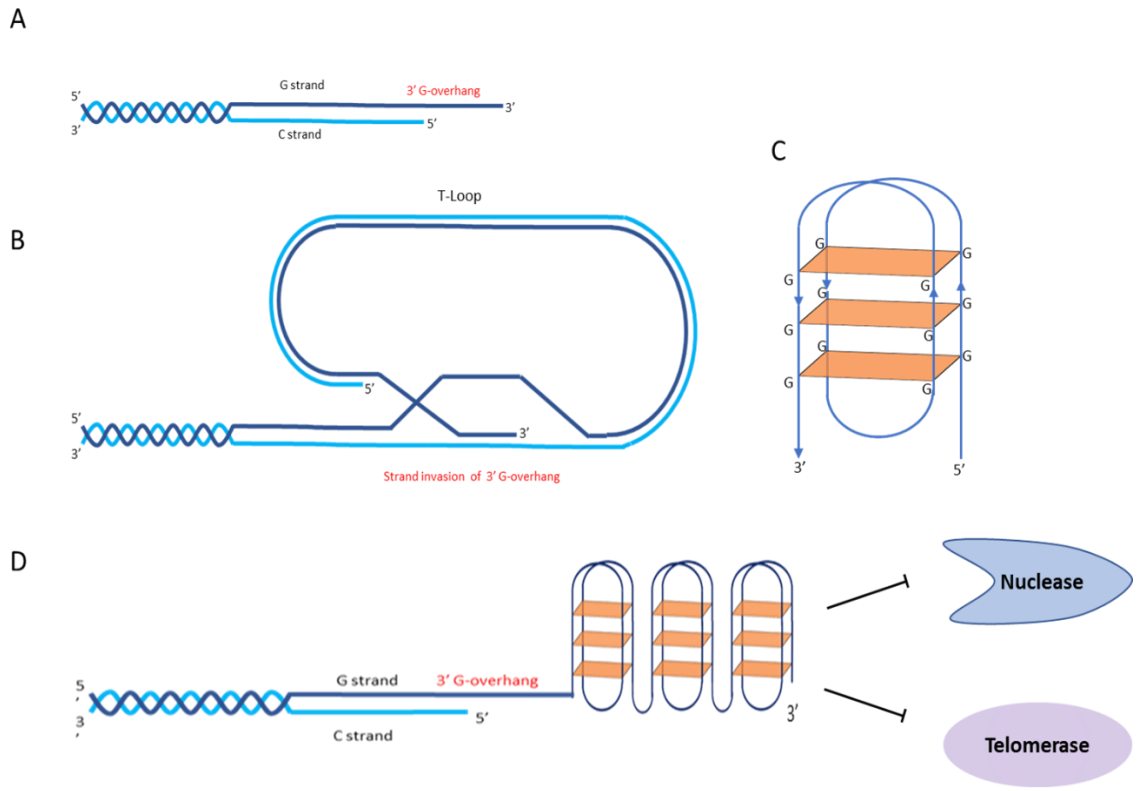

Figure 1.1. Telomeres structure. (A) Telomeric DNA is formed of double-stranded and single-stranded DNA. One of the strands is C-rich, and the opposite G-strand protrudes toward the end of the chromosome to form a 3′ G-overhang. **(B)** A telomere forming a T-loop, the 3′ G-overhang invades of double-stranded DNA, forming an internal D-loop. **(C)** G-quadruplex formed from G-quartets, which are square, planar arrays of four guanines (Gs) that are hydrogen-bonded by Hoogsteen base pairing. **(D).** G-quadruplexes that may offer end protection against nucleases or regulate telomerase activity. Adapted from **(Giardini et al., 2014)**

3.1.2 3′ G-overhang

In eukaryotes, telomeres end in a G-rich single-strand tail called the 3′ overhang(Chai et al., 2006). The structure is essential for forming T- loop, in which the overhang is inserted into the duplex telomeric DNA region, presumably helping protect chromosome ends from being recognized as damaged DNA and preserving genome stability (Palm and de Lange, 2008).

During DNA replication, the end of the G-rich strand of the telomere is synthesized by leading strand synthesis, and the terminal of C-rich strand is replicated by lagging strand synthesis(Muraki et al., 2012). The end of the lagging strand is not completely replicated due to presence of RNA primers resulting in telomere shortening(Muraki et al., 2012). However, the synthesis of leading strand generates a blunt end that requires processing by nucleolytic enzymes, Apollo and Exonuclease1(Exo1)(Wu et al., 2012). This resection is necessary to generate the 3 G-overhang and ultimately the formation of T-loop. Two components of the shelterin complex, TRF2 and POT1 play essential role in telomeric end processing. TRF2, binds to double-stranded telomeric DNA, mediates the localization of Apollo to the telomeric end whereas POT1, binds to single-strand telomeric DNA act as a negative terminating Apollo function(Wu et al., 2012). EXO1 acts on both leading and lagging strand of telomeric DNA and creates further resection in both ends. The 3′ G-overhangs is protected by single-stranded DNA binding protein POT1(Loayza and De Lange, 2003).

The 3′ G-overhang of mammalian telomeres have been found to vary from 50 to 500 nucleotides(Hwang et al., 2014). The length of 3′ G-overhang has been shown to be correlated with telomere length(Rahman et al., 2008). Like telomeres, 3′ G-overhang progressively shortens with cell division indicating that they can affect telomere stability and therefore impact cell proliferation(Rahman et al., 2008). Disruption of the 3′ G-overhang induces a growth arrest with features of replicative senescence(Rahman et al., 2008)

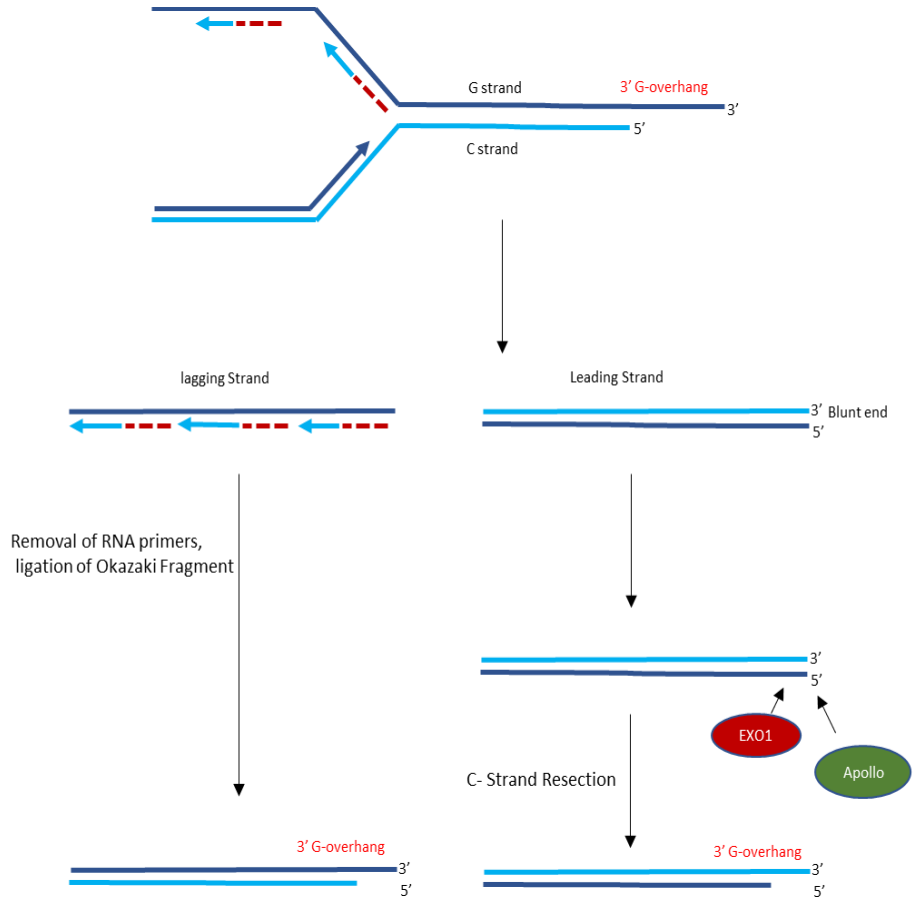

Figure 1.2. Generation of 3′ G-overhang in both lagging strand and leading strand. Modified from ((de Lange, 2009)

3.1.3 T-loop

The telomeric DNA forms additional structure help in protecting telomeric DNA from being recognized as damaged DNA known as T-loop(de Lange, 2004). The lariat structures function as a sequestration of the 3′ end hindering nucleases access to the 3′ G-overhang (de Lange, 2004). The size of the T-loop is highly variable. Super-resolution fluorescence imaging revealed variation in T-loop size depending on both the invasion point and telomere length(Doksani et al., 2013).

T-loops were first identified mammals by Griffith et al(Griffith et al., 1999). Microscopic data show that T-loops are created through the strand invasion of the 3′ G-overhang into the duplex part of the telomere DNA and anneal with the complementary strand (Griffith et al., 1999). TRF2 and POT1 telomere binding proteins are involved in the assembly of T-loop(Stansel et al., 2001). Experiments on telomeres using TRF2 null cells revealed that T-loops were absent in these cells indicating the TRF2 role in T-loop formation(Doksani et al., 2013).

The protective function of T-loop has been studied using high resolution microscopy. DNA damage response activation occurred specifically in linearized telomere ultimately causing telomere deprotection and telomeric end fusion(Van Ly et al., 2018). The microscopic data also showed that loss of T-loop resulted in longer average telomere length compared with T-loop positive cells(Van Ly et al., 2018). These findings highlight the importance of observing telomere structure integrity over telomere length in studying telomeres dynamics to avoid false positive results. Formation of these lariat DNA structures is important contributor to the protection of telomere ends from DNA repair mechanism.

3.1.4 The shelterin complex

In human telomere, the T-loop is formed and maintained by a complex of six telomere-specific proteins called the shelterin complex (Palm and de Lange, 2008). In general, the shelterin complex protects the telomeric DNA by repressing DNA repair mechanism(Heidenreich and Kumar, 2017).The six subunits are telomeric repeat-binding factor 1 and 2 (TRF1) (TRF2), repressor/activator protein 1 (RAP1), TRF1-interacting nuclear factor 2 (TIN2), TPP1 (also known as adrenocortical dysplasia protein homolog) and protection of telomeres1(POT1)(Maciejowski and de Lange, 2017b). The interactions between members of the shelterin complex and the telomere DNA sequence stabilize the telomere structure and regulate access of proteins involved in DNA repair and lengthening(de Lange, 2018).

Human telomeres are condensed into tight globular structures in vivo, like those seen in mouse cells(Bandaria et al., 2016). The condensation of telomeres is primarily mediated by shelterin components and telomeric DNA, not by histone deacetylation, DNA methylation, or histone trimethylation(Bandaria et al., 2016). Removal or manipulation of shelterin components leads to decompaction of telomeric chromatin, which triggers access of DDR signals at telomere ends(Bandaria et al., 2016). Shelterin proteins collectively protect telomeres from DNA damage signals. However, each component of the shelterin has a different role in this process. TRF1, TRF2 and POT1 bind TTAGGG repeats specifically. The remaining member of the complex do not bind directly to telomeric DNA(de Lange, 2018).

Human TRF1 and TRF2(hTRF1 and hTRF2) hold a very similar amino acid sequence closely related to the Myb domain(Court et al., 2005). The DNA binding domain of hTRF1 and hTRF2 recognize the central AGGGTT sequence in telomeric DNA where TRF1 DNA binding is four times stronger than TRF2(Hanaoka et al., 2005). The reason of the difference in binding

activity is attributed to difference in amino acid sequence between these two proteins(Bandaria et al., 2016). POT1 protein bind to G-overhang at the ends of chromosomes (de Lange, 2018). The crystal structure of POT1 (hPOT1) has two important domains required for its function: an N-terminal OB fold necessary for DNA binding, and a protein interaction domain, mediating association with the TRF1-TRF2 complex (Loayza and De Lange, 2003). hPOT1 binds to single-stranded human telomeric TTAGGG repeats but not to double-stranded telomeric DNA nor to the C-rich telomeric repeat strand (Loayza and De Lange, 2003). hPOT1 binding requires a single strand telomeric DNA of at least ten bases(Lei et al., 2004a). This binding is concentration and sequence dependent(Lei et al., 2004b). Body of work has defined the role of TRF2 and POT1 proteins in repressing all DNA damage response pathways (Hockemeyer et al., 2006; Konishi and de Lange, 2008). TRF1 on the other hand is involved in telomeres replication and prevents ATR activation at fragile telomeres in metaphase(Sfeir et al., 2009). Super-resolution fluorescence imaging showed that only TRF2 is required telomeric DNA T-loop configuration whereas deletion of TRF1 and POT1 had no effect on the T-loop formation(Doksani et al., 2013).

TIN2 does not bind to telomeric DNA. Instead TIN2 connect TRF1 and TRF2 which stabilizesTRF2 on telomeres. TIN2 also binds to TPP1, which in turn binds to POT1(de Lange, 2005). Therefore, TIN2 responsible for the stabilization of single stranded and double stranded telomeric DNA binding protein component of shelterin. The function of TIN2 was conformed by TIN2 depletion study which greatly affected the stability of the shelterin complex(Ye et al., 2004).

TPP1 is composed 3 domains: N-terminal OB-fold domain required for telomerase recruitment(Grill et al., 2018), a central domain that directly binds to POT1, and a C-terminal domain necessary for its association with TIN2, which integrates both TPP1 and POT1 into the shelterin complex(Palm and de Lange, 2008). TPP1 does not have a DNA binding domain

therefore no direct interaction between TPP1 and telomeric DNA is observed. TPP1 interaction with POT1 was shown to be essential for telomerase recruitment to telomere(Xin et al., 2007).

RAP1 lacks any DNA binding activity. Rap1 interacts with TRF2 forming a complex essential for TFR2 binding to telomeric DNA(Necasova et al., 2017). Removing RAP1 from telomere either by gene deletion or mutation in TRF2 showed higher incidence of homology directed repair (Sfeir et al., 2010).

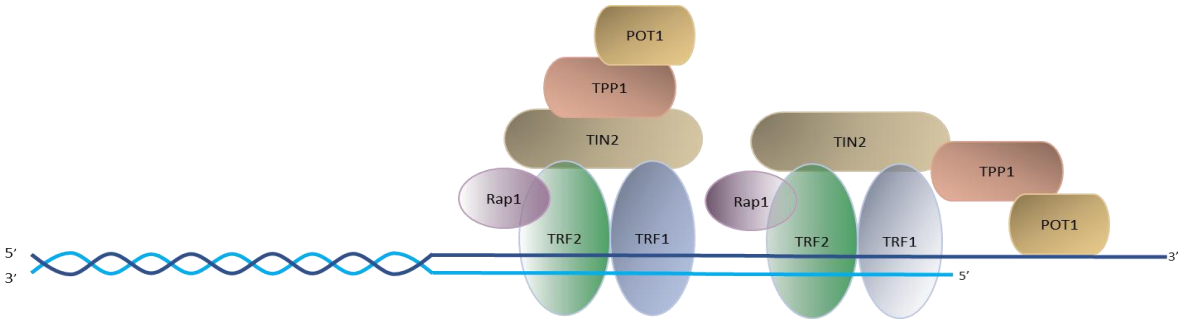

Figure 1.3.Shelterin protein complex. Shelterin is a six-subunit complex that specifically associates with telomeric repeats. Shelterin is formed by TRF1, TRF2, POT1, TIN2, Rap1 and TPP1. TRF1 and TRF2 bind to double stranded telomeric DNA through their ability to recognize duplex TTAGGG repeats. POT1 binds to single-stranded TTAGGG repeats. TIN2 and TPP1 do not process a DNA binding sequence. Modified from (de Lange, 2018)

2.2 Telomere-Length

Telomere length is highly variable among individuals of the same species. In human, telomere length is reset at the time of fertilization and decreases as the fetus develops(Turner et al., 2010). Telomere length is equivalent in different somatic tissues of the human fetus and newborn in part to the activity of telomerase(Blackburn, 2005). Different tissues have different telomere length for example, muscle tissue have longer telomeres than leucocytes(Daniali et al.,

2013). Variation is not exclusive to tissue, telomere length also varies between chromosomes and their respective arms within one cell(Londono-Vallejo et al., 2001). Several studies have demonstrated that the telomere length on homologous chromosomes can differ(Suda et al., 2002; Zou et al., 2004). Additionally, telomere length is correlated with the size of the corresponding chromosome(Wise et al., 2009). A positive relationship between chromosome size and telomere length has been observed within human and other species(Wise et al., 2009). With no clear explanation why this pattern exist, a recent hypothesis termed the centromere-from telomere hypothesis has been proposed as a possible mechanism to explain such correlation(Slijepcevic, 2016). In Brief, the closer the telomere to centromere can lead to instability. However more studies are needed in this field.

Telomere length (TL) has emerged as a promising biomarker to assess age-related disease risk , neurodegenerative disease and cancer(Fasching, 2018). To date, several methods have been made available to measure the length of telomeres. Understanding the benefits and drawbacks of TL measurement methods is important because short telomeres, not average TL, limit long-term stem cell divisions essential for tissue renewal(Lai et al., 2018).

2.3 Telomere localization

Chromosomes are organized in gene-poor and gene-rich regions where gene-poor regions being more peripheral, and gene rich regions are closer to the nucleus(Pombo and Dillon, 2015). Localization depends on the interaction genomic loci and nuclear lamina(Wang et al., 2016). Telomeres are heterochromatic domains with preferential locations close to nuclear periphery(Gonzalo and Eissenberg, 2016; Ottaviani et al., 2009). Nuclear lamins with other proteins contribute in nuclear stiffness and mechanical stability(Swift et al., 2013). Telomere enrichment at the nuclear rim is mediated by physical tethering of telomeres to the nuclear

envelope(Crabbe et al., 2012). Studies showed telomere binding to nuclear lamins in vivo is mediated by the shelterin factor TRF2(Wood et al., 2014). The interaction between TRF2 and lamin A was shown to protect and stabilize the telomeric T-loop(Wood et al., 2014). Defective telomere tethering to lamins (Gonzalo and Eissenberg, 2016) has the same impact as lamin loss in affecting distribution of telomeres and results in telomere shortening, defects in telomeric heterochromatin, and increased genomic instability(Gonzalez-Suarez et al., 2009). TRF1 and TRF2 were reported to be implicated in telomere attachment the nuclear envelop(Smith et al., 2018; Wang et al., 2018) through interaction with two different proteins(TERB2 and MAJIN) that are responsible for this tethering(Shibuya et al., 2015). Disruption of TERB2-MAJIN interaction abolishes the telomere attachment to the nuclear envelop and causes aberrant homologous leading subsequent meiosis defects (Wang et al., 2019).

Telomeres are also dynamic structures, exhibiting highly variable non-directional motion(Gonzalo and Eissenberg, 2016). Deprotected telomeres are more mobile the functional telomeres(Wang et al., 2008). The increased mobility mostly seen at the site of damage where 53BP1 accumulates facilitating DNA repair reactions(Dimitrova et al., 2008). Altogether, alterations telomere attachment to nuclear envelop can cause telomere dysfunction-driven genomic instability.

2.4 Human chromosomes protected by shelterin

Telomeres critical for maintenance of genome stability and cell viability. Dysfunctional telomeres occur due excessive shortening of telomeric repeats, loss of the capping, or the protective T-loop structure leading to genome instability and tumorigenesis(Gonzalo and Eissenberg, 2016).

The vital function of telomeres is to prevent the activation of the DNA damage response at the ends of chromosomes(de Lange, 2018). Naked DNA is prone to activate ATM (ataxia-

telangiectasia mutated), and ATR (ataxia telangiectasia and Rad3-related protein) pathways where ATM activated by DNA double strand break (DSB) and ATR activated in single strand break (Maréchal and Zou). In response DBS, the MRN complex (Mer11-Rad50-Nbs1) is the recruited to the DSBs. The MRN acts as a sensor for ATM and is required for ATM binding and activation(Lee and Paull, 2005; Uziel et al., 2003). Following localization to the site of damage, ATM induces phosphorylate histone variant H2AX within minutes of after DNA damage and spreads over large chromatin domain(Maréchal and Zou). Formation of these DNA damage foci has been implicated in signal amplification and DNA repair. The two master checkpoint kinases also phosphorylate CHK1 and CHK2 enforce G1/S or G2/M arrest thereby block cell cycle progression(Ronco et al., 2016). Chk1 and Chk2 also cooperate with ATM and ATR to activate p53, which further inhibits cell cycle progression through induction of the Cdk inhibitor p21(Kousholt et al., 2012).

TRF2 seems to be the main player in repassing telomeric DNA damage response(Takai et al., 2011). TRF2 is required for T-loop formation and maintenance as deletion of TRF2 resulted in telomere fusion, and disappearance of T-loops (Palm and de Lange, 2008). Change of telomeric structure as a result of TRF2 deletion is prominent as telomeres gained linear elongated structure(Doksani et al., 2013). In addition, microscopic data shows telomeric fusion occurs as long joined chromosomes in metaphase spread(Doksani et al., 2013). Since ATM signalling is required for NHEJ of telomere, ATM-/- cells showed reduction in telomere fusion(Doksani et al., 2013). Whereas T-loop is essential for telomere protection, the structure itself can be a substrate for endonuclease attacks. The 5′ transition of the telomeric double strand into single strand is the vulnerable site and TRF2 binding with telomeric DNA prevent the endonuclease cleavage thereby repressing telomere loss(Schmutz et al., 2017). Although only TRF2 was reported to activated

MRN-dependent ATM activation at deprotected telomeres, studies regarding involvement of other members showed that loss of the stabilization of the complex ,for example TIN2 deletion can result in ATM activation(de Lange, 2018). ATM is not only activated by double strand DNA breaks, in human nuclear extracts ATM was also shown to be activated by short single stranded DNA overhangs(Shiotani and Zou, 2009). ATM and ATR signalling are required for efficient non-homologous end-joining (NHEJ) of dysfunctional telomeres(Denchi and de Lange, 2007).

ATR kinases activation involves the binding of Replication protein A (RPA) to single strand DNA(Cimprich and Cortez, 2008). Interaction of ATR kinase with RPA coated single strand DNA mediated by ATR-interacting protein (ATRIP)(Cortez et al., 2001). Subsequently, the complex direct the Rad9-Rad1-Hus1 (9-1-1) complex loading 5′ on the double strand/single strand transition by the Rad17(Cimprich and Cortez, 2008). Ultimately, this will lead to phosphorylation of downstream kinase Chk1 and other ATR effectors.

Shelterin component POT1 is a critical repressor ATR signaling at single strand telomeric DNA(Denchi and de Lange, 2007). POT1a depletion increased RPA accumulation at telomeric ends in mouse model suggesting the antagonistic effect of POT1a for RPA binding(Gong and de Lange, 2010). In human, POT1 showed similar results where loss of POT1 activated ATR signalling by inhibiting RPA localization to single strand telomeric DNA(Barrientos et al., 2008). Other shelterin components are involved indirectly in this process. TIN2 for example showed important role in stabilizing TPP1/POT1 tethering to telomeric DNA, thereby preventing RPA accumulation and ATR activation(Takai et al., 2011).

ATR activation by TRF1 deletion was reported by one study(Martinez et al., 2009).TRF1 depletion causes rapid induction of senescence, which is concomitant with abundant telomeric gamma-H2AX foci and activation of the ATR pathway(Martinez et al., 2009) therefore leading to

increased telomere fragility and fusions. Collectively, shelterin complex components crucial for telomeric DNA protection from DNA repair mechanism.

Structural organization study of telomeric chromatin in human cells showed that telomeres form compact globular structures through telomere shelterin interactions(Bandaria et al., 2016). Telomere compaction driven by shelterin complex was demonstrated as reduction in telomeric volume upon overexpression of shelterin component TRF1 and TRF2. Abrogation of the shelterin complex resulted in telomere decompaction and accumulation of DDR signals(Bandaria et al., 2016).

2.5 Telomeres non-canonical function

Telomeric DNA has been shown to be epigenetically active by either impacting transcription by position effect or by direct transcription(Robin et al., 2014). Telomeres impact gene expression in different ways. First to be reported was Telomere Position Effect (TPE) which described in repressing gene expression up to 100kb from telomere. The human genome is composed of self-interacting loops known as topologically associating domains (TAD)(Dixon et al., 2012). These looping in the chromosome brings long telomere close to genes whereas short telomere are separated from the same loci(Robin et al., 2014).This mechanism was described extensively in *Saccharomyces cerevisiae* by placing genes adjacent the telomeric repeats. Genes close to telomeres are silenced in with long telomeres and become expressed when telomeres are short(Gottschling et al., 1990). This reversible gene repression has also been demonstrated in humans. The presence of TPE in human cells was first described by Baur Ja et al where the expression of luciferase reporter adjacent to telomeres was less compared to control(Baur et al., 2001). ISG15 (Interferon Stimulated Gene 15 kDa) was the first TPE gene upregulated upon telomere shortening(Lou et al., 2009b). Later on, different reports described expression of multiple

genes regulated by TPE in telomere length dependent manner(Lou et al., 2009a; Robin et al., 2015; Stadler et al., 2013). Interestingly, hTERT gene which is 1.2 Mb far from the end of chromosome 5p is in part regulated by the length of the telomere(Kim et al., 2016). In vitro experiments demonstrated that hTERT mRNA levels were significantly lower in cells with long telomeres compared to cells with short telomeres. This suggests that chromatin loops in hTERT locus are formed in cells with long telomere(Kim et al., 2016).

Telomeres length does not only affect expression of near by genes. Robin et al. analyzed the effect of TPE on 1423 sub telomeric genes. 144 telomere length dependent genes were identified which were located as far as 10Mb from telomere. This effect was called as Telomere position effect over long distance (TPE-OLD)(Robin et al., 2014).

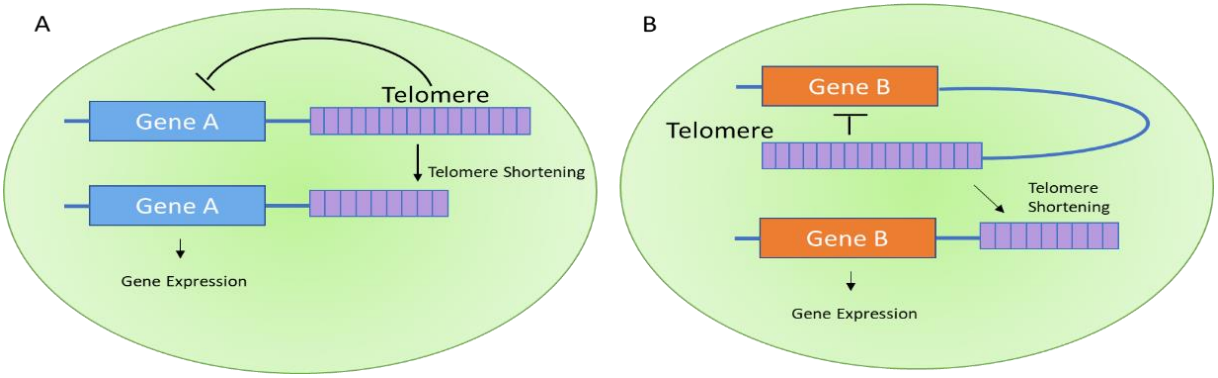

Figure 1. 4 Telomere position effect. (A) Telomere position (TPE). Telomeres reversibly silence expression of genes near telomeres. Progressive telomere shortening remove the inhibitory effect activating gene transcription. **(B)** Telomere portion effect over long distance (TPE-OLD). Telomeres control expression of genes far away from telomere. Progressive telomere shortening remove the inhibitory effect activating gene transcription

Until recently, Telomeres have been considered as transcriptionally silent. Azzalin CM et al, were the first to report that mammalian telomeres are transcribed into telomeric repeat-

containing RNA (TERRA) (Azzalin et al., 2007). The non-coding RNA are transcribed by polymerase II from sub-telomeric regions contains the canonical telomeric repeat sequence, UUAGGG, as well as sequences unique to the sub-telomeric region of each chromosome ranges in size from 100 bases to >100 kb (Chu et al., 2017). Recent study has shown that TERRA depletion by single-stranded antisense oligonucleotides causes dysregulation of TERRA target genes(Chu et al., 2017). Same study identified functional antagonism between TERRA and ATRX gene and also possible upregulation of telomerase activity with TERRA knockdown suggesting TERRA depletion would cause telomere dysfunction(Chu et al., 2017).

Taken together, the aforementioned functions of telomeres show a new area of research where telomere shortening may increase expression of an oncogene suppressed by telomere position or supress the expression the tumor-suppressor gene silenced by TERRA.

3. Telomerase: a specialized reverse transcriptase

The existence of a reverse transcriptase that can synthesize telomeres was discovered by Greider and Blackburn about 45 years after the discovery of telomere (Blackburn, 2001). Telomerase is a ribonucleoprotein (RNP) complex that synthesizes telomeric DNA repeats at the end for linear chromosome (Harley, 2008a). The holoenzyme is composed of catalytic protein component, telomerase reverse transcriptase (TERT), RNA template (TERC) and accessory proteins for the assembly, subcellular trafficking, processivity and localization to telomeric ends(Greider and Blackburn, 1985).

3.1 TERT

Human TERT(hTERT), the catalytic component of telomerase , is a 40kb gene located on the short arm of chromosome 5 and predominantly governed at transcriptional levels(Jafri et al.,

2016). hTERT is a 127 kDa protein 1,132 amino acids long, with four functional domains. The central reverse transcriptase (RT) domain composed of evolutionarily conserved motifs that are essential for catalysis(Blackburn and Collins, 2011). The TERT N-terminal domain (TEN) plays a key role in telomerase recruitment to telomeres and participates in the catalysis of telomeric repeat synthesis , the TERT RNA binding domain (TRBD)and the C-terminal extension(Lu et al., 2013).

hTERT is expressed solely in cells that exhibit telomerase activity and is not expressed in most normal somatic cells(Yi et al., 2001a). Therefore, hTERT is considered as the rate-limiting role in the telomerase holoenzyme. Body of studies demonstrated that overexpression of hTERT is enough to reconstitutes telomerase activity normal human cells(Bodnar et al., 1998; MacKenzie et al., 2002).

3.2 Telomerase RNA.

hTERC was first cloned in 1995. It was noted that hTERC is ubiquitously expressed in all normal human (Feng et al., 1995). TERC is expressed as a 451 nucleotide RNA polymerase II-driven non-coding RNA(Feng et al., 1995). TERC has a well characterized secondary structure that can be divided into functional regions, the 5′ domain and 3′ domain(Arndt and MacKenzie, 2016b). TERC functional domain 5′ pseudoknot structure that interacts with TERT and includes a region that serves as a template for telomere synthesis(Mitchell and Collins, 2000). The 5 ′domain (also known as the core domain) folds into pseudoknot that contains the RNA template. The template pseudoknot in the 5′ domain binds to hTERT and aligns the enzyme complex with the 3′ overhang of telomeric DNA(Arndt and MacKenzie, 2016b).

The 3′domain of hTERC contains the H/ACA box which binds to telomerase accessory proteins necessary for the stability and accumulation of TERC(Arndt and MacKenzie, 2016b).

Several accessory proteins associated with the telomerase holoenzyme, including telomerase Cajal body protein 1 (TCAB1),the four H/ACA-motif RNA binding proteins dyskerin ,NHP2, NOP10, and GAR1 (Xu and Goldkorn, 2016)**.** Interaction between hTERC and these proteins is essential for stable telomerase complex(Xu and Goldkorn, 2016). TERT utilizes the template region (3′-CAAUCCCAAUC-5′) of TERC to add TTAGGG repeats and thereby extend single stranded 3′ telomeric strands(Xu and Goldkorn, 2016).

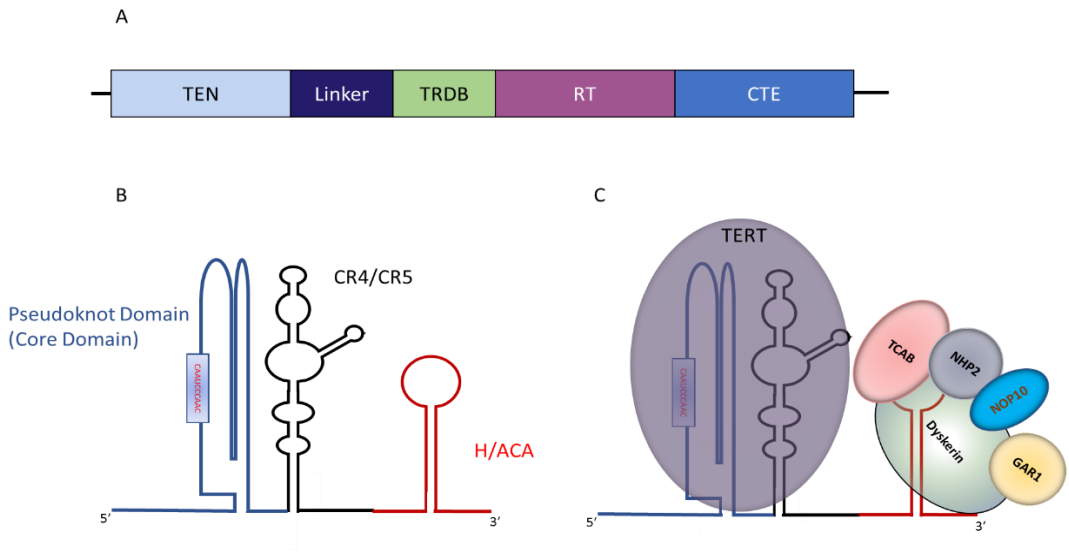

Figure 1.5 (A) hTERT protein domains. **(B)** The human telomerase RNA (hTERC) contains three major structural and functional domains, the core domain, the CR4/CR5 domain, and the H/ACA. **(C)** Secondary structure and known protein components of the human telomerase holoenzyme. Modified from (Jafri et al 2016).

3.3 Human TERT regulation

Telomerase activity is regulated at both the transcriptional and post transcriptional levels. At transcriptional level, the pre-messenger RNA of hTERT gets spliced into various alternative transcripts carrying a disrupted catalytic domain, ultimately resulting in a decreased pool of mRNA for catalytically active hTERT(Liu et al., 2017). Splicing pattern changes with cell type and

development stage suggesting that alternative splicing is likely to control telomerase activity. Post-translational regulation of telomerase activated occurs through phosphorylation and ubiquitination(Jie et al., 2019).

3.3.1 Alternative splicing of hTERT

Alternative splicing affects almost all genes, allowing generation of over 100,00 proteins from about 20,000 protein coding sequence(Wong et al., 2014). hTERT contains 15 introns and 16 exons that can spliced into 22 identified isoforms(Wong et al., 2014). Of all identified isoforms, only the full-length transcript with all 16 exons process telomere elongation capacity(Listerman et al., 2013) since the full-length hTERT include conserved domain the encodes reverse transcriptase activity. Major splice variant identified are termed minus alpha(hTERTα) or minus beta(hTERTβ) which encodes for truncated protein that lacks reverse transcriptase domain but retain the RNA binding motifs(Listerman et al., 2013). hTERTα results from a partial in-frame deletion of 36 bp within exon 6, leading to the partial loss of RT-motif A(Colgin et al., 2000). The missing 12 amino acids in hTERTα are from the conserved reverse transcriptase domain ,therefore hTERT does not posses any telomerase activity(Yi et al., 2000).hTERTα has been detected in developing human tissue while the full length hTERT was almost absent (Ulaner et al., 1998).

hTERTβ results from a 182-nucleotide out-of-frame deletion which skips exon 7 and 8 joining exon 6 to exon9 introducing termination codon. The truncated protein possess dominant-negative on telomerase positive cells(Yi et al., 2000). hTERTα and hTERTβ overexpression inhibited telomerase activity (dominant negative) in telomerase positive cell line by competing with hTERT for binding to hTERC (Colgin et al., 2000; Listerman et al., 2013). However, the relatively low abundance of hTERTα and hTERTβ transcripts makes it less likely to affect telomerase activity in telomerase positive cells(Mavrogiannou et al., 2007).

In addition to the inhibitory effect they have on telomerase activity, splice variants of hTERT have been shown to enhance cell proliferation thought enhancing Wnt signalling pathway(Hrdlickova et al., 2012). Moreover, hTERTβ localization to mitochondria protected breast cancer cell from cisplatin -induced apoptosis(Listerman et al., 2013). The expression of these variants in normal cells and telomerase negative cells provide supporting evidence of the non canonical function of hTERT as discussed below.

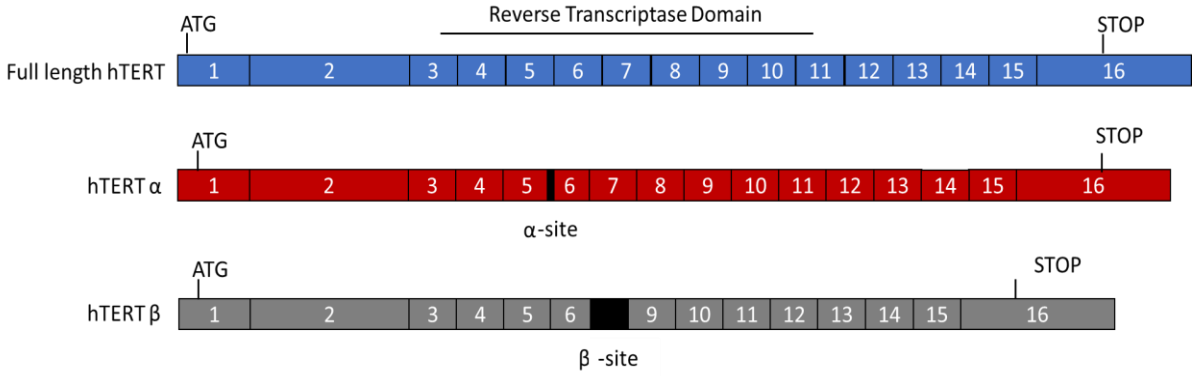

Figure 1. 6. Telomerase (hTERT) mRNA and major splicing variant. The full-length transcript (blue) contains all 16 exons that can make telomerase with reverse transcriptase activity. hTERTα (red) with the minus alpha leading to missing 36 bp within exon 6. hTERT β(gray) with the minus beta isoform missing exon7 and 8, both occurring in the reverse transcriptase domain leading to truncated protein that lack telomere extension activity.

3.3.2 Transcriptional Regulation of hTERT

It is well known that hTERT gene is predominantly governed at transcriptional level. hTERT Transcription is regulation is extremely complex and involves various positive and negative factors(Jafri et al., 2016). The core promoter of the hTERT gene contains several regulatory elements. TERT promoter does not have typical transcription regulatory elements , TATA and CAAT boxes (Jafri et al., 2016). TERT promoter contains binding sites for many

transcription factors SP1, ETS, E2F, AP1, HIF1 and c-Myc(Akincilar et al., 2016). However non of these factors alone promote immortalization in somatic cells(Zhu et al., 2010). c-Myc binds to E-boxes in the promoter region of TERT leading to upregulation of TERT expression(Khattar and Tergaonkar, 2017). However, c-Myc alone is not sufficient to drive the activation. Interaction of ETS with cMyc is critical for hTERT gene expression and breast cancer cell proliferation(Xu et al., 2008). Specificity protein 1(Sp1) acts cooperatively with c-Myc to induce to TERT expression(Kyo et al., 2000; Ramlee et al., 2016). Additional factors contribute to the activation of hTERT transcription including estrogen which has been shown to activate the transcription of hTERT via activation of c-Myc in breast cancer cell line(Boggess et al., 2006). Survivin phosphorylation of c-Myc and Sp1 enhances the expression of TERT in colon cancer(Endoh et al., 2005).

Transcription repressor of hTERT studies uncovered several factors that can downregulate the expression of hTERT. For example, MAD1 competes with c-Myc for the E-box motifs and mediates its repressive effect(Ramlee et al., 2016). E2F1 which binds to promoter region of hTERT leading to its downregulation(Lacerte et al., 2008). Wilms tumor protein (WT1) exhibits hTERT repressing characteristic shown in clear cell renal cell carcinoma by directly binding to hTERT(Sitaram et al., 2010) . P53 gene has two binding sites upstream of the transcription start site of hTERT promoter, -1240 and -1877. Overexpression of P53 was found to repress the expression of hTERT. However, overexpression of TERT alone did not immortalize cells suggesting downregulation of the former combined by the overexpression of the later are required for cell immortalization(Shats et al., 2004).

3.3.3 Post-translational activation/repression of hTERT

Regulation of hTERT also takes place during posttranslational mechanism which plays a pivotal role in modulating telomerase activity. Posttranslational regulation of hTERT can occur via reversible phosphorylation of hTERT at specific serine/threonine or tyrosine residues can may affect the structure, localization and enzyme activity(Wojtyla et al., 2011). For example, Phosphorylation of hTERT by protein kinase C(PKC) isoenzymes enhance telomerase activity(Chang et al., 2006). hTERT phosphorylation by PKC is essential for telomerase holoenzyme assembly, leading to telomerase activation and oncogenesis(Chang et al., 2006). Additional example on hTERT phosphorylation is Akt-mediated phosphorylation of hTERT was found to increase the hTERT localization to the nucleus(Chung et al., 2012a). Moreover, phosphorylation enhances the non-canonical function hTERT where Src phosphorylation hTERT increase hTERT localization to mitochondria in response to oxidative stress(Buchner et al., 2010) (Haendeler et al., 2003) phosphorylation can negatively impact the activity of the enzyme. For example, protein phosphatase 2A PP2A dephosphorylation of hTERT reduces the nuclear telomerase activity (Xi et al., 2013). Similarly, c-Abl phosphorylation of hTERT at proline-rich was shown to have negative effect on telomerase activity. (Kharbanda et al., 2000).

Reduction in hTERT levels due to degradation and turnover of the protein occurs through ubiquitination. Makorin Ring Finger Protein 1 (MKRN1) is the first factor identified as an E3 ubiquitin ligase for hTERT in mammalian cells(Chung et al., 2012b). MKRN1 ubiquitination of hTERT occurs at the C-terminal domain (residues 946–1132). Moreover, overexpression of MKRN1 decreased activity of telomerase and therefore telomere length in HT1080 cell line(Kim et al., 2005). CHIP (C terminus of Hsc70-interacting protein) is another post-translation modifier of hTERT(Lee et al., 2010). Binding of CHIP to hTERT inhibits nuclear translocation of hTERT

by dissociating p23 thereby inhibiting telomerase activity (Lee et al., 2010). Hdm2 (E3 ligase) has also been shown to reduce telomerase activity by inducing hTERT ubiquitination and degradation. (Oh et al., 2010).

Taken together, the effect of phosphorylation and dephosphorylation on hTERT provide substantial evidence that posttranslational modifications of hTERT play a role in modulating telomerase activity.

3.3.4 hTERT Transport

As mentioned above, hTERT requires localization to the nucleus to perform its function. Reports suggested TERT transport to the nucleus occurs first then the assembly start to happen in the nucleus(Jafri et al., 2016). Several factors are involved in the transportation and localization into the nucleus. 14-3-3 signalling molecule was found to be involved in hTERT translocation which seems to block the binding of hTERT to exporting receptors, CRM1(Seimiya et al., 2000). In general, nuclear transport occurs thought interaction of nuclear transporter with nuclear pore complex (NPC)(Wente and Rout, 2010). Nuclear transport receptor recognizes molecules containing nuclear localization signal (NLS) (Wente and Rout, 2010). N-terminal region of hTERT contains NLS that was found to be substrate for Nup358 and importin 7 which are responsible to nuclear import of hTERT(Frohnert et al., 2014). hTERT translocation from nucleus to cytoplasm mediated by CRM1 nuclear pores requires its phosphorylation by Src (Haendeler et al., 2003). (Haendeler et al., 2003).

3.4 Telomerase Assembly.

Telomerase biogenesis is a sequential and cell cycle-dependent process which requires interaction between chaperone and assembly factors(Egan and Collins, 2012). hTERT is

synthesized in the cytoplasm and is chaperoned to the nucleus for assembly hTERT(Dey and Chakrabarti, 2018). The transcription activity of hTERT peaks in S phase(Xi and Cech, 2014) and telomerase access to the telomere is restricted to S where telomerase action is started after DNA replication is done(Tomlinson et al., 2008a).

Chaperones HSP90 and p23 interact with hTERT in the cytoplasm and move to the nucleus(Jafri et al., 2016). Pontin and Reptin proteins are required for the assembly where they bind to hTERT once it is in the nucleus(Schmidt and Cech, 2015). Blocking the interaction between the hTERT and the chaperon proteins inhibits telomerase assembly therefore decreasing its activity(Holt et al., 1999).

hTERC diffuses to nucleus and stabilized by the dyskerin complex association with its 3′ domain. ((Hamma and Ferre-D'Amare, 2010; MacNeil et al., 2016a). Telomerase complex localizes to Cajal bodies for most of the cell cycle via interaction with the CAB box of hTERC. The interaction between hTERC and telomerase cajal body protein 1(TCAB1) is important for the recruitment of telomerase to telomeres(Venteicher et al., 2009). Cajal bodies trafficking of telomerase complex occurs in S-phase of cell cycle to few telomere suggesting not all telomeres are being elongated every cell cycle(Jády et al., 2006). Localization of hTERC to cajal bodies and telomeres is hTERT dependent since no localization was found in hTERT negative cells(Tomlinson et al., 2008b).

3.5 Telomerase recruitment to telomeres

Active recruitment of telomerase to telomeres is necessary for telomere elongation. At telomere extension site, TPP1 and POT1 are the processivity factors required for telomerase recruitment and activity(Wang et al., 2007). Specific sequence of amino acids in TPP1 domain mediate hTERT - TPP1 interaction and telomerase recruitment to single strand telomeric

DNA(Sexton et al., 2012). Mutation in this amino acid sequence showed failure in telomerase recruitment to telomere causing a medical condition known as dyskeratosis congenita(Schmidt and Cech, 2015).

3.6 Telomerase activation and telomere length regulation

Number of telomeric repeats added each cell cycle dereddens on several factors such as TERT expression, telomerase assembly, interactions between telomere and telomerase. Chromosomes do not replicate at the same time as well as telomeres replication occurs at preferential moments during the S-phase(Arnoult et al., 2010). Some chromosomes are being replicated during early S phase while others are replicated in late S phase. In General, Telomeres replication occurs in early S phase adding around 60 nucleotides in a single round of extension(Zhao et al., 2009). The number of nuclides added by telomerase varied substantially between individual telomerase extension events(Teixeira et al., 2004a). Following the hybridization of the RNA template with the telomeric DNA, telomerase complex adds telomeric sequence to the 3` end of telomers. The active site of telomerase binds to the RNA/DNA hybrid catalyzing RNA-dependent DNA synthesis(Qi et al., 2012). Template translocation occurs to regenerate the RNA template after each synthesized repeat. This process involves separation of RNA template from DNA, translocation and realignment with DNA for additional repeats synthesis(Qi et al., 2012).

Telomeres extension is dependent on telomere length and telomerase activity. Experiment conducted by Teixeria et al. showed that telomerase does not extend every telomere in every cell cycle rather telomerase acts preferentially on short telomeres(Teixeira et al., 2004b). Telomere extension is dependent on number of telomerase complex available. Xi L and Cech estimated

about 240 telomerase monomers which is similar to that of telomeres in late S phase(Xi and Cech, 2014).

Once the 3'overhange extension is completed, telomerase activity is terminated by the CTC1–STN1–TEN1 complex (CST) through primer sequestration and physical interaction with POT1/TPP1 telomerase processivity factor(Wang et al., 2007). This interaction increases during late S/G2 phase leading to inhibition of telomerase recruitment to telomeric ends. CST complex also stimulates the DNA polymerase α/primase for the synthesis of the complementary strand thereby completing telomere synthesis(Chen et al., 2012).

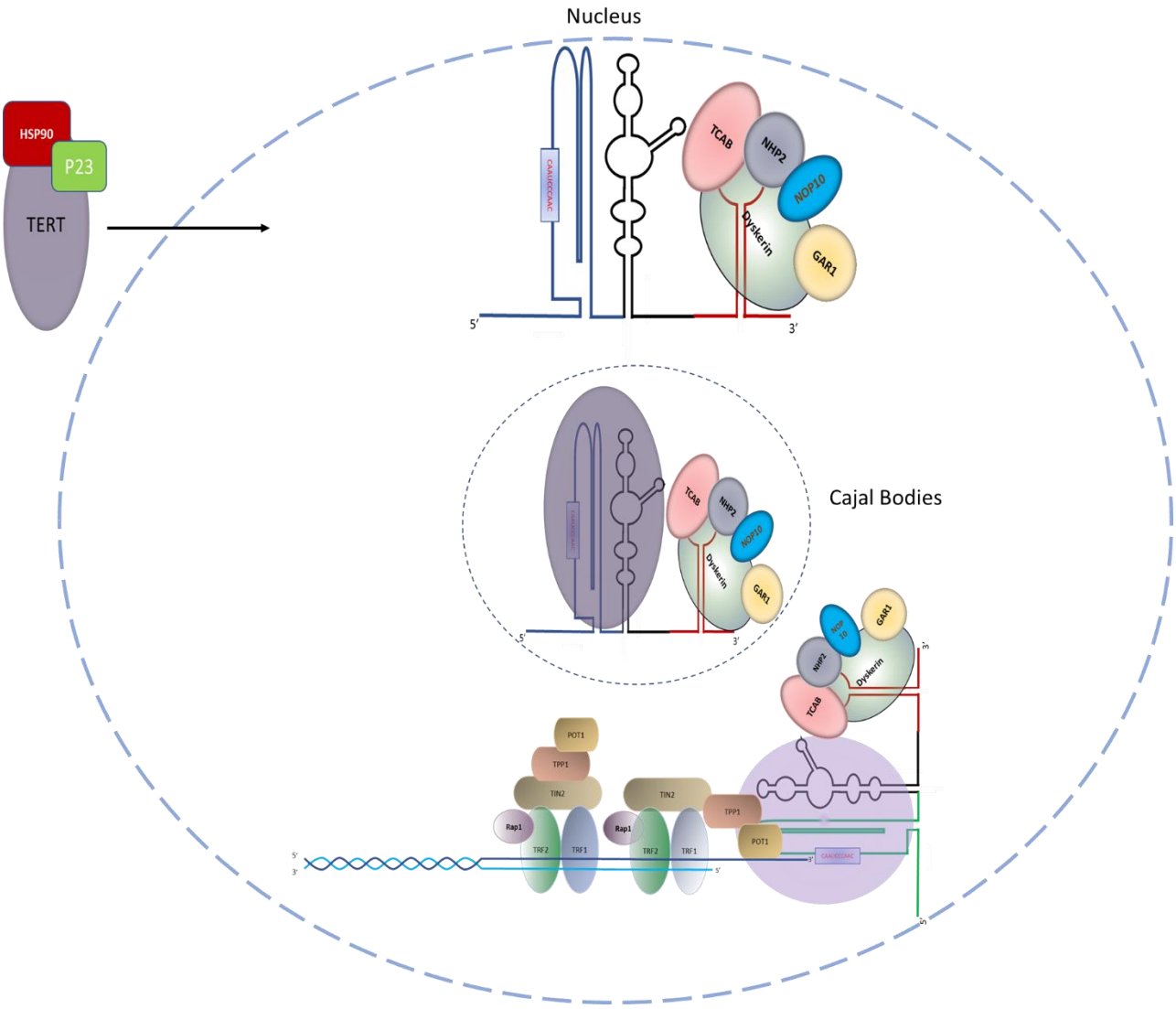

Figure 1.7. Telomerase assembly, recruitment to the telomere, and telomeric DNA synthesis. Intracellular trafficking of hTERT by chaperon proteins Hsp90 and p23. In the nucleus hTERT assembly mediate by Reptin ad pontin. hTR accessory protein TCAB guide the complex to cajal bodies. Telomerase holoenzyme recruitment to telomere occurs during S phase starting telomere elongation modified from reference (Jafri et al., 2016).

3.7 Telomerase activity

Although hTERC is essential for the activity of telomerase, the limiting factor for telomerase activity is strictly dependent on transcription of hTERT mRNA(Cong et al., 2002a). Telomerase activity is strongly correlated with TERT mRNA expression but not with hTERC expression regardless of it′s ubiquitous expression [127].

Telomerase activity has been detected germ cells, stem cells, immune and some somatic cells(Hiyama and Hiyama, 2007). Higher activity of telomerase was detected in early stages of embryogenesis which decreases with development(Magnenat et al., 1999). The activity decreases with development until it is completely absent (Wright et al., 1996). In stem cells, telomerase expression is enough to slow down rather than to prevent telomeres shortening. hTERT transcripts can be detected in a variety of telomerase-negative cells and tissues, but the mRNA produced is not full-length mRNA capable of producing active telomerase(Hrdlickova et al., 2012).

3.8 Telomerase non canonical function

The well-described function of telomerase is to maintain the integrity of chromosomal end structures enabling cell proliferation(O'Sullivan and Karlseder, 2010). In addition to telomeres maintenance, accumulating reports described the extra-telomeric activities for telomerase. TERT has been shown to facilitates tumor angiogenesis by up-regulating VEGF expression through direct interactions with the VEGF gene and the Sp1 transcription factor(Liu et al., 2016b). TERT overexpression was also reported to increase cell adhesion(Liu et al., 2016a), tumorigenesis(Stewart et al., 2002), DNA damage response and apoptosis regulation(Cong and Shay, 2008). It was recently demonstrated that TERT regulates NF-κB-dependent gene transcription. TERT was found to bind to bind to p65 and localize to promoter of NF-κB-dependent gene such as interleukin-6 and TNF-α increasing their transcription(Ghosh et al., 2012).

Telomerase has also been found to regulate the transcription activity of Wnt/ß catenin complex. Deregulation of the complex has been involved in cancer development. TERT acts as a cofactor in the ß catenin transcription complex(Li and Tergaonkar, 2014).

In addition to its role in activation of gene transcription, hTERT is localized to mitochondria. hTERT localization protected mitochondria from high levels of reactive oxygen species (ROS)(Haendeler et al., 2009). Authors demonstrated TERT binding to mitochondrial DNA (mtDNA) has a protective function from damage, oxidative stress-induced apoptosis and protect the respiratory chain complex(Haendeler et al., 2009).

Collectively, these reports provide more insights into TERT function in tumor progression in addition to its role in telomere maintenance (Ghosh et al., 2012). Understanding the non-canonical function is thus important to develop strategies to target telomerase and its extratelomeric effect than the then conventional telomerase inhibitors that depend entirely on telomere erosion for therapeutic impact.

4. Telomere shortening

The end of chromosomes gets shorter with every cell division. Telomeric repeats shorten at a rate of 50-200 bps with every cell divisions(Muraki et al., 2012). This shortening results from failure to replicate the ends of linear DNA molecules, termed the end replication problem as DNA polymerases is unable to copy 10-14 bases at the end of the chromosome in the lagging strand(Chow et al., 2012). During DNA replication, the end of the G-rich strand of the telomere is synthesized by leading strand synthesis, and the terminal of C-rich strand is replicated by lagging strand synthesis. The end of the lagging strand is not completely replicated due to presence of RNA primers resulting in telomere shortening(Muraki et al., 2012). As cells divide,

progressive telomere shortening occurs up to a point where cells become senescent(Victorelli and Passos, 2017). Therefore, telomere length is a fundamental feature of dividing cells and directly related to the age. Short telomeres lose their protective capacity, if accompanied with defective cell cycle check points, chromosomal fusion and unequal distribution of genetic martial between the daughter cells may occur(Zhu et al., 2016).

Although the telomere length varies between tissue, leukocytes, muscle, skin and fat displayed similar rates of age-dependent telomer shortening. The difference in length is believed to be established at early stages of development(Daniali et al., 2013). Since telomere length is variable between the chromosomes of the same cells, the question to ask is how many short telomers trigger replicative senescence. Hemann et al reported that the length of the shortest telomeres is a key biomarker of the onset of senescence rather than the average length(Hemann et al., 2001). Shay and Wright also indicated that a single short telomere is sufficient to induce replicative senescence(Shay and Wright, 2004).

Dysfunctional telomere does not allow T-loop formation. Defects in formation of the telomere protective cap leads to cell cycle arrest and is often associated with end-to-end chromosome fusion by non-homologous ends joining(O'Sullivan and Karlseder, 2010) .When telomere become critically short, they cannot fulfil their normal protective functions therefore the telomeric end will be recognized as double-strand break (DBS). The DNA damage response factors such as such as 53BP1, γ-H2AX, Rad17, ATM, and Mre11 accumulate at the site of uncapped telomere often called telomere-associated DNA damage factors as a Telomere dysfunction-Induced focus (TIF)(Kaul et al., 2011).

There have been many publications correlating human diseases with telomere shortening. An inverse correlation with the length of telomeres has been linked with development of cardiovascular disease, neurovegetative disease and cancer(Bernadotte et al., 2016). Telomeres studies revealed most cancer telomerase-positive cells display rather short telomeres as telomerase upregulation is considered a late event during malignant transformation whereas stems cells process long telomeres with active telomerase(Artandi and DePinho, 2010).

4.1 Telomere shortening and genome instability

Telomeres loses their genome guardian property when they become too short to from T-loop even with presence of long TTAGGG repeats(Longhese, 2008). Dysfunction in the chromosome end cap formation process leads to telomeric DNA recognition by the DDR machinery and activation of senescence or apoptotic pathways(de Lange, 2004). Cells loses their ability to senesce because of mutations in p53 protein in which the continue to divide eventually entering ‘crisis’ where extensive telomere shortening results in chromosomal fusion and cell death(Ozaki and Nakagawara, 2011).

Chromosomal rearrangement are very common event occurring are at early stages of tumorigenesis(Shih et al., 2001) and stabilize in advanced malignancy. Telomere-driven genome instability as first reported In 1938 by McClintock upon chromosomes irradiation with X-ray(O’Sullivan and Karlseder, 2010) . The cycles are initiated when a chromosome without a telomere replicates, and the sister chromatids fuse at their end(Sabatier et al., 2005). The progressive loss is first identified as breakage and subjected to DNA repair mechanism as mentioned above. As the cell replicate, sister chromatids fuse at their ends bridge during anaphase. Fusion can occur between two arm of different chromosome, the former type of fusion occurs when uncapping occurs in single telomere(Maciejowski and de Lange, 2017a). Fusion

preferentially occurs between chromosomes bearing short telomeres. The break occurs when the centromeres are pulled in the opposite directions leading to unequal distribution of genome between the daughter cells. The Break-Fusion-Bridge cycle will continue as the cell divide due to lack of telomere(Murnane, 2006). Cycles can continue for multiple cell generations, leading to extensive DNA amplification and progressive terminal deletions, duplication of whole chromosomes, aneuploidy, gene amplifications, translocations, inversions and deletions(De Lange, 2005) and ends when the chromosome eventually acquires a new telomere and again become stable(Gobbini et al., 2014). Telomere restabilising mechanism requires activation of telomerase.

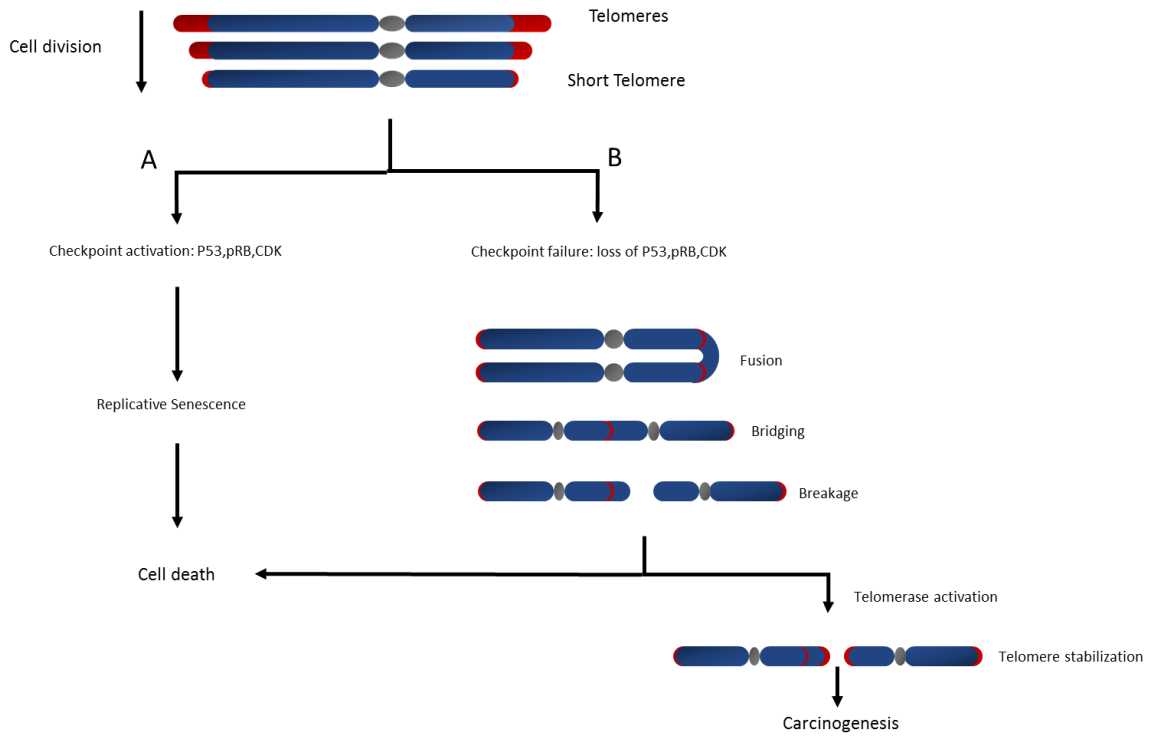

Figure 1.8. Telomere shortening and genome instability. Telomere shortening with each cell division. A) P53 and pRB activation induces replicative senescence B) if P53 is mutated or lost chromosome goes thought Breakage–fusion–bridge (BFB) cycles can occur when telomere fusion generates a dicentric chromosome. Activation of telomerase stabilizes telomere leading to carcinogenesis

5.Telomere and telomerase in cancer

5.1 Telomerase in cancer

Telomeres shorting may be a powerful mechanism to suppress tumor through proliferation arrest induced by DNA repair proteins at the damaged end to chromosome. However, loss of telomere protection can lead to telomere crisis leading to genome instability that can promote cancer progression. Telomere crisis occurs frequently during the development of human epithelial cancers, which lack telomerase when cell fail to undergo senescence (Valls Bautista et al., 2009). Cancer cells survive cellular crisis through telomere maintenance mechanisms(Barthel et al., 2017)

In telomerase negative cells, telomere shorten with every cell division eventually going through replicative senescence also known as mortality stage one (M1). This process is triggered by P53-depedent DNA damage response. However, some cells can escape M1 phase and keep dividing until they enter a state known as crisis or mortality stage 2(M2). This process occurs when there is a mutation in cell cycle check points. Telomere shortening in this stage drive genome instability due to breakage-fusion-bridge cycle eventually leading to cell death. Some cells are able to escape cell death by acquiring telomere maintenance mechanism. However, to escaping M2 is very rare human cell (about 1 in 10 million)(Shay and Wright, 2004). Linking telomere shortening to replicative senescence have been studied extensively and can be demonstrated by producing telomerase activity in telomerase-negative cells for indefinite replication. This provide clear evidence that telomere control replication.

In general tumors have shorter telomeres compared to normal tissue. Although Telomerase was reported by many to be overexpressed in different cancers, large number of cell lines studies failed to find correlation between its activity and telomeres length(Maes et al., 2007). A systematic analysis of telomere length in 18,430 samples across 31 and matching normal tissue showed

shorter telomeres in most tumors(Barthel et al., 2017). Tumors that rely on alternative telomere lengthen mechanisms have longer telomeres compared to tumors with telomerase(Barthel et al., 2017).

Several mechanisms were involved in hTERT activation. Mutation, amplification, and rearrangements of hTERT gene are most common. Advanced genome sequencing technology revealed high percentage of mutation in coding and noncoding regions in hTERT promoter in multiple cancers including melanoma(Thomas et al., 2018), hepatocellular carcinoma(Lee et al., 2017),ovarian(Pilsworth et al., 2018),Thyroid(Liu and Xing, 2016) and breast cancer(Shimoi et al., 2018). Mutation are rarely found in sarcomas because of the absence of telomerase.(Saito et al., 2016)

5.2 hTERT Promoter Mutations

Reactivation of telomerase expression occurs in the vast majority of cancer (85%) [43]. In most cases, reactivation is associated with TERT promoter mutations [44]. Mutations in the hTERT promoter are highly recurrent in cancer(Akincilar et al., 2016). Mutations in core promoter regions occurring upstream from the ATG start site at −124 bp and −146 bp are C>T transitions have been shown to increase the binding of ETS, transcriptional activator, to the hTERT promoter region in lung cancer(Jafri et al., 2016). Moreover, these mutation were found to be associated with large percent of melanomas, glioblastomas, hepatocellular carcinomas, bladder cancers, of basal cell carcinomas, cutaneous squamous cell carcinomas, thyroid cancers and oligodendrogliomas(Jafri et al., 2016).

Less frequent hTERT promoter mutation, −57 bp upstream from the ATG start site, resulting in an A>C transition [5]. Expression of estrogen exhibits a strong concordance with hTERT transcription. Mutations in the estrogen receptor (ER) binding sites of hTERT promoter dramatically reduced hTERT transcription. Kyo et al. demonstrated that the effect of estrogen was completely abrogated upon mutating E-boxes in proximal hTERT promoter(Kimura et al., 2004).

5.3 TERT Rearrangements

Chromosomal rearrangement is a mutation is a common mechanism for the conversion of normal genes into cancer genes(Stephens et al., 2009). This can result in duplication, amplification and deletion. TERT gene can also be a target of this alteration. This type of rearrangements occurs in the 5p15.33 region consistently clustered in a region 50 kb upstream of the TERT transcriptional start site without directly affecting the gene or its core promoter region(Peifer et al., 2015). High levels of TERT rearrangements identified in high-stage neuroblastoma associated with very poor prognosis(Valentijn et al., 2015).

5.4 hTERT amplifications

Gene amplification is a frequent event in tumors which results from increased copy number of specific genes(Leao et al., 2018). TERT gene is frequently target of amplification for leading to telomerase activation in malignancies(Zhang et al., 2002). Certain single nucleotide polymorphisms (SNP) contribute to TERT expression and telomerase activity. hTERT amplifications presented a substantial prevalence in lung adenocarcinoma (18%) and lung small cell carcinomas LSCC (25%), colorectal carcinoma (48%), and cervical carcinomas (88%)(Vinagre et al., 2013).

Amplifications of the hTERC gene has also been reported in multiple cancer including lung, ovarian and cervical tumours(Barthel et al., 2017). Invasive cervical carcinomas have been reported to carry extra copies of chromosome arm 3q resulting in amplification of hTERC(Heselmeyer-Haddad et al., 2005). hTERT and hTERC amplification are associated with high grade tumors. Moreover, increased hTERT copy number is associated with acquired drug resistance in breast, skin and thyroid cancer(Leao et al., 2018).

5.5 Epigenetic Mechanisms

The epigenetic process of DNA methylation is crucial in gene expression regulation. CpG sites methylation in non-coding regions by DNA methyltransferases consist of methyl group addition to on the 5-carbon of a cytosine (C) base followed by guanine (G) base(Leao et al., 2018). DNA methylation of hTERT has been investigated to assess the possible association between epigenetic modifications of hTERT and Telomerase activity.

Although DNA methylation is thought to promote gene silencing, hTERT promotor methylation has been found to be positively correlated with gene expression and activity suggesting hTERT promotor methylation affects hTERT expression different manner from other genes regulated by promoter methylation (Guilleret et al., 2002). Brain, prostate, colon, and blood tumors have shown high frequency of hypermethylation signature in a specific region upstream of hTERT core promote(Leao et al., 2018).

6. Exploiting telomere and telomerase to target cancer cells

Given the fundamental role to telomerase in cancer cell immortality, its high expression in vast majority of cancer versus low expression or non-existence in normal cell, effort to target telomere/telomerase system is continuous equally by industry and academia. Different approaches have been designed in the search for telomerase inhibitors: small-molecule inhibitors, antisense oligonucleotides, G-quadruplex stabilizers, immunotherapy and gene therapy using telomerase promoter-driven expression of a suicide gene (Arndt and MacKenzie, 2016b; Buseman et al., 2012; Harley, 2008b).

Despite the recognized relation between its expression and tumor development, there is no pharmacological inhibitor available for telomerase yet(Arndt and MacKenzie, 2016a). The effort to find an effective and specific small-molecule inhibitor has failed to date. This could be attributed to the focus on inhibiting telomerase by blocking the interaction between telomerase and telomeres overlooking the non canonical functions of hTERT. The mechanisms underlying extratelomeric activities of TERT may provide alternative approach to identify compound that directly ablate TERT transcription. Such approach can have direct effect on cell proliferation other than telomeres attrition.

G-quadruplex ligands, which stabilize the G-quadruplex structures that tend to form in the G-rich 3′ strand of telomeric DNA to block telomerase access(Shin-ya et al., 2001). The putative function of G-quadruplex structures is to protect telomere ends from nuclease attack(Bochman et al., 2012). Telomestatin (SOT-095) , a natural product isolated from Streptomyces anulatus(Shin-ya et al., 2001), is the most studied inhibitors of this class, which induces telomere stabilization(Tauchi et al., 2003). Telomestatin stabilizes the intermolecular G-quadruplex structure thereby interfering with telomerase activity (Kim et al., 2002). Although Telomestatin

was reported to decrease telomerase activity and telomeres length in leukemia cell lines(Tauchi et al., 2003), binding to non-telomeric G-quadruplex structures in gene promoters and RNA–DNA hybrids may cause toxicity in non-malignant cells(Arndt and MacKenzie, 2016b). Another well studied G4 ligand BRAC019, promotes the formation of G4 structures at the end of telomeres invitro(Read et al., 2001). Despite its low cytotoxicity, BRAC019 has not progressed to clinical trials due to low membrane permeability(Roh et al., 2013).

The unique interaction between TERC and telomeric DNA between is a rational approach to target telomerase active cells. Imetelstat is first-in-class modified oligonucleotide is a 13-mer (5′-TAGGGTTAGACAA-3′) that is complementary to nine nucleotides in the template region(Xu and Goldkorn, 2016). Imetelstat binding to TERC disrupts telomerase ribonucleoprotein assembly and enzymatic activity at telomeres. Imetelstat treated tumor cells progress to apoptosis in a telomere length-dependent manner(Asai et al., 2003). However, no change in telomeres length over the course of treatment. Additionally, Imetelstat has been studied in two telomerase-positive non-small cell lung cancer and breast cancer with no clinical benefit(Armanios and Greider, 2015). In addition, toxicities such as thrombocytopenia, lymphopenia, and neutropenia has been reported in phase clinical studies(Ding et al., 2019).

Non-competitive Small molecule BIBR1532 inhibitor has been shown to Inhibit human telomerase activity(Pascolo et al., 2002). BIBR1532 inhibits the interaction between hTERT and hTR eventually leading to telomere attrition(Pascolo et al., 2002). Although BIBR1532 has shown good result int vitro, no clinical trail available yet for this inhibitor(Gomez et al., 2016).

Tankyrase belongs to the poly (ADP-ribose) polymerase (PARP) protein superfamily that is involved in various cellular processes, including telomere length regulation(Smith et al., 1998). Telomere lengthening requires dissociation of TRF1 from the telomere for telomerase to access

the telomere (Smogorzewska and de Lange, 2004). Tankyrase inhibitors reduce the TRF1 dissociation from telomeres and prevent binding of telomerase. Although several tankyrase inhibitors such as IWR1 ,JW55 were reported to reduce telomeres length(Smogorzewska and de Lange, 2004), none of these inhibitors have entered clinical trial yet.

6.1 Is Telomerase a viable target?

Although telomere looks exciting anticancer target, perhaps direct telomerase inhibition is not the best strategy. Almost all previously mentioned therapies are based on the telomere attrition theory which constitute major challenge whereas long lag period required to observe telomere attrition ultimately cell death. This requires a continuous administration of treatment over a long period of time. The long treatment course as a consequence may allow tumor cells to adapt and find alternative pathway to maintain their telomeres intendent of telomerase. The long period of treatment may increase cytotoxicity of the telomerase inhibitors. For example, development serious hematological toxicities were reported with Imetelstat treatment in children with recurrent CNS malignancies(Salloum et al., 2016).

Tumor cells can develop resistance to therapies. Likewise, anti-telomerase cancer therapy might force telomerase activity cancer cells switch to the alternative lengthen of telomere (ALT) mechanism(Cesare and Reddel, 2008; Hu et al., 2012; Queisser et al., 2013). It has been suggested that alterations in telomere capping might facilitate the activation of ALT in human cells, most likely by allowing HR reactions at telomeres(Cesare and Reddel, 2008). The capability of tumor cells to switch from telomerase to ALT following anti-telomerase therapy is a new field to of predicting therapy failure. Both in-vitro and in-vivo studies demonstrated ALT switch after anti telomerase treatment of telomerase positive cells(Bechter et al., 2004; Chen et al., 2010; Hu et al., 2016; Xue et al., 2011). Induction of ALT after inhibiting telomerase causes ASF1 depletion, a

histone chaperone protein, strongly supports the hypothesis that ALT is a consequence of histone management dysfunction(O'Sullivan et al., 2014). Additionally, mutation ATRX/DAXX genes have been found in many ALT cancers(He et al., 2018). Concomitant inhibition of telomerase with these mutation favours the switch to ALT in telomerase positive cells (Hu et al., 2016). All these studies suggest telomerase/ALT switch is behind the failure of anti telomerase drugs. Additionally, Anti telomerase therapies may cause cell to go though telomere-based crisis therefore leading to further genome instability. With no ALT targeting drugs available yet, it could be speculated that they may exert very powerful selective pressure in ALT-positive tumors, favoring the reactivation of telomerase(De Vitis et al., 2018).

Interesting approaches have been taken by research to target telomeres and telomerase associated proteins. For example, Geldanamycin was used to target telomerase activity by inhibiting chaperone HSP90 mediated trafficking into the nucleus and block telomerase assembly. low solubility and high hepatotoxicity precluded it from progressing to clinical trails(Gomez et al., 2016). Moreover, abrogation of shelterin complex component have been studied on small interfering small RNAs levels. Recent study showed that telomere binding proteins Loss of Rap1 induces telomere recombination favoring telomeres/ Alt switch(Sfeir et al., 2010).

Despite all the hurdles telomerase targeting in cancer, it remains as the promising candidate in cancer treatment. A major challenge for telomerase directed therapy is the lag period to observe telomere shortening allowing tumor cells to grow and adapt. Therefore, more research should be invested in field and finding new strategies that cancer address both the canonical and non canonical function of telomerase providing a rapid and effective way of inhibiting telomerase.

7. Exploiting genetic approaches to selectively kill cancer cells

A major challenge in developing anti-cancer therapies is to find chemical inhibtors with high speicifty to cancer cells with no or minal effect on normal cells. Lack of specifity is the main reason behind the higher toxicty in nomal tissue which led to clinical trial termination for many of newly deveopled inhibtors. Understadning the differences between the normal tissue and cancer tissue can be beneifical in increasing the specificty to cancer cell. Indeed cancer cells accumlate mutliple mutation during cancer progression that give them different genetic makeup than normal cell. These difference can be explioted to kill cancer cell while sparing the normal cells.

Most of the recently designed anticancer therapies take the advantage of oncogene addiction phenomena to target cancer cell growth(Pagliarini et al., 2015). As the name suggest, cancer cells growth and survival can often be impaired by the inactivation of a single oncogene(Weinstein and Joe, 2008). Kinases inhibitors comprise a perfect example of oncogenic addition and therefore have been a major focus of cancer drug. However, not all tumors have a druggable gain of function genes (for example RAS and MYC) (Mullenders and Bernards, 2009)or in some cases designing selective inhibitor can be challenging as catalytic domain of some targets within the same families show high-degree homology(Hopkins and Groom, 2002; Utsugi, 2013). Due to these limitations the field of genetic interaction has received more attention in identifying drug targets.

Integrating Genetic interactions into the discovery of anticancer drugs have promising direction in the development of selective and less toxic anticancer drugs by targeting the genetic differences between cancer tissues and normal tissues. Genetic interactions can reveal information about the functional relationships between genes. A gene effect can be modified by the effect of one or several other genes often called modifier genes(Ashworth et al., 2011).These interactions

are important for delineating functional relationships among genes and their corresponding proteins, as well as elucidating complex biological processes and diseases.

An important type of genetic interaction is synthetic sickness or synthetic lethality which involves two or more gene in which the loss of either gene alone has little impact on cell viability, but the combined perpetuation of both genes results in decrease in fitness (sickness) or cell death (lethality)(Nijman, 2011).

7.1 Synthetic lethality

Synthetic lethality is defined as the interaction between two genes such that loss of the function of either gene separately results in cell survival, but loss of the function of both genes results in cell death(O'Neil et al., 2017). Synthetic lethal can be achieved chemically or genetically where a coessential gene function can be inhibited. In recent years, synthetic lethality received high attention as it provides a new perspective for therapy and may explain the sensitivity of cancer cells to certain drugs.

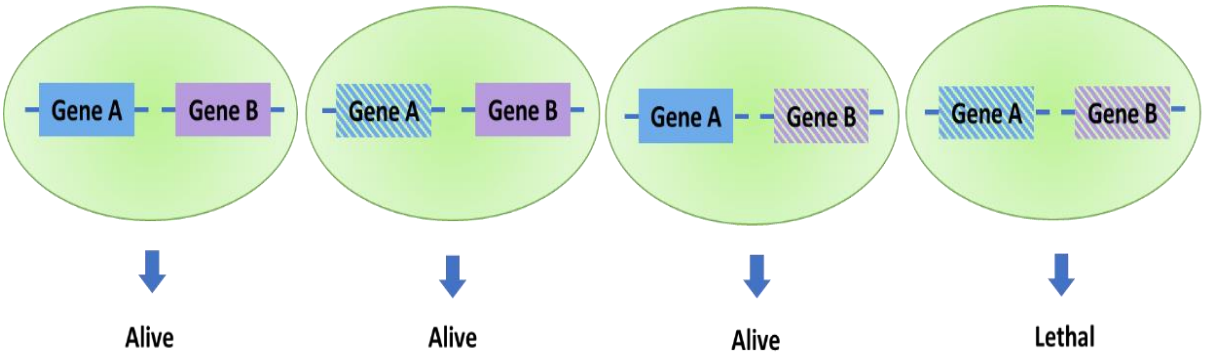

Figure 1.9.Schematic representation of synthetic lethality. Two genes are termed synthetic lethal when loss of either gene has little effect on cell viability while loss of both genes (gene A and gene B) results in decrease of fitness(sickness) or cell death (lethality).

7.2 Synthetic Dosage Lethality

Another form of genetic interaction Synthetic dosage lethality which is defined as the interaction between two genes such that inhibiting the function of one gene accompanied by overexpression of the other gene results in cell death, while sparing the wild type(Boone et al., 2007). The inhibition can be achieved by siRNA, shRNA, gRNA, or specific chemical inhibitor for the target gene. loss-of-function of one of the target gene can affect the other gene at any level such as epigenetic level. The interaction between the two genes can be predicated in which gene X can be a part of the gene Y pathway. However, SDL interactions is not always due to predicated connection between the two genes.

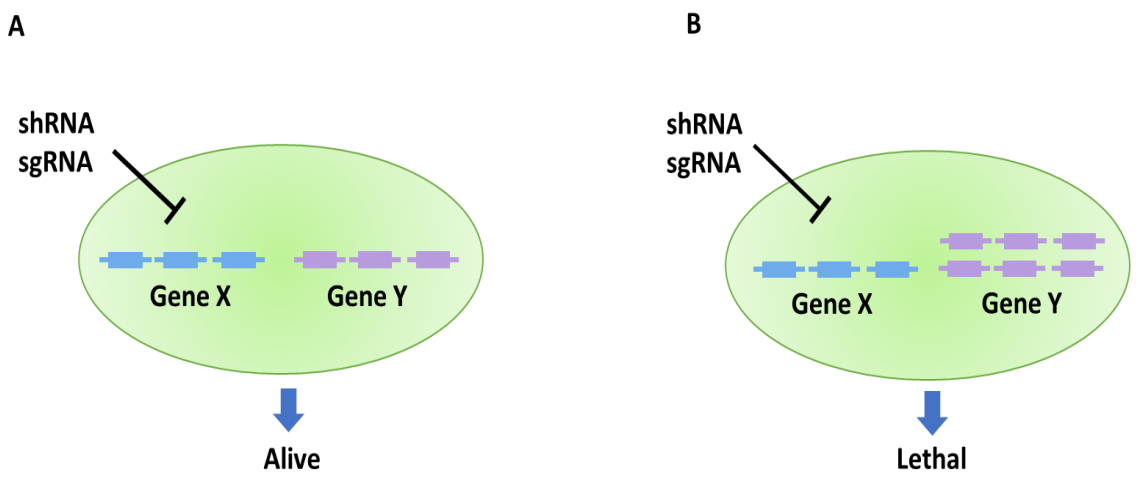

Figure 1.10. Synthetic dosage lethal (SDL): A. Cells have an normal expression or activation of gene Y (Wild Type) when gene X is inhibited by a specific drug or siRNA cell survive. **B.** Cells have overexpression or overactivation of gene Y. when are treated to inhibit gene X by a specific inhibitor or siRNA cells die.

7.3 Genome wide screening

Genome wide screen provide an unbiased approach for exploring gene function. Genome-wide screening requires no prior knowledge of pathways involved therefore; it is considered as a blind, unbiased search that requires large-scale genetic screening technology. Advanced technologies have made it possible to screen for genes involved in synthetic lethal interactions including c, siRNA, shRNA, and CRISPR-cas9 screen(Mullenders and Bernards, 2009). Loss of function screen can be performed using chemical, siRNA or CRISPR cas9 technology mainly relying on the comparison between cell lines. In genetic screens, the assessment can be done in arrayed screening format where siRNAs, shRNAs or sgRNAs are separately introduced to cells or pooled screening format where a mixture of shRNA or sgRNAs is applied to large number of cells, resulting in the individual shRNA or sgRNA per cells. Pooled screens require designing library of shRNA or sgRNA where identification of sh/sgRNA readouts is based on to determine lost

sh/sgRNA lost during the screen. The statistical difference of readouts between the cell matching cell lines is used for assessing the dropout sh/sgRNAs. Appropriate technology selection based mostly on the biological question asked.

7.4 Genome-wide screen using shRNA.

Short hairpin RNA (shRNA) is an evolutionarily conserved post-transcriptional gene silencing mediated by double-stranded RNA (dsRNA). Upon integration into the genome, the shRNA is then transcribed to pre-shRNA which is exported from the nucleus(Lee and Kumar, 2009). This pre-shRNA is then processed by ribonuclease Dicer and loaded into the RNA-induced silencing complex (RISC). The RISC aids siRNA to bind to mRNA that has a complementary sequence leading to its cleavage(Luo et al., 2008).

Pooled screens using shRNA technology have received wide acceptance due to easy of not requiring additional proteins as in CRISPR/Cas9 system. Limited validation have been shown to be a major draw back of this technology(Schuster et al., 2018).

7.5 Genome-wide screens using CRISPR–Cas9.

The clustered regularly interspaced short palindromic repeats (CRISPR/Cas) system was discovered as a form of immunity in bacteria and adapted for use in genome editing. The CRISPR/Cas9 ribonucleoprotein complex is composed of a single-guide RNA (sgRNA) that enables targeting of the Cas9 endonuclease to specific sequences in the genome, where Cas9 introduces a blunt-ended double-strand break (DSB) that then needs to be repaired.

Recently (CRISPR)/Cas9 technology became a powerful tool large-scale function-based screening(Shalem et al., 2014). The simplicity of the CRISPR/Cas9 system made it an excellent approach for targeted genome editing. In CRISPR/Cas9 system is based on introducing double-

stranded breaks into eukaryotic DNA. at target loci that are repaired through either homology-directed repair (HDR) or more often, non-homologous end joining (NHEJ)(Mali et al., 2013). As a result, loss-of-function mutations can occur as frameshifting indels occurs from the repairing process producing a premature stop codon and subsequent nonsense-mediated decay of the transcript or generate a non-functional protein. These features make Cas9 ideal for genome editing applications.

Whole genome covering CRISPR/Cas9 and shRNA libraries have been developed and are commercially available, which can be used in loss of function genetic screens. Pooled libraries contain several shRNA/sgRNA targeting the same genes. Increasing the number of sh/sgRNAs per gene is beneficial in eliminating off target effect(Schuster et al., 2019). Library presentation should be considered when conducting pooled screen. Low number of representation has greater impact on the quality and robustness of the screen introducing false positive dropouts(Joung et al., 2017a).

For both lentiviral pooled screen platforms, single-copy integration is critical for pooled screening applications to avoid off target effects(Blakely et al., 2011).This integration can be achieved through limiting number of virus particles to large number of cells available for transduction. Low multiplicity of infection (MOI) reduces the likelihood of multiple integrations per cell(Shalem et al., 2014). Subsequently, uninfected cells can be eliminated by puromycin selection. Both lentiviral screening strategies rely upon readout of the changes in abundance of hairpin over a defined period of time. Decreased number of representations of specific hairpin implies the essentiality of the gene to cell viability.

Screen endpoints is another important aspect of conducting pooled screen. Generally, population doubling time dictates the duration of the screen. However, multiple time points is more

beneficial in determining actual dropout reducing false positive results. There is a debate about the poor overlap between the shRNA screens and CRISPR/Cas9 screens. However, it is not known whether the difference is of technical or biological source. Regardless of the technique used, pooled genetic screens can help finding synthetic lethal targets that can be utilized in targeting telomerase in cancer cells with less effect on normal cells

Chapter2: Rational and Hypothesis

2.1 Research Question

Genetic interactions such as SDL are a powerful approach for revealing novel cellular targets and exploiting molecular alterations such as hTERT overexpression without directly targeting hTERT itself. Body of research has shown that hTERT overexpression is a pervasive in 80-90% of cancers and can be used as a therapeutic target, but clinical trials have not been reflective of this potential. This poses the question, is there any other way to take advantage of hTERT overexpression as a tumour-agnostic targeted therapy?

2.2 Rationale and Hypothesis

Telomerase is a proposed anti-cancer target that is a crucial for limitless self-renewal in cancer.

The potential clinical applications of telomerase-dependent anti-cancer arises from its significantly expressed in ~90 % of human cancers. Despite strong evidence showing Telomerase inhibition decreases tumour growth in pre-clinical work, no telomerase inhibitor is available in clinic yet. Small-molecule telomerase inhibitors and immunotherapeutic approaches failed clinical trial for solid tumors. This raises a question of its broader applicability as therapeutic target in cancer treatment. Because short telomeres trigger genome instability, it is extremely important to understand the prices mechanism of telomerase inhibitors.

We propose to identify potential therapeutic targets by applying a basic biological concept called synthetic dosage lethality (SDL) where overexpression of a gene is lethal when another mutation or deletion is present. Discovering SDL interactions could reveal new therapeutic targets for cancer treatment in this situation, cancer cells overexpressing hTERT

2.3 Objectives

A. Genomic-wide pooled shRNA *and* CRISPR/Cas9 screening for identification of potential hTERT SDL genes

I. Genome-wide screening for SDL using a pooled shRNA lentiviral library and an isogenic models o of hTERT overexpression, and evaluation of the potential interactions and their functions

II. Genome-wide screening for SDL using a pooled CRISPR lentiviral library and an isogenic model of hTERT overexpression, and evaluation of the potential interactions and their functions.

III. Prioritization of a subset of the potential interactions using a variety of computational analysis to evaluate SDL interactions and relevance to hTERT-overexpressing cancers.

B. Validation of the identified hits in the model cell lines on a gene-by-gene basis

C. Evaluating the targets across multiple cell lines representing different tissue types that naturally overexpress telomerase and generate a list of highly validated targets

D. Prioritize the candidate targets for animal studies

E. Evaluating the targets connection with telomerase

.

Chapter 3 Materials and Methods

3.1 Reagents

Table 3.1: Reagent used in this study

Reagents	***Source***
X-tremeGENE	Sigma-Millipore
Hexadimethrine bromide (Polybrene)	Sigma-Aldrich (St. Louis, MO, USA)
Opti-Mem	Gibco
Puromycin	ThermoFisher Scientific (Burlington, ON, Canada)
Blasticidin	Invitrogen
Fetal bovine Serum FBS	Sigma
Penicillin/Streptomycin (P/S)	HyCloneTM
Bovine Serum Albumin	GE Healthcare Life Sciences, Utah, USA
Phosphate buffer saline (P/S)	HyCloneTM
Methanol	Fisher Scientific
Ethanol	Fisher Scientific
Hygromycin B	Invitrogen
Formaldehyde	Fisher Scientific

3.2 Cell Culture

Table 3.2: cell lines used in the project with its culture medium for each cell line and supplementation

Cancer Cell lines	Culture medium
HT1080	DMEM (HyClone^{TM}) 10% FBS ,1% P/S
HT1080-hTERT	DMEM (HyClone^{TM}) 10% FBS ,1% P/S
GM00847	DMEM (HyClone^{TM}) 10% FBS ,1% P/S
GM00847-hTERT	DMEM (HyClone^{TM}) 10% FBS ,1% P/S
DLD-1	RPMI (HyClone^{TM}) 10% FBS ,1% P/S
HCT15	RPMI (HyClone^{TM}) 10% FBS ,1% P/S
ASPC-1	RPMI (HyClone^{TM}) 10% FBS ,1% P/S
MiaPaca-2	DMEM (HyClone^{TM}) 10% FBS ,1% P/S
SKOV3	DMEM (HyCloneTM) 10% FBS ,1% P/S
ES2	McCoy's 5A (HyClone^{TM}) 10% FBS ,1% P/S
MDA-MB-231	RPMI (HyClone^{TM}) 10% FBS ,1% P/S
HCC70	RPMI (HyClone^{TM}) 10% FBS ,1% P/S
22RV-1	RPMI (HyClone^{TM}) 10% FBS ,1% P/S
LnCap	RPMI (HyClone^{TM}) 10% FBS ,1% P/S
HEK293T	DMEM (HyClone^{TM}) 10% FBS ,1% P/S
PaCaDD 119	Keratinocyte Serum-Free Growth Medium (Invitrogen)
PaCaDD 135	Keratinocyte Serum-Free Growth Medium (Invitrogen)
PaCaDD 137	Keratinocyte Serum-Free Growth Medium (Invitrogen)
PaCaDD 159	Keratinocyte Serum-Free Growth Medium (Invitrogen)
PaCaDD 161	Keratinocyte Serum-Free Growth Medium (Invitrogen)
PaCaDD 165	Keratinocyte Serum-Free Growth Medium (Invitrogen)

PaCaDD 183	Keratinocyte Serum-Free Growth Medium (Invitrogen)
PaCaDD 188	Keratinocyte Serum-Free Growth Medium (Invitrogen)

Each cell line was maintained in corresponding medium in Table (3-2) All media were supplemented with containing 10 % FBS (Gibco, Life Technologies), 1 % penicillin/streptomycin (Gibco, Life Technologies) and incubated at 37°C and 5% CO2. Primary pancreatic cancer cell lines were gift from Dr. Prama Pallavi, Heidelberg University, Mannheim, Germany(Ruckert et al., 2012). All primary pancreatic cell lines were cultured in Dresden media which is a mixture of Keratinocyte Serum-Free Growth Medium (Invitrogen) and DMEM 20% FBS ratio 1:2. Incubated at 37°C 5% CO_2.

3.3 Lentivirus Production

shRNA and gRNA lentiviral particles were generated by transfecting HEK-293T cells with psPAX2, pMD2.G, and with the lentiviral vector encoding the genes of interest. Transfection took place in 10 mL of tissue culture medium with 540 µL Opti-Mem (Gibco, Life technologies) and 36 µL X-treamGENE DNA Transfection Reagent (Roche, Mississauga, ON, Canada). Medium was changed after 18 hr and replaced with DMEM containing 20% w/v bovine serum albumin (Sigma) and viral particles were collected after 24 and 48 hr. Viral harvests were pooled and centrifuged at 1000 rpm for 3 min and stored at -80C◦ for subsequent use.

3.4 Generation of Cas9 Stable Cell Lines

Stable Cas9-blast cell lines were generated by transfecting each cell line with the lentiviral cas9-blast particles. Cells were trypsinzed and counted for each cell line and seeded in a density of $1.0X10^6$ in 10 cm plate. Polybrene's final concentration of 8uG/mL was added to the cells with

Cas9 lentivirus for 24 hr. Medium was changed and blasticidin was added in concertation specific for each cell determined by the killing curve. Media with blasticidin was changed every 2 to 3 days until the uninfected cells showed complete cell death. Harvested cells cryopreserved and stored in liquid nitrogen for subsequent use.

3.5 Cell line selection protocol

Generating a stable cell line expressing a transgene of interest requires determination the minimum concentration of antibiotic required to kill non-transduced cells. Antibiotic selection typically begins 24 hr after transduction. To determine the concentration of antibiotics needed for each cell line were seeded in six-well plates at a density of $1x10^4$ cells per well. Cells were left to grow until they reach 70% confluent. Replace media on all wells with fresh media and different concentrations of selection antibiotic. One well was left as control without antibiotic added. Puromycin concentrations used were 0.5,1,2,4,6 µg/mL and 1,2,4,6,8 µg/mL for blasticidin. Cells were monitored after 48 hr until untransduced cells die. The lowest concentration that causes 100% cell death was used as the for selection.

3.6 Bacterial transformation

Plasmid DNA was transformed as stated in the manufacturer's protocol of the DH5α Competent Cells (ThermoFisher Cat. No. 18265017). Two µL (1 ng) of plasmid DNA was added to 1 µL of the competent cells in a centrifuge tube and gently mixed. The mixture was incubated on ice for 20 min. The mixture was heat-shocked at 42°C for 45 seconds and returned into ice for 2 min for the bacteria to absorb the plasmid. Two hundred µL of LB medium without antibiotic was added to the mixture and incubated at 37°C for 40 min at 225 RPM. Fifty µL of the bacterial cells were then streaked on LB agar plate with an appropriate antibiotic and incubated at 37°C for

overnight. An individual colony from the agar plate was inoculated into 5 mL of LB medium supplemented with an appropriate antibiotic (Ampicillin) and incubated, grown at 37°C for overnight at 225 RPM. Plasmid DNA was purified from the bacteria for downstream experiments.

3.7 Bacterial Plasmid Purification

DNA purification was performed as per the manufacturer's protocol (Qiagen). In brief, bacterial culture was spun down at 10,000 x g for 10 min, and the supernatant was discarded, leaving behind the bacterial pellet. The pellet was resuspended, and lysis buffer was added and incubated for 5 min at room temperature. Neutralization buffer and left on ice for 15 min. Then, the mixture was centrifuged at 16,000 x g for 10 min. The supernatant was transferred to the binding membrane pre-equilibrated column and left to pass through the column. The flow-through was discarded. The binding membrane was washed twice with washing buffer. The column was placed in a new centrifuge tube, and elution buffer was added to get eluted DNA. The eluted DNA was then washed with isopropanol and centrifuged at 16,000 x g for 30 min. The DNA pellet was collelec70% ethanol and t centrifuged at 10,000 g for 10 min. the pellets were resuspended with TE buffer and measure the concentration of the DNA. The DNA was stored in -20 freezer for subsequent use.

3.8 Pooled Screening

3.8.1 Determination of Multiplicity of Infection

The volume of lentivirus used in the screen was determined by multiplicity of infection (MOI). Cells transduction at a low MOI to ensure that most cells receive only one stably integrated RNA guide. MOI was done in cell lines, HT1080, HT1080-hTERT, GM00857, GM00847-hTERT, cells were infected with 0, 0.25, 0.5, 0.75, 1.0, 2.0, 4.0, or 8 mL of the 90K lentiviral

*sh*RNA library in 15 cm tissue culture dishes. 8 μg/mL of polybrene was added to each plate. After 24 hr, media was removed and replaced with fresh medium containing 2 μg/mL puromycin except for the control. Each cell line was incubated for 48 hr after the addition of the puromycin medium. After the selection was done cells were counted for each concentration and the number of living cells with each volume of the lentivirus was compared to the corresponding control in order to determine the percentage of survival. The percentage of survival, therefore, indicated the percentage of cells that were successfully transduced and acquired puromycin resistance. The viral volume resulting in 30- 40 % survival indicates a multiplicity of infection (MOI) of 0.3-0.4.

CRISPR Cas9 MOI was done using CRISPR lentiCRISPR v2 library (Source) using the same concentration and conditions as mentioned above in the shRNA MOI. The viral volume resulting in 30- 40 % survival indicates a multiplicity of infection (MOI) of 0.3-0.4.

3.8.2 Pooled shRNA screen

HT1080-Parental and HT1080-*h*TERT cells were transduced with 90K lentiviral shRNAs at a density of 1.80x108 from the RNAi Consortium lentiviral library (Sigma-Aldrich) in 15 cm tissue culture dishes at MOI of 0.3-0.4. Cells were transduced in the presence of 8 μg/mL polybrene. After 24 hr, media was removed and replaced with fresh DMEM containing 2 μg/mL puromycin to eliminate uninfected cells. Cells were incubated in the presence of puromycin for 48 hr before being collected and divided into 3 replicates of 1.8×10^7 cells per cell line. This was time point zero (T0) of the screens, and in addition, 3 tubes of 2×10^7 cells from each cell line were pelleted and frozen for T0 genomic DNA. After 6 doublings, cells were harvested and pelleted a total of 100×10^7 cells for T6 time point and 8×10^7 were seeded again in fresh DMEM medium the final harvest was on after 12 doublings where all cells were collected and pelleted for T12 time point. T0, T6 and T12 harvest of the infected cells were used for genomic DNA isolation and

shRNA library preparation. GM847-Parental and GM847-*h*TERT shRNA screens were done similarly.

3.8.3 Microarray probe preparation

DNA microarray-based method employs PCR-amplified shRNA template sequence pools. Genomic DNA was amplified by large-scale PCR. Each 50 µl reaction contained 800 ng template gDNA, 200 µM dNTP, 0.5 µM primers, 1.5 µl DMSO and 1-unit Platinum Pfx polymerase (Invitrogen).

PCR_F	5'- Biotin-AATGGACTATCATATGCTTACCGTAACTTGAA-3'
PCR_R	5' TGTGGATGAATACTGCCATTTGTCTCGAGGTC-3'

The master mix was divided into 50 µL aliquots for PCR. PCR was performed at 98 °C for 3 min, followed by 30 cycles of (98 °C for 10 sec, 55 °C for 15 sec, 72 °C for 15 sec) 72 °C for 5 min, then cooling to 4 C. The Parallel reaction products were pooled and purified using the QIAquick PCR Purification Kit (Qiagen) according to the manufacturer's instructions. Purification was done immediately to avoid conversion of linear *sh*RNAs to cruciform structures. The resulting amplicons were digested into half-hairpins with XhoI (New England Biolabs, Whitby, ON, Canada) by mixing 120 µL of PCR product with 10x NEB buffer 2 (New England Biolabs) and 100x BSA and the reaction was carried out at 37 °C for 2 hr, followed by 65 °C for 20 min, then cooling to 4 °C. The digested product was then purified using low-melting agarose. The quantity one the final product was assessed using Nanodrop spectrophotometry (Thermo).

3.8.4 Microarray Hybridization

Hybridization of the hairpins was carried out on UT-GMAP 1.0 microarrays (Affymetrix Inc, Santa Clara, CA, USA). Microarray Washing was carried out in GeneChip Fluidics Station 450 (Affymetrix) according to the manufacturer's instructions using the FlexFS450_0001 protocol. Briefly, hybridization mixture was prepared for each sample containing 66 µL of 2x hybridization buffer (Sigma), 1.32 µL of 50 mg/mL BSA, 1.32 µL of 10 mg/mL herring sperm DNA (Invitrogen), 1.3 µL of 5 nM B213 (Sigma), 1.38 µL of spike-in controls (Sigma), 25 µL of 20 µM blocking oligo mixture (Sigma), and 13.2 µL DMSO. The hybridization mix was added to 28.5 µL containing water and 2 µg of purified probe sample. The hybridization mix was incubated at 99 °C for 10 min, followed by incubation at 40 °C for 5 min, and then centrifuged at 15,000 xg for 5 min. The hybridization mix was then added to the preconditioned microarray and the microarray was incubated in the hybridization oven at 40 °C for 24 hr at 60 RPM. Microarray Scanning was done using a GeneChip Scanner 3000 (Affymetrix). CEL files generated were read using the Saskatchewan Cancer Agency differential essentiality mapping system (SCADEMS) in order to determine individual *sh*RNA probe intensities.

3.8.5 Microarray Deconvolution and Scoring of shRNA Dropout

Microarray scanning was carried out using a GeneChip Scanner 3000 (Affymetrix). The generated CEL files were read using the Saskatchewan Cancer Agency differential essentiality mapping system (SCADEMS) (http://homepage.usask.ca/~frv603/scadems.php) to determine individual *sh*RNA intensities for scoring calculations.

For each *sh*RNA, the microarray signal intensity was converted to log2 scale for each time point of each replicate of each population ($hTERT^{-low}$, $hTERT^{-high}$). Hairpins with a log2 barcode signal below 8 at T0 were considered background noise and discarded. Hairpins with a fold change

≥ 1.25 at one time point relative to the previous time point were also discarded. For each replicate, the weighted differential cumulative change (WDC) fitness score between the TERT^{-low} and TERT^{-high} populations were calculated for each time points relative to the corresponding previous time point for each individual hairpin using the formula as done previously(Paul et al., 2016):

$$DCC = \sum_{t=1}^{T}(x_{t,k}^{pc3} - x_{t-1,k}^{pc3}) - \sum_{t=1}^{T}(x_{t,k}^{w} - x_{t-1,k}^{w})$$

Where X is the signal intensity for the indicated sample at timepoint t and replicate k and α is a small constant. The WDC fitness score calculation for each individual gene was performed by taking the two lowest hairpin WDC values for each gene in the following formula:

$$WDC_{Gene} = arg\frac{WDC_{g,h} + WDC_{g,h'}}{2}$$

Where h and h' are the individual hairpins for gene g.

Finally, the p-value for the WDC scores was calculated using a permutation performed by randomly shuffling the WDC scores. This process was repeated to construct an empirical distribution of the WDC fitness scores over all of the genes was constructed, and then used in the following formula:

$$p - value = \frac{1}{NL}\sum_{r=1}^{NL} I(WDC_{Random} < WDC_{Gene})$$

Where N is the number of genes, L is the number of repeats performed in the construction of the empirical distribution, and I is a binary indictor where when WDC Random < WDC Gene is true, I = 1, and when WDC Random < WDC Gene is not true I = 0.

All genes with a negative WDC fitness score and a p-value < 0.05 were considered *TERT* screen hits.

3.8.6 Precision Recall Analysis

For comparison to an established set of essential and non-essential genes, a Bayes factor was calculated based on the raw microarray intensity signal from all timepoints in all replicates by the following formula(Hart et al., 2014a):

$$Bayes\ factor = \prod_{i,j} \frac{\Pr\left(fc_{i,j}|essential\right)}{\Pr\left(fc_{i,j}|non-essential\right)}$$

Where Pr is a density function of the fold-changes of all hairpins targeting essential (or for non-essential) genes in the training set was estimated by Gaussian kernel density estimation using the scipy stats gaussian_kde function in Python, across hairpin observations i and timepoints j.

Genes were ranked ordered by the Bayes factor value to get a Bayes factor score. True positives were determined as the number of genes in the essentials test set with a Bayes factor score greater than the current gene, and false positives as the number of genes in the non-essential test set with a Bayes factor score greater than the current gene(Hart et al., 2014b) .The true and false positives were used to calculate precision and recall in the following formulas:

$$Recall = \frac{true\ positives}{(total\ essential\ genes)}$$

$$Precison = \frac{true\ positives}{(true\ positives + false\ positives)}$$

Finally, the F-measure was then calculated by the formula, where an F-measure > 0.75 indicates satisfactory identification of the reference essential and non-essential genes:

$$F - measure = 2 \times \frac{precision \times recall}{precision + recall}$$

3.8.7 Pooled CRISPR screen

HT1080-Parental-Cas9, HT1080-hTERT-Cas9, GM00847-Parental-Cas9, and GM00874-hTERT-Cas9 cells were transduced with CRISPR library lentiviral in 15 cm tissue culture dishes at a MOI of 0.3-0.4 of the correspondent cell line. Cells were transduced in the presence of 8 μg/mL polybrene. After 24 hr, media was removed and replaced with DMEM containing 2 μg/mL puromycin to eliminate uninfected cells. Cells were incubated in the presence of puromycin for 48 hr then collected and divided into 3 replicates of 1.2 x 10^7 cells per cell line, passaged every 3 days, and maintained at 200-fold coverage. This was time point zero (T0) of the screen. After 6 doublings, cells were harvested and pelleted a total of 1 x 10^7 cells for T6 time point and 1.2 x 10^7 were seeded again in fresh DMEM medium the final harvest was on after 12 doublings where all cells were collected and pelleted for T12 time point. T0, T6 and T12 harvest of the infected cells were used for genomic DNA extraction. and CRISPR library preparation. GM847-Parental-Cas9 and GM847-hTERT-Cas9 CRISPR screens were done similarly.

3.8.8 CRISPR library preparation

CRISPR library preparation for next-generation sequencing (NGS) was generated by a two-step PCR. The first PCR was used to amplify the sgRNA region utilizing primers recognizing constant lentiviral integration sequence and a second PCR adds Illumina i5 and i7 sequences as well as barcodes for multiplexing directly in front of the variable 20 bp sgRNA sequences. For the first PCR, the amount of genomic DNA (gDNA) for each sample was calculated in order to achieve 200X coverage over the GECKO library, which resulted in 90 μg DNA per sample. For each sample, we performed 12 separate 100 ul reactions using Platinum™ Pfx DNA Polymerase

(Invitrogen) and then combined the resulting amplicons. Primers sequences to amplify lentiCRISPR sgRNAs for the first PCR are in the table below.

10x PCR Amplification Buffer	240 uL
10x PCRx Enhancer Solution	240 uL
10 mM dNTPs	36 uL
20 uM Primer Mix	54 uL
50 mM $MgSO_4$	24 uL
Platinum™ Pfx DNA Polymerase	18 uL
DNA Template	X uL
DNAase-free ddH_2O	588-X uL
Total reaction volume	1200 uL

The PCR was carried out by denaturing once cycled at 98C for 30s and 24 cycles of (98°C for 1s, 62°C for 5s, 72°C for 35s) and 72°C for 1 minute then cooling to 4 °C.

After the first PCR is completed the content of the 12 PCR tubes were pooled together and ready for the second PCRA second PCR was done to attach Illumina adaptors that gives each sample unique barcode. The second PCR was done in a 100 ul reaction volume using 5ul of the product from the first PCR. Primers for the second PCR include both a variable length sequence to increase library complexity and an 8bp barcode for multiplexing are in the table 3.3.

The component assemble for the second PCR in 100uL volume using 20ul of 10x PCR Amplification Buffer, 20uL of 10x PCRx Enhancer Solution, 3ul of 10mM dNTPs ,4.5 uL of 20 uM Primer Mix, 2uL of 50mM $MgSO_4$, 1.5 uL of Platinum™ Pfx DNA Polymerase 5uL of DNA (amplicon from the first PCR) 49uL of ddH_2O .The amplification PCR reaction was carried out by denaturing once at 94 °C for 5 min, followed by 20 cycles of (94 °C for 15 sec, 63 °C for 30 sec, 72 °C for 23 sec) 72 °C for 5 min, then cooling to 4 C. A test sample of PCR product (178 bp) was run on a 2% agarose gel to ensure that amplified *sh*RNAs did not form into cruciform structures (370 bp). The entire amplicon form the second PCR was run on a 2% low melting

agarose gel using the taped combs using low range sm1203(ThermoFisher) ladder with 6x orange DNA loading dye. Bands were excised of expected 370 bp band on a UV Transilluminator.

Product quantity and quality were evaluated using Qubit fluorometric quantification (Qubit 3.0 and dsDNA high-sensitivity assay; Thermo Fisher Scientific) and Bioanalyzer gel electrophoresis (section 3.8.10).

Table 3. 2 CRISPR library sequencing primers supplementation

First PCR primers	
F	*AATGGACTATCATATGCTTACCGTAACTTGAAAGTATTTCG*
R	*CTTTAGTTTGTATGTCTGTTGCTATTATGTCTACTATTCTTTCC*
Second PCR Primers	
F1	*AATGATACGGCGACCACCGAGATCTACACTCTTTCCCTACACGACGCTCTTCCGATCTTAAGTAG AGTCTTGTGGAAAGGACGAAACACCG*
F2	*AATGATACGGCGACCACCGAGATCTACACTCTTTCCCTACACGACGCTCTTCCGATCTATACACG ATCTCTTGTGGAAAGGACGAAACACCG*
F3	*AATGATACGGCGACCACCGAGATCTACACTCTTTCCCTACACGACGCTCTTCCGATCTGATCGC GCGGTTCTTGTGGAAAGGACGAAACACCG*
F4	*AATGATACGGCGACCACCGAGATCTACACTCTTTCCCTACACGACGCTCTTCCGATCTCGATCAT GATCGTCTTGTGGAAAGGACGAAACACCG*
F5	*AATGATACGGCGACCACCGAGATCTACACTCTTTCCCTACACGACGCTCTTCCGATCTTCGATCG TTACCATCTTGTGGAAAGGACGAAACACCG*
F6	*AATGATACGGCGACCACCGAGATCTACACTCTTTCCCTACACGACGCTCTTCCGATCTATCGATT CCTTGGTTCTTGTGGAAAGGACGAAACACCG*
R1	*CAAGCAGAAGACGGCATACGAGATAAGTAGAGGTGACTGGAGTTCAGACGTGTGCTCTTCCGAT CTTTCTACTATTCTTTCCCCTGCACTGT*
R2	*CAAGCAGAAGACGGCATACGAGATACACGATCGTGACTGGAGTTCAGACGTGTGCTCTTCCGAT CTATTCTACTATTCTTTCCCCTGCACTGT*

R3	*CAAGCAGAAGACGGCATACGAGATCGCGCGGTGTGACTGGAGTTCAGACGTGTGCTCTTCCGATCTGATTCTACTATTCTTTCCCCTGCACTGT*
R4	*CAAGCAGAAGACGGCATACGAGATCATGATCGGTGACTGGAGTTCAGACGTGTGCTCTTCCGATCTCGATTCTACTATTCTTTCCCCTGCACTGT*
R5	*CAAGCAGAAGACGGCATACGAGATCGTTACCAGTGACTGGAGTTCAGACGTGTGCTCTTCCGATCTTCGATTCTACTATTCTTTCCCCTGCACTGT*
R6	*CAAGCAGAAGACGGCATACGAGATTCCTTGGTGTGACTGGAGTTCAGACGTGTGCTCTTCCGATCTATCGATTCTACTATTCTTTCCCCTGCACTGT*

3.8.9 Sequencing and Scoring of sgRNA Sequences

The *sg*RNA sequences were PCR amplified from the genomic DNA using primers targeting the surrounding *sg*RNA scaffolding region and illumina barcode ligation was done as describe previously (see section (3.8.7) CRISR Library preparation for details). Samples were sent to Applied Biological Materials for Illumina next-generation sequencing (NGS). Individual *sg*RNA read counts were analyzed using same analysis method as the pooled genome-wide screen. (Section 3.8.4 and 3.8.5)

3.8.10 Quality assessment of CRISPR library using a Bioanalyzer

CRISPR library was quality controlled using the Bioanalyzer 2100 with DNA High Sensitivity chip (Agilent). This step was done to monitor size distribution after fragmentation and adapter ligation and detection of artifacts post-PCR amplification. The procedure was carried according to manufacturer protocol. Preparing the Gel-Dye Mix was done by Pipetting 25 µL of the dye concentrate into DNA gel matrix vial. The mixture was transferred to spin filter and spinned for 15 min at room temperature at 2240 g. the gel-dye mix was allowed to equilibrate to room temperature for 30 minutes before being loaded into a Bioanalyzer DNA 1000 chip. 5 µL of DNA marker was loaded into the chip to allow fragment size determination. 1 µl of 500 pg/µl of

each sample was applied to the chip. A sharp peak was expected for a pure library sample. Presence of multiple peaks and/or broad peak larger than the expected library suggested formation of a heteroduplex.

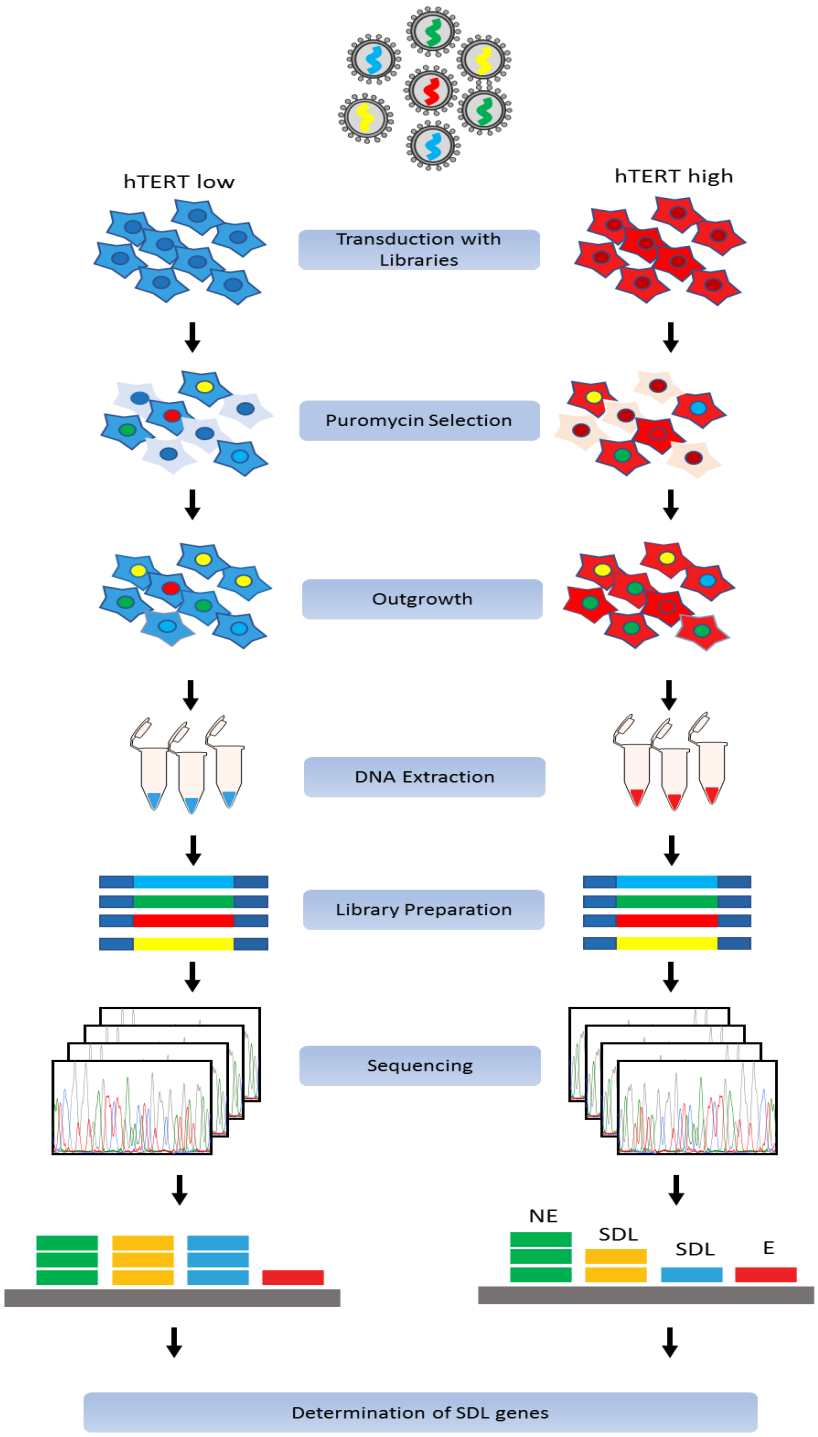

Figure 3. 1 Genome-wide pooled screening for SDL. Schematic of the methodology of genome-wide screening for hTERT$^{-low\ versus}$ hTERT^{-High}. SDL genes identification is based on sequences that dropped out of the hTERT^{-High} population at higher levels than in the hTERT^{-low} population. Example signals labelled with SDL, or E for essential gene, or NE for non-essential gene.

3.9 Gel electrophoresis

One % of the agarose powder was melted in Tris/Borate/EDTA (TBE) buffer (0.5 g/50 mL) in an Erlenmeyer flask using the microwave. 5 µL of the Syber green (sybersafe) was added into the agarose liquid. At moderate temperature, agarose was poured 29 out into the gel tank (Bio-Rad Cat.1704467), and a comb was placed at the (-) electrode for creating the wells for loading the samples. After 15 min, the samples were run at 120 V for an hour. The gel was then visualized and captured using Gel Doc™ XR+ Gel Documentation System (BioRad).

3.10 DNA gel extraction

DNA Gel extraction was done using QIAquick Gel Extraction Kit (Qiagen, Germany) DNA bands were visualized on top of a gel bright illuminator box. Individual bands of interests were excised and trimmed from any gel excesses using a new and clean blade and placed into an individual centrifuge tube. 3 volumes of the dissolving gel buffer were added to the gel inside the tube and incubated at 50°C for 10 minutes or until the gel is dissolved completely. The melted gel slice was allowed to go through the binding membrane of the column and centrifuged for 30 seconds. The binding membrane was then washed with 700 µL of the washing buffer and centrifuged for 3 minutes. The elution buffer was preheated at 50°C, and 6 µL was added to increase the DNA yield.

3.11 Genomic DNA Extraction

Frozen cell pellets from the pooled screen were thawed, resuspended in 4.5 mL PBS, and vortexed thoroughly. Genomic DNA was then extracted from the cell suspensions using the QIAamp DNA Blood Maxi Kit (Qiagen, Toronto, ON, Canada), according to the manufacturer's

instructions. Following elution in buffer AE (Qiagen), the eluted DNA solution was made up to 500 µL with the addition of water. 20 µL of 5 M NaCl (Sigma) was added to the DNA, followed by 1 mL of -20 °C 96 % ethanol. Tubes were mixed by inversion, and centrifuged for 15 min at 15,000 xg and 4 °C. The supernatant was aspirated, and the DNA pellet was washed by the addition of 500 µL of -20 °C 70 % ethanol and subsequent inversion. Tubes were centrifuged for 10 min at 15,000 xg and 4 °C, followed by aspiration of the supernatant and air-drying for 5 min. DNA pellets were resuspended in 10 mM Tris-HCl pH 7.5 for a final concentration of 400 ng/µL and heated for 1 hr at 50 °C. Extracted genomic DNA was stored at -20 °C until the probe preparation.

3.12 Genome editing

Genome editing was done using GeneArt® Genomic Cleavage Detection Kit (Thermofisher, Carlsbad, CA 92008 USA). The locus being investigated for the gene of interest were amplified by PCR. primers designed with Tm >55°C., a length of 18–22 bp and have 45–60% GC content. Primers designed to amplify a length of approximately 600 bp upstream the gRNA and approximately 300 bp downstream the gRNA. Cell infected with gRNA of interest were collected and spun down at 200g. Cell pellets were resuspended in 50 µL cell lysis buffer with 2 µL Protein degrader in an Eppendorf tube. Resuspended pellets were transferred to a PCR tube and run the following program in a thermal cycler 68°C for 15 min 95°C for 10 min then 4 °C. 2 µL of cell lysate were mixed with, 1 µL of 10 µM F/R primer mix and 25 µL AmpliTaq Gold® 360 Master Mix Volume was completed to 50 µL with water. The amplification PCR reaction was carried out by denaturing once at 95 °C for 10 min, followed by 40 cycles of (95 °C for 30 sec, 55 °C for 30 sec, 72 °C for 30 sec) final extension at 72 °C for 5 min, then cooling to 4 °C. the product was verified by running 3 µL of the PCR product on 2% agarose gel. The product from the first PCR was run denaturing and re-annealing reaction using the following

program 95°C for 5 min, 95°C–85°C –2°C/sec, 85°C–25°C, –0.1°C/sec and then cool down at 4°C. The heteroduplex DNA generated from the previous step was cleaved by adding 1 µL of detection enzyme followed by incubation for 1 hr at 37°C. the final product was run 2% agarose gel and imaged using imager (ChemiDoc MP Imaging System, Biorad).

Table 3.3 :List of Primers used in gemone editing assay

Gene	Primer Sequence	Gene	Primer Sequence
PCDHB16-F1	GCAGTGTCTACTCATAGTGT	DSCC1-F1	ACAGGGTGGAGGGATATAAC
PCDHB16-R1	TGAGAGCTTGGGCTGATTTT	DSCC1-R1	GCGCTTTCAAACGCTCAGGT
SH3GL3-F1	CAACCAGAAAGTCCAGGAAT	DSCC1-F2	CAAACTCCTGAGGTCCGACA
SH3GL3-R1	AACCTTTGCTCAGTGCTCTC	DSCC1-R2	GGGCAGAGGCAGCATCAAAA
SH3GL3-F2	TCAGCAATGTGCCCCATCAT	CPA6-F1	ACCTAGACCAAACCCCTGGT
SH3GL3-R2	CAACAGAGTTTAATTGGGCC	CPA6-R1	ACCCCGTCTCTACTAAGAGG
CGRRF1-F1	ACACTATGAGAGTGGTAGGT	CPA6-F2	CATGAAGTGACCCTGGACTT
CGRRF1-R1	TTTCCCGGTCATCCTCATCA	CPA6-R2	CACTCTTCCATTGTGCTTCC
ARHGAP15-F1	TCTGGGGTCTGTTTTGCTCT	PRKRA-F1	CCCCAGTCCCAACTTAGCTA
ARHGAP15-R1	GTAGAGGCCCTTAAAATGAG	PRKRA-R1	CCTCTGCCTGCTTCTTCAAA
ARHGAP15-F2	GGGGGCGCTGTAAAACAATT	MED14-F1	GGGGGGACATAGTTGACCCC
ARHGAP15-R2	GAGAAATCTTTGTGGCAAGG	MED14-R1	GTGTTATGCCCTTCACACCT
TSPAN9-F1	GACTGCCTCCTTTCTCCATC	MED14-F2	GGTTGTGGAGATGTTGGAGG
TSPAN9-R1	CCACTGCCATCTCTGGTCAT	MED14-R2	CCCAGAATCTGGAATCAGAG
GCN1L1-F1	AGCTAGGGTGTTATTAGTCC	KMT2E-F1	CATGTTGATACCAGTACTCC
GCN1L1-R1	CCCATCTCTTGGCACTGACA	KMT2E-R1	ATTCTCACTCTCCTGCCTCT
LRRFIP1-F1	GTGCTGAGAAGTGACTGGAC	KMT2E-F2	TTCTGGGATTACAGGCAAGA
LRRFIP1-R1	TCAGACCCTGAACATTTTGG	KMT2E-R2	CATTGAGAGCAGAGTTCAGT
LRRFIP1-F2	GGAGTTCCTCACACACAAGG	PLK1-F1	GACAACCCACAAGTCAGTAT

LRRFIP1-R2	GCCATTGATGGTGCACTACA	PLK1-R1	TTTCAGACACAGGCCCTCTC
PLK4-F1	TGAACTGTGATCATGCCACT	BCAS4-F1	TGAGTAGAGACGGGGTTCTG
PLK4-R1	GCAGCTTGGGATGTAGGAAA	BCAS4-R1	GGCTCCTCTGCGGAATAAAA
PLK4-F2	TGCATGTAAGCGGGGGGATA	BCAS4-F2	CTGATATCAGTGATCAAGGG
PLK4-R2	CATGCCACCACACTCAACTA	BCAS4-R2	ACCTGGCCTGGAAACAAATT
PACSIN1-F1	GCCTCTATGCATTGTGTCTT	PMVK-F1	AGAGTAACCTCTCCTGCCTT
PACSIN1-R2	ACACCTGCTCCATGTTCTCC	PMVK-R1	GGTCAGTCTGGCTACTGTGT
SNRPC-F1	GATGACTGTTCCTCTTTGGT	WDR61-F1	CACATCCTTGCTAACACTTG
SNRPC-R1	TCTTAGATCCACACTTGGGA	WDR61-FR1	AGCTATGATCACACCACTGC
NEK2-F-1	CAAAGGGAACCAAGGAAAG	WDR61-F2	TGGGGAGATGAGAGCAGTCT
NEK2-R1	ATAGTGACATGCACCTGTAG	WDR61-R2	GCATTTAAAGGCTGTGGGGC
PCYOX1L-F1	TATCCTAGCTGCCTATCCAC	BIRC5-F1	CCTTAATCCTTACAGTGGGC
PCYOX1L-R1	AGGGAGACCATTACTGGACC	BIRC5-R1	CAATGTGGTGAAACCCCATC
PCYOX1L-F2	TGGGCAACATTTCAAAGGCC	FANCA-F1	CAGGCTCACCCACAGTTATC
PCYOX1L-R2	GTCCCAGAATCAGGCAGGAT	FANCA-R1	GGAGCTGTGACAGCTCACAC
SEPT4-F1	AGAGAAGATTGGCGCTGGGT	FANCA-F2	GCTGAGGCAGGTGAATCACA
SEPT4-R1	AGGAAATGCCGGTGGCTGTT	FANCA-R2	ACAGGAAGATGACGAGTGAC
RRM2-F1	CGGGAGATTTAAAGGCTGCT	PRPF19-F1	AACTCCCTCACTGCATCACT
RRM2-R2	TCACGCCTGTAATCCCAACA	PRPF19-R1	GTCATGCTGCACAGCTTCAC
PPARGC1B-F1	GCCCAGAGGTGCTAAGTATG	BUB1B-F1	GATGCATTCAATGGTAGGCA
PPARGC1B-R1	CTAGGTGGGAAAGGTTAAGT	BUB1B-R1	GCTTATCACTGCCCCCTGTA
TOP2A-F1	ATGGGAAGATGTGCCACCCT	BUB1B-F2	GTCGGGATTACAGGCATCAG
TOP2A-R1	TGAGCTCCAGTATTTTGAGC	BUB1B-R2	GCGATCAATCTTAAAAGGGC
TOP2A-F2	GTTTGAGATGGAGTTTCGCC	LMNB1-F1	TACAGTTGTGCAGTCATGGC
TOP2A-R2	AGGCTGATAGCAGCATCATC	LMNB1-R1	CGGTAACAGCTTGAGTTCTC
MET-F1	CAGCTACTCAGGAGGCTAAT	PKMYT1-F1	GCTCCCTCCACATTTGACTT
MET-R1	ATTTCTGGCCTCTTCTCTTC	PKMYT1-R1	CAGGTTACACAAAGTGGCTC
ABCA3-F1	ACCATGTTGGCCAGGCTTGT	FTSJ3-F1	GACCATTATGTACCTCTCCT

ABCA3-R1	TAGTGATGCGGGAAGAAGCA	FTSJ3-R1	TAAATCAAAAGGCTCAGGCC
ABCA3-F2	AACTCCCACTGTGAGTGCTG	IPO13-F1	GAGGTACTGGGGATTAAGAT
ABCA3-R2	TGTCACCAAGATCCCCTTGG	IPO13-R1	TGAAGGCCTTTTATACTGCC
RTTN-F1	GTCAGTATGAAAGGGAGCAC	DNHD1-F1	TGCCTACAGGAGCGAGTACA
RTTN-R1	AGAGGAGGGGAAAAAGGTC	DNHD1-R1	ACTGGAGAAAAACCTCACAG
RTTN-F-2	TGACCTTACGGTCTTCAAGT	DNHD1-F2	GTACAGTGAGCTGAGATCGT
RTTN-R2	TGTGGCACAAGAATCGCTTG	DNHD1-R2	AAGTGACAGAACCATGGGGT
AHNAK-F1	ATCAGGGTGGTTGGTACCCA	ACSF3-F1	CTGAGGGAGGGTAAAGCATC
AHNAK-R1	AGCACAGCCACATGTCACAC	ACSF3-R1	TTCCTGCAGGGGAATCATGC
HLA-A-F1	TGTTCTAAAGCCCGCACGCA	CAMK2D-F1	GGGTGACCTGAGTAAATAAG
HLA-A-R1	TTCTCCAGGTATCTGCGGAG	CAMK2D-R1	GAGAACCACTCATGACATCA
UBE2G2-F1	GCTGCTTGACTCTTAACCTT	CAMK2D-F2	ACCACATCCCTTCTTAAGTC
UBE2G2-R1	GCATAACCCCTTCTGAGCAC	CAMK2D-R2	TTCAAGACCAGCCTGGCCAT

3.13 Western Blotting

Cells were rinsed with ice-cold PBS and lysed using lysis RIPA buffer containing. Cell debris was removed by centrifugation. lysates were then resolved using SDS-PAGE, followed by transfer to nitrocellulose membranes (Amersham, GE Healthcare Life Sciences). Membranes were blocked with 5 % non-fat dry milk in 0.1 % PBS/Tween-20 for 1 hr and incubated overnight with primary antibodies at 4 °C. After incubation with primary antibodies, membranes were rinsed 3 times with PBS or TBS, incubated for 2hr with secondary antibodies at room temperature. After washing three times with TBST, the protein bands were visualized using ECL Western Blotting chemiluminescent substrate (Thermo Scientific, 34077) and ChemiDoc MP Imaging System (BioRad).

Table 3.4: Primary antibodies used in this study

Cas9 (Anti-CRISPR-Cas9 antibody)	ab204448 (abcam)
TERT (Anti-Telomerase reverse transcriptase antibody)	ab183105
GAPDH	SC-47724 (Santa Cruz Biotechnology

3.14 RNA Extraction and quantification

RNA extraction was done using PureLink™ RNA Mini Kit as per manufacturer protocol. Briefly, an appropriate number of cells (approximately 106 cells) were suspended, vortexed and homogenized with 0.6 mL lysis buffer. Equal volume 70% ethanol was added to the cell homogenate. Sample was transferred to spin cartage and centrifuged at 12,000 x g. spin cartridge was washed twice with washing buffer. RNA was eluted from the spin cartridge using RNAase-free water and centrifuged at 12,000 x g for 2 min. RNA concertation was measured a Nanodrop 2000 Spectrophotometer (Thermo Scientific, Logan, UT) and stored in -80^{0}C for subsequent use.

3.15 Real-time RT-PCR

For reverse transcription reactions, the High-Capacity Reverse Transcription Kit with RNase inhibitor (Life Technologies) was used. 1µg of RNA based on Nanodrop quantification was reverse transcribed to cDNA according to the manufacturer's instructions. The reaction was carried out in a Bio-Rad Cl000 Thermal Cycler with the following cycle parameters: 25°C for 10 min, 37°C for 2 hr, 85°C for five min, and 4°C hold. For RT-PCR experiments that utilized TaqMan® gene expression assay pre-designed FAM labeled probes, the TaqMan® Universal PCR Master Mix was utilized (Life Technologies). For all experiments where custom primers were used with

SYBR® green detection, the Universal SYBR® Green Master Mix was used: with an initial heating at 94°C for 90 s. followed by 35 cycles of 95°C for 25 s, 68°C for 50 s, and 72°C for 50 s. which targeted regions that contained the α and β splice sites. The remainder of the primers and RT-PCR assay information can be found in Table 1. For real-time RT-PCR, the samples were placed in a Cl000™ Thermal Cycler (BioRad, 32 Mississauga, Canada) and incubated at 50°C for 2 min followed by 10 min at 95°C. Samples were then amplified at 95°C for 15 seconds followed by 1 minute at 58°C for 46 cycles. All samples were normalized to GAPDH as an internal control, and fold changes calculated using the following equations.

$$Fold\ change = 2^{(-\Delta\Delta Ct)}$$

Where $\Delta\Delta C_t$ is calculated by:

$$\Delta\Delta Ct = \Delta Ct_{target\ sample} - \Delta Ct_{control\ sample}$$

And ΔC_t is calculated by:

$$\Delta Ct = Ct_{target\ gene} - Ct_{reference\ gene}$$

Where Ct is the cycle threshold or number of cycles when gene expression exceeds background levels.

Table 3. 5 : RT-PCR primers used in this study

Gene	Forward Primer	Reverse Primer
hTERT 1	GCCGATTGTGAACATGGACTACG	GCTCGTAGTTGAGCACGCTGAA
hTERT 2	CCAAGTTCCTGCACTGGCTGA	TTCCCGATGCTGCCTGACC
hTR-1	TTGCGGAGGGTGGGCCT	CGGGCCAGCAGCTGACATT
hTR-2	AAGAGTTGGGCTCTGTCAGC	GACTCGCTCCGTTCCTCTTC
MED14	AACCGCACTTGGGTAGCAGAGT	CTACCACCAACAGGCTCAGACA
BIRC5	TCATTCACAACCCTTCCCAG	TGAAAGCTTCCTCGACATCTG
FTSJ3	GACTGGCATGTTCTCCTTGAGC	GTGTCATCACCGTCGTCCTCAA
ACSF3	GTGATGATGCCTGAGTTCAGCC	GGCTGGGTAAAATGCCTGTCGT
BUB1B	GTGGAAGAGACTGCACAACAGC	TCAGACGCTTGCTGATGGCTCT

PRKRA	CCCTTAATGCCTGACCCTTCCA	CAGGAAGTCTCCAGCCATGATG
PMVK	GCCTTTCGGAAGGACATGATCC	ACTCTCCGTGTGTCACTCACCA
DSCC1	CGCTGAGTTTCAAGAAGTGTGGC	CCTCAGGTAAATCATCTACTTTCAG
TOP2A	GTGGCAAGGATTCTGCTAGTCC	ACCATTCAGGCTCAACACGCTG
PLK1	GCACAGTGTCAATGCCTCCAAG	GCCGTACTTGTCCGAATAGTCC
FANCA	CAGAACCCAACTCTGCTGAGGA	ATCACTGCCACCTGTGCCGATA
RRM2	CTGGCTCAAGAAACGAGGACTG	CTCTCCTCCGATGGTTTGTGTAC
PRPF19	TGGGCTTTCTCTGACATCCAGAC	CCTGTTCCAAAGATGAGTCCGTC
GAPDH	CATGTTCGTCATGGGTGTGAACCA	ATGGCATGGACTGTGGTCATGAGT

3.16 Tumor Xenograft Studies

Male and Female NOD SCID gamma mice were housed in sterile cages and maintained in pathogen-free aseptic rooms, while being fed autoclaved food pellets and water *ad libitum*. All animal protocols were reviewed and approved by the University of Saskatchewan Animal Research Ethics Board. Xenograft tumors were established by injection of $4x10^6$ Miapaca2, 1X106 ES-2, $1.5x10^6$HCC70, $1x10^6$ 22RV1 in 50 μL PBS and 50 μL of Matrigel (Corning, NY, USA) into the flank region of 6-8-week-old animals. Tumor measurement was initiated when tumors became palpable. Measurements were done twice per week for at least 20 days. Digital caliper measurements were taken every 3 days and tumor volume was calculated by the formula:

$$Tumour\ volume = \frac{A}{2} \times B^2$$

(where A and B were the long and short diameters of the tumor respectively). At the end of the experiment's animals were sacrificed and tumors were removed and weighed. Tumors were fixed in 10% buffered formalin for paraffin embedding.

3.17 TeloView

3.17.1 Slide preparation

Teloview experiment was done according to Knecht H and Mai S protocol (Knecht and Mai, 2017).for genes selected for Teloview experiment, Miapaca2-Cas9 cells transfected with pooled lentivirus of two gRNA per gene in presence of polybrene presence of 8 μg/mL polybrene. After 24 hr, media was removed and replaced with DMEM containing 2 μg/mL puromycin to eliminate uninfected cells. Cells were incubated in the presence of puromycin for 48 hr then fresh media was added to the cells and left to grow for 96 hr. After that cells were trypsinzed, collected and counted. $1x10^6$ cells were seeded on slides pre-soaked with 70%ethaol for 24 hr. The slides were removed for the ethanol and let to air dry inside the incubator. Dry slides were placed in $10cm^2$ and cells were added with fresh medium and then placed in the incubator at 37C overnight. Medium was removed and the slides where washed with 1X PBS. Each slide was fixed in 3.7 % formaldehyde/1× PBS for 10 min flowed by 3 times wash in 1× PBS for 5 min. Slides were then incubated in 0.5 % Triton X-100 for 10 min followed by incubation in 20 % glycerol for 1 hour. Freeze-thaw slides by dipping the slide into liquid nitrogen and thaw them. After the freeze thaw process slides were washed 3 times in 1× PBS for 5 min. Slides were then incubated in fresh 0.1 M HCl for 5 min and then washed twice in 1× PBS for 5 min. Slides equilibrated slides in 70 % formamide/2× SSC pH 7.0 for 1 hour at room temperature before hybridization. 8uL of Telomere PNA FISH Kit/Cy3 Probe (Dako Denmark) were applied to the selected area and cover with coverslip and sealed with rubber cement. Denaturation step was done for 3 min at 80 °C, and hybridization for 2 hr at 30 °C (Hybrite™, Vysis/Abbott). Slides were placed in 70 % formamide/10 mM Tris (pH = 7.4) for 15 min then washed with1× PBS. Slides were washed for 5 min at 55 °C in 0.1× saline-sodium citrate (*SSC)* buffer (SSC) then washed 2 × 5 min in 2×

SSC/0.05 % Tween 20. The nuclei were counterstained with 4′,6-diamidino-2-phenylindole (DAPI) and coverslips mounted using VECTASHIELD (Vector Laboratories, Burlington, Ontario, Canada). The slides were kept in 4°C degree for until imaged.

3.17.2 Image acquisition and analysis

Imaging of nuclei was performed with a Zeiss DECON-1 microscope (Zeiss, Toronto, ON, Canada). Images were acquired by using AXIOVISION 4.8 (Zeiss, Toronto, ON, Canada). 30 cells were imaged nuclei per time point using an AxioImager Z2 microscope (Carl Zeiss, Toronto, Ontario, Canada). A 63×/1.4 oil objective lens (Carl Zeiss Canada Ltd.) was used for image acquisition. Sixty z-stacks were acquired at a sampling distance of x,y: 102 nm and z: 200 nm for each slice of the stack. The ZEN 2.3 software (Carl Zeiss Canada Ltd.) was used for 3D image acquisition and processing (the constrained iterative algorithm was used for deconvolution). Deconvolved images were analyzed using the Teloview v1.03 software program(Vermolen et al., 2005) (3D Signatures Inc., Toronto, ON, Canada). TeloView (3D Signatures Inc.) loads 3D images and determines telomeric signal intensity (telomere length), the number of telomeric signals and the number of telomere aggregates. For every fluorochrome, the 3D image consists of a stack of 60 images with a sampling distance of 200 nm along the z and 106 nm in the x, y directions.

3.18 Generation of CRISPR Lentiviral validation Library

Selected hits form the screen (194 hits) were validated in array format screen. gRNA of the selected hits was cherrypicked from our CRISPR Library. The glycerol stocks of bacteria harbouring each gRNA of interest were inoculated into deep 96-well growth plates containing 1.3 mL of LB media containing 100 µg/mL Ampicillin. The plates were sealed with permeable membrane, and incubated them at 37°C, 300 rpm overnight. Plates were spun down at 1800 g for

10 min and plasmid isolated using sigma Kit Lentiviruses were generated using HEK293T cells in 96 well format using same protocol mentioned above **(section 3.3).** For hits validation in each cell line, cells were seeded in 96 well plate each well received lentivirus of pooled gRNA targeting single gene with polybrene final concentration of 8uG/mL for 24 hr. Media was replaced with fresh media containing puromycin of 2uG/mL and left for 48hr to eliminate uninfected cells. After the selection is done, fresh media added to the cells and plates were placed in Live-Cell Analysis System IncuCyte S3® (Essen BioScience Inc. MI 48108, United States). Cells were left to grow for 7 days to compare the growth difference between the knockouts and the control with media change every 48 hours.

3.19 Potential hits validation using CRISPR/Cas9 system

194 hits were validated in HT1080-Parental-Cas9, HT1080-hTERT-Cas9, GM00874-Parental Cas9, GM00874-hTERT-Cas9. Validation was done in image based arrayed format where each well in 96 well plates received gRNA targeting single gene. Number of cells is determined based on the length of the experiment doubling time of the cells and size of the cells to be used in the experiment. After determining the optimal number of cells for the validation experiment, cell was seeded in 96 well plate. Each well was transduced with a mixture of two gRNA targeting single gene of a volume of 100ul per well. Additional wells were kept for nontargeting control and puromycin control. All plates were let to grow for 24hrs (incubator temp and humidity CO_2). After 24hr, fresh medium with puromycin concentration of 2ug/ml were added to the plates in addition to Hygromycin and blastcidin and then placed in IncuCyte (IncuCyteS3®- Sartorius) for proliferation monitoring for 7 days. Medium was replaced with fresh medium every 3 days until

the experiment is done. Subsequent hits validation was done as mentioned previously in telomerase naturally expressing cell lines (Table 3.2) after generating Cas9 stable cell line and validation was done as mentioned above. For primary Panarctic cell lines, Validation was done using shRNA as Cas9 generation for these cells line was not successful.

3.20 TRAP Assay

Telomerase activity were measure using TRAPeze® Telomerase Detection Kit | S7700 – (EMD Millipore, USA). Briefly, cultured Cells, were lysed in CHAPS buffer for 30 min on ice and centrifuged at 12,000 x g for 20 min at 4°C. Protein concentrations were determined using the BCA protein assay (Pierce, Rockford, IL). Telomerase activity was assayed using 2 μg of protein per reaction.

3.21 Statistical Analysis

GraphPad prism software was used for all tests. A one-tailed unpaired student t-test was used for analysis. Data are presented as mean ± standard deviation (SD). A probability value $P < 0.05$ was considered statistically significant.

4. Chapter 4 Results

4.1 Establishing isogenic models to screen for SDL interactions of hTERT

To identify SDL interactions of the telomerase, we choose an isogenic pair of cell line system where genes that are essential for the survival of hTERT over expression can be identified by comparing with an isogenic parental non-overexpressing control cell line. To do this, we used telomerase-positive fibrosarcoma cell line HT1080 that has an endogenous level of hTERT expression. A derived isogenic cell line that overexpressed *h*TERT were used. The HT1080-Parental represents hTERT^{-low} and HT1080-hTERT as hTERT^{-high} model. A constitutively active pBABE-hygro-GFP-hTERT vector was used to allow the over-expression of hTERT in HT1080 cell line.

In Addition, to eliminate cell line specific effects, we used immortalized cell lines that are telomerase negative. The SV40 transformed fibroblast GM0847 that is telomerase negative (GM847-Parental), and derived hTERT overexpressing isogenic cell line (GM847-hTERT). In these cells, telomere length maintenance can be achieved by a telomerase-independent mechanism, Alternative Lengthening of Telomeres. Thus, these two pairs of isogenic cell line system (HT1080-Parental and HT1080-hTERT) and (GM847-Parental and GM847-hTERT) were used to perform our genome-wide shRNA screens. For convenience, these cell lines hereafter will be referred as HTelo-, HTelo+ and GTelo-, GTelo+.

Prior to performing proof-of-principle screens, we assessed GTelo-/GTelo+ and HTelo-/HTelo+ cells by measuring the protein levels of hTERT by western blotting using anti-hTERT antibody and the expression of hTERT by RT-PCR. Results of the protein levels protein levels and expression levels in assessed GTelo-/GTelo+ **(Figure.4.1A) and** HTelo-/HTelo+ **(Figure.4.1B)**

clearly demonstrate the significant difference between the isogenic cell lines and the model fulfil the requirements of the SDL screen . Additionally, previous studies have shown consistent correlation between telomerase activity and TERT gene copy number(Cao et al., 2008), we wanted test if the engineered cell lines still keep relationship between functionally active telomerase and major telomerase components hTERT. To test that the model has enzyme activity of telomerase using the telomeric repeat amplification protocol (TRAP) relevant its expression in GTelo-/GTelo+ **(Figure.4.1C)**. and HTelo-/HTelo+ **(Figure.4.1D)**. The TRAP assay shows a strong correlation between expression and activity in our model cell lines. Moreover, we tested if the stable expression of hTERT affected ALT pathway in the GTelo isogenic model system. The stable expression of hTERT in GTelo+ ALT cell lines reconstitutes telomerase activity without the abrogation of molecular characteristics of the ALT pathway, including formation of ALT-associated promyelocytic leukemia (PML) bodies **(Fig.4.1E).** Quantitation of the PML bodies shows no significant difference between the GTelo- and GTelo+**(Fig.4.1F).** This is important because hTERT has been telomerase might have non-canonical roles that are not related to telomere maintenance. The isogenic cell line systems would serve as an ideal model to identify SDL targets by exploiting canonical and non-canonical functions of telomerase.

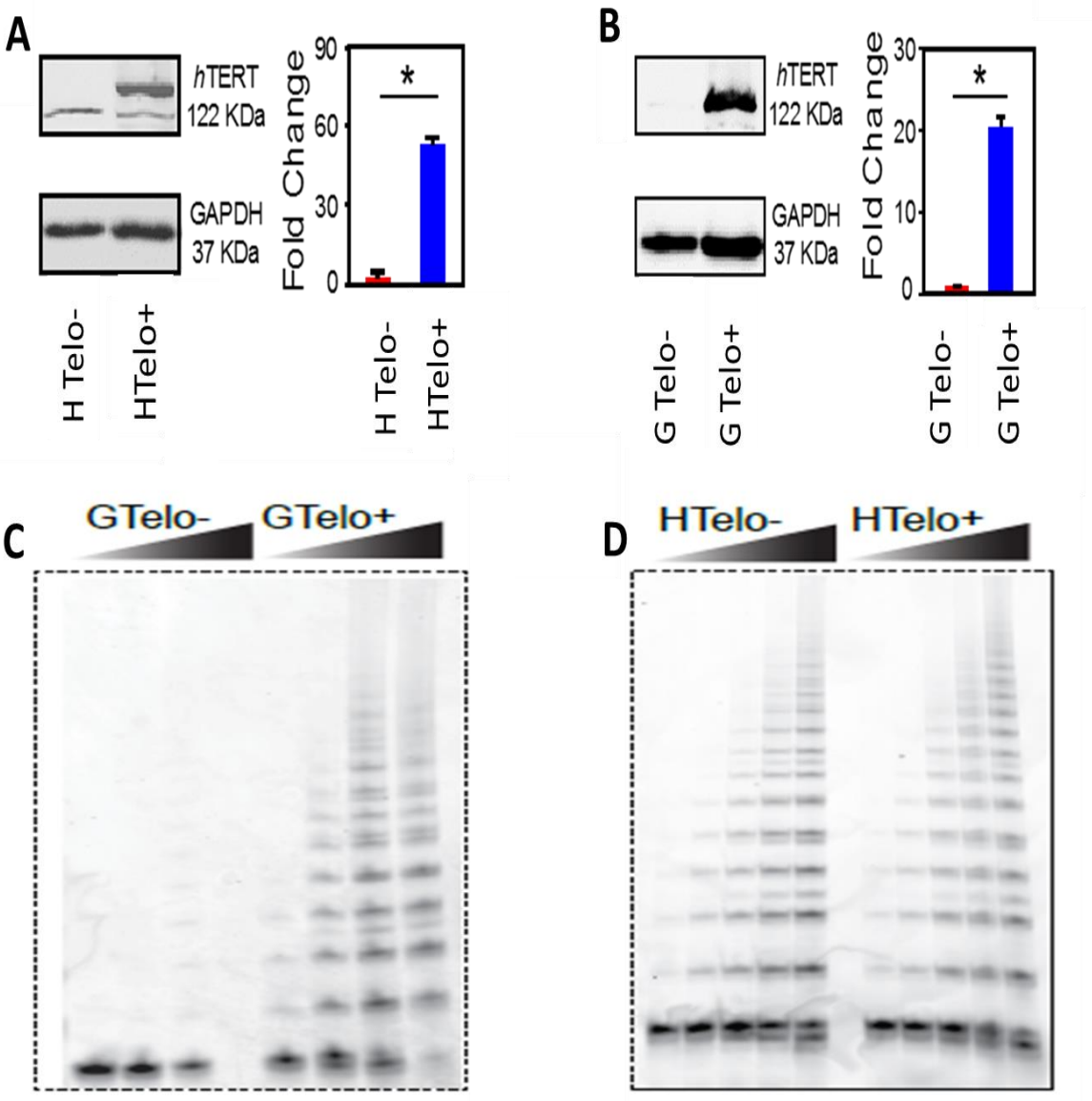
A
hTERT
122 KDa
GAPDH
37 KDa
H Telo-
HTelo+
Fold Change
90
60
30
0
*
H Telo-
HTelo+
B
hTERT
122 KDa
GAPDH
37 KDa
G Telo-
G Telo+
Fold Change
30
20
10
0
*
G Telo-
G Telo+
C
GTelo-
GTelo+
D
HTelo-
HTelo+

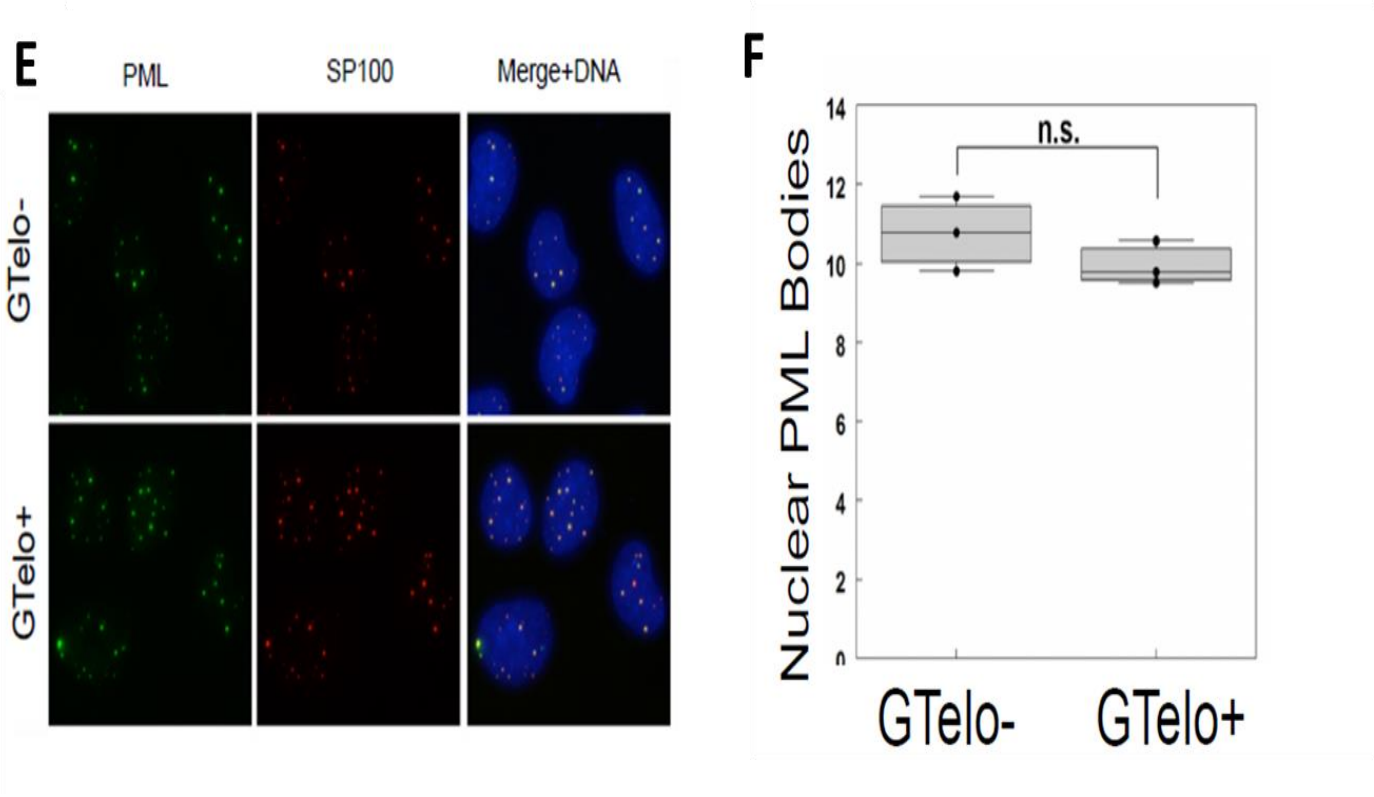

Figure 4.1 Establishing isogenic models to screen for SDL interactions of hTERT. (A) Western blot transformed fibroblast cells GM0847 that are telomerase negative (GTelo-) and derived a hTERT^{high} isogenic cell line (GTelo+) and expression of hTERT by RT-PCR.**(B)** Western blot of hTERT in hTERT^{low} HT1080 (HTelo-) cells and established a hTERT^{high} HT1080-hTERT isogenic cell line (HTelo+) and expression of hTERT by RT-PCR. **(C**) Enzyme activity of telomerase using the telomeric repeat amplification protocol (TRAP) in GTelo-/GTelo+ cells. **(D)** TRAP in HTelo- and HTelo+ cell lines. **(E)** ALT-associated promyelocytic leukemia (PML) bodies in GTelo- and derived isogenic cell line GTelo+. **(F)** Quantitation of PML bodies in GTelo- and GTelo+ cells lines.

For CRISPR Screens, Cas9 stable cell lines were generated by transfecting the four cell lines with a lentti-cas9-Blast vector. Blasticidin was used for selection of cas9 positive cells. Newly generated Cas9 stables cell lines were verified by western blot using anti CRISPRAnti-CRISPR-Cas9 antibody for GTelo-/+ **(Figure4.2A)** and HTelo-/+ **(Figure4.2B).** Western blots show successful generation of stable cas9 cell of the isogenic cell lines. To test the functionality of stably integrated Cas9 nuclease in the genome we measurement of genome editing ability of cas9 stable cells were tested using GeneArt Genomic Cleavage Detection Kit **(Figure 4.2C).** The gemone editing results indicated that the stable cas9 cell lines have the nuclease activity that allows for sequence editing upon gRNA introduction.

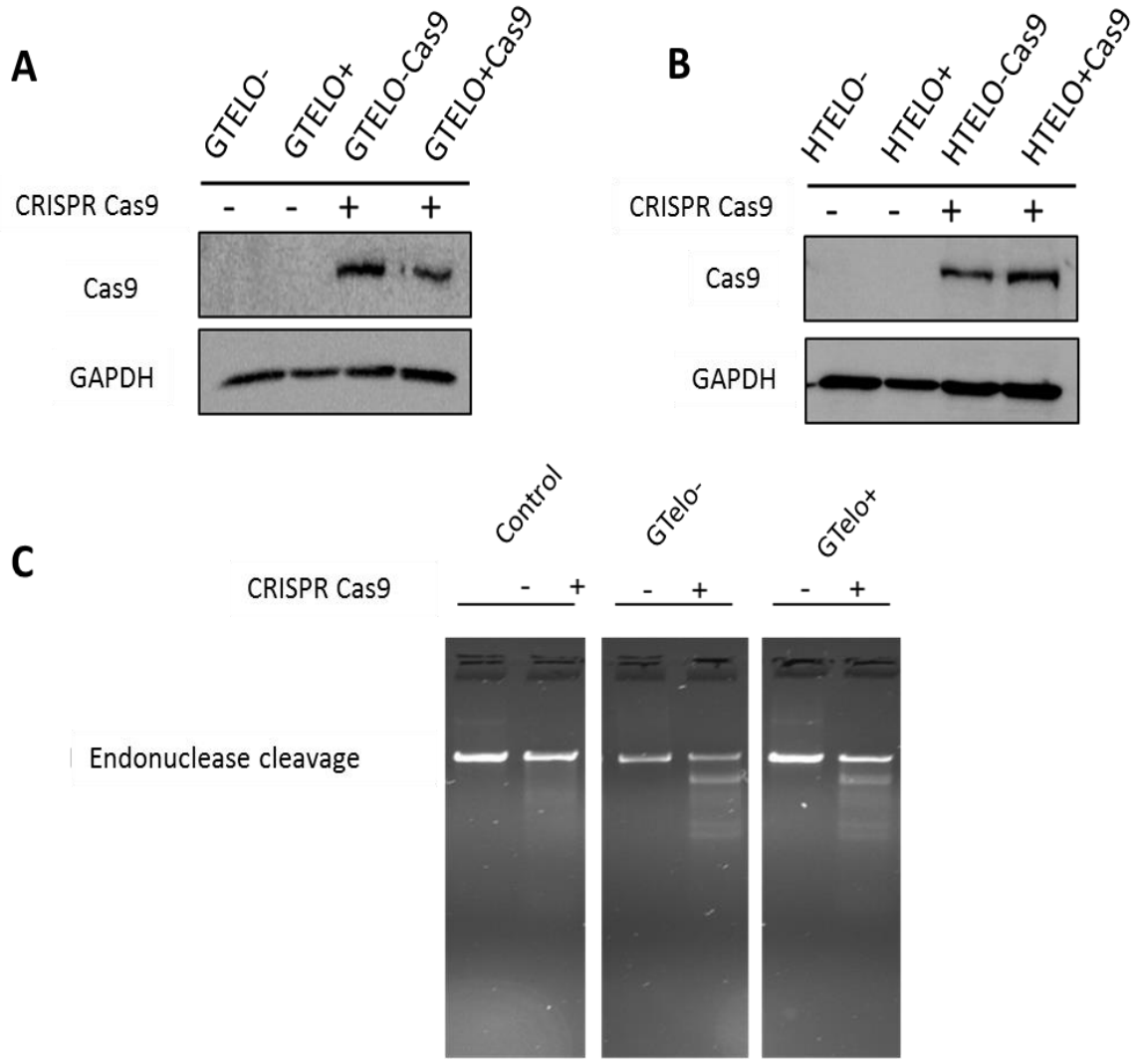

Figure 4.2 Cas9 nuclease has been stably integrated in the genome. (A) Western blot of GTelo-/GTelo+ stable Cas9 cell lines using anti-Cas9 antibody showing successful integration of Cas9 in the gemone. **(B)** Western blot of HTelo- and HTelo+ cell showing Cas being expressed. Verification of genome editing capacity of stably integrated Cas9 cell lines. **(C)** Assessment of Cas9 nuclease on gene editing using genome editing assay.

4.2 Pooled genome-wide shRNA-based screens in hTERT-^{low}/ hTERT-^{high} model

To find SDL in hTERT overexpression context, genome-wide pooled screening was done using a lentiviral pooled library of 90 000 shRNA sequences that target 18 000 human genes with approximately 5 hairpins per gene target. Screens were done in each isogenic cell line pairs. screen conducting, cell numbers and lentivirus particles were optimized by conducting MOI to ensure no more than one lentiviral particle per cell for transduction, ensuring a single gene is knocked down. We took MOI of 0.3 for all cell lines which means that only 30% the cells will be transduced. Transduction at a such low MOI increases the odds that a single cell receives only one lentivirus particle therefore, ensuring that adequate representation of integrated hairpins in the population **(figure4.3).** To ensure there is adequate depth and distribution of sequences (> 200-fold of gRNA numbers), the transduction was done with a high number of cells. The large number of cells was more than adequate for subsequent bioinformatic analysis.

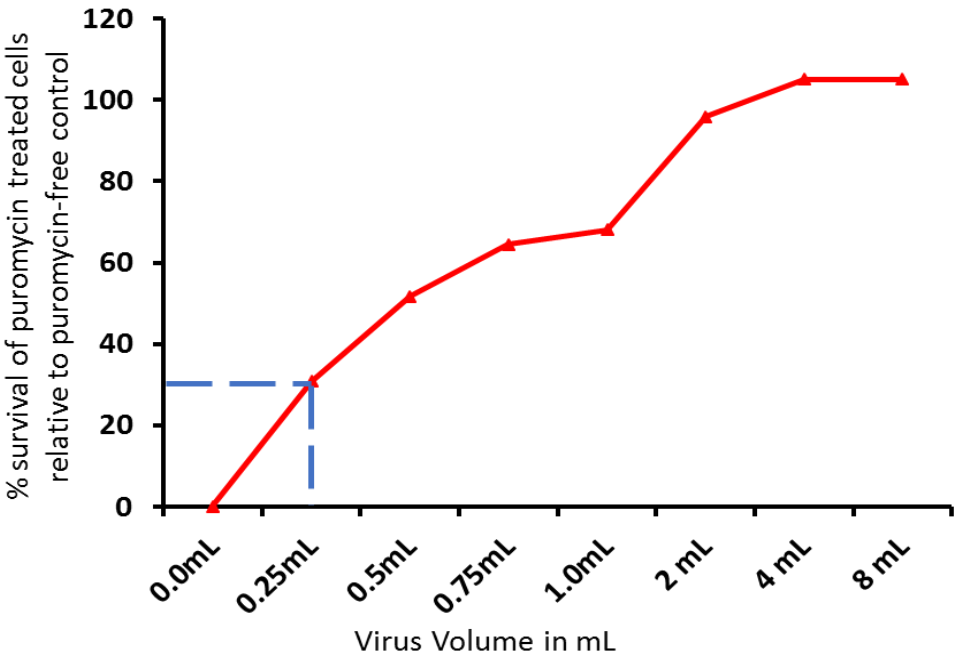

Figure4.3 Pooled lentiviral library. MOI determination Scatter plot graph of lentivirus volume versus cell survival after puromycin selection relative to an untransduced and unselected growth control. A MOI of 0.3 is achieved by the ratio of lentivirus to cells that gives 30% cell survival, in this case, 0.4 mL of lentivirus per 3000 cells.

Microarray signals generated from each integrated *sh*RNA were used to evaluate changes in hairpin representation over time in each population as described in method section (3.8.4 Microarray Deconvolution and Scoring of shRNA Dropout). A drop-in signal intensity of hairpin from one timepoint to the next timepoint within the same replicate is referred to as dropping out of the population. Hairpin is identified as SDL hits if they show significant dropout from one time point to the next in the hTERT- high population relative to hTERT-low population. Volcano plot of all results of the genome-wide pooled screen showing SDL identified from each isogenic cell line **(Figure4.4A)** and Negative genetic interactions, or genes that significantly decreased the fitness and precision recall curve are shown in **(Figure4.4B)**

The quality of the shRNA screens was assessed by analyzing changes in reference sets of essential and nonessential genes. Bayesian Analysis of Gene Essentiality (BAGEL) (Hart et al., 2014) recorded good performance scores for each screen **(Figure4.4B).** In total, 829 genes were identified GTelo shRNA as essential (SDL hits) with p-value < 0.05 while 1278 genes where found essential in HTelo shRNA screen. The full list of identified hits is in Appendix A.1

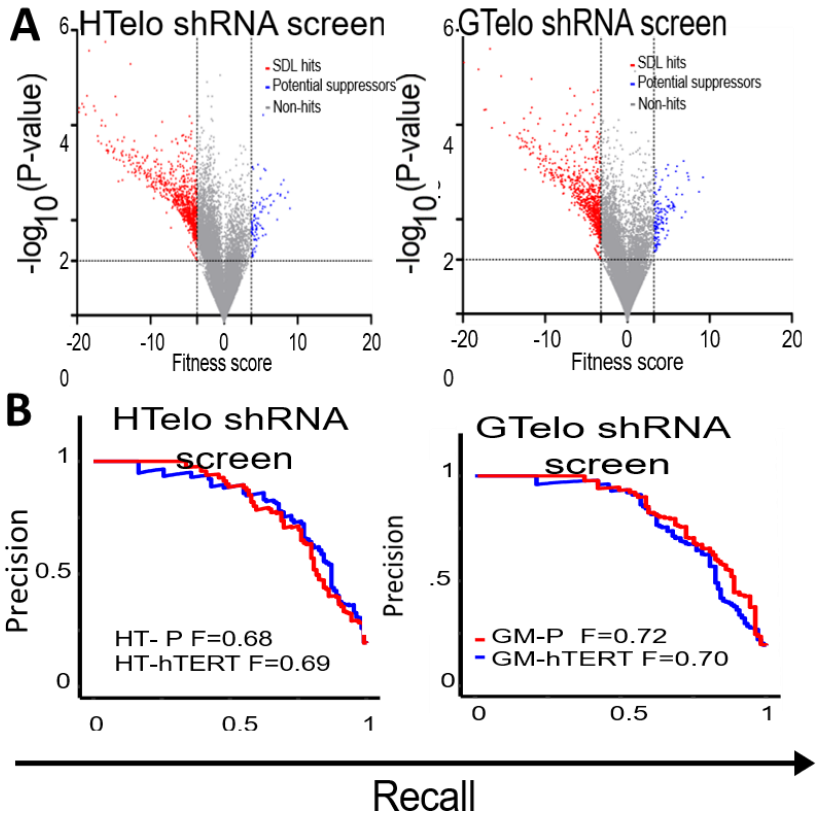

Figure 4.4. Microarray analysis of the genome-wide screen for genes SDL with telomerase (A) Volcano plot of the genome-wide pooled screens in two isogenic models by two different methods. The x-axis represents the fitness score that identifies the SDL hits (red dots) on the left and potential suppressors (blue dots) **(B)** Precision-recall analysis of the telomerase genome-wide screens the y-axis shows the significance of these hits. Precision-recall curve evaluating the quality of the screen as described in HART et al 2013. Higher F-measure, lower is the error rate.

4.3 Pooled genome-wide CRISPR/Cas9-based screens in 4 cell lines with low/high TERT

To uncover novel essential genes whose depletion endows cells death in hTERT-^{high} scenario, we carried out genome wide CRISPR screens in HTelo-, HTelo+, and GTelo-, GTelo+ cell lines. The guide RNA (gRNA) library we chose was the human GeCKO (Genome-Scale CRISPR Knock-Out) lentiviral pooled, which contains 58,360 gRNAs targeting 18,053 protein-coding genes (Sanjana et al., 2014; Shalem et al., 2014). Cells were infected with lentiviruses particles encompassing the GeCKO library at MOI of 0.3. Similar to shRNA screen, the collected cell from different time point were used for library preparation. Subsequently, the sgRNA amplicon was amplified by PCR followed by agarose gel electrophoresis to confirm the size of the amplicon **(Figure4.5).**

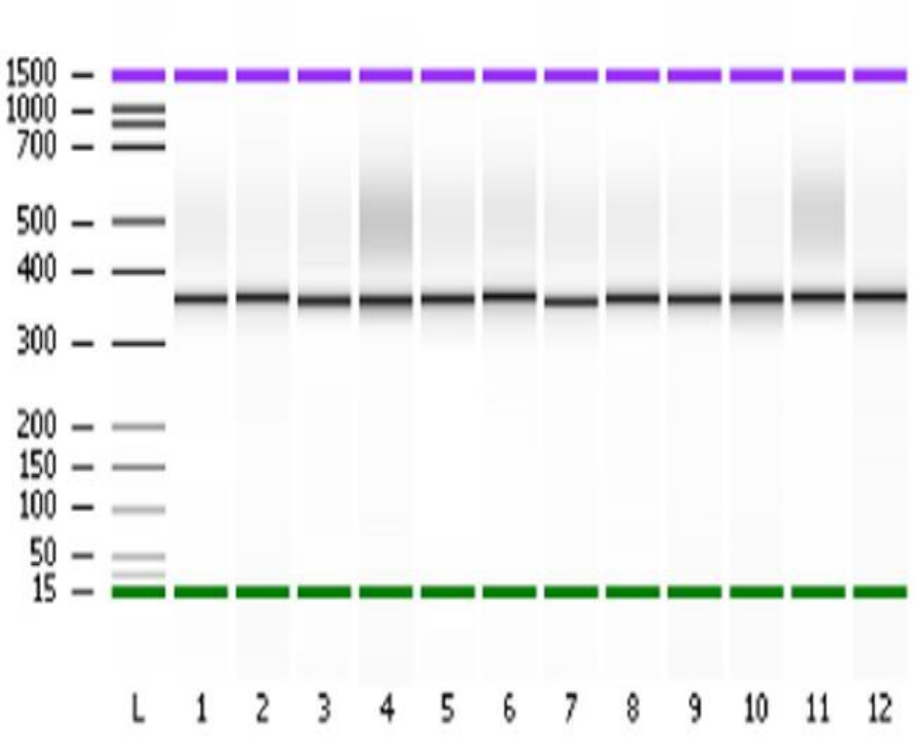

Figure 4. 5 CIRSPR library preparation. Image of agarose gel of CRISPR library amplicons after illumina barcode attachment.

Additionally ,1 µl of amplified library of each sample was analysed on the Agilent Bioanalyzer instrument with the Agilent High Sensitivity DNA chip in order to be accepted for further processing, amplicon libraries needed to have multiple peaks and size range between 360–450bp **(Figure 4.6)**. Amplified libraries typically had concentrations of 20nG. After quantification, and dilution, the amplicons were Next-generation sequencing (NGS) was performed on 350-bp amplicons with upwards of 1.8×10^7 reads, of which approximately 90% were mapped to the gRNA library.

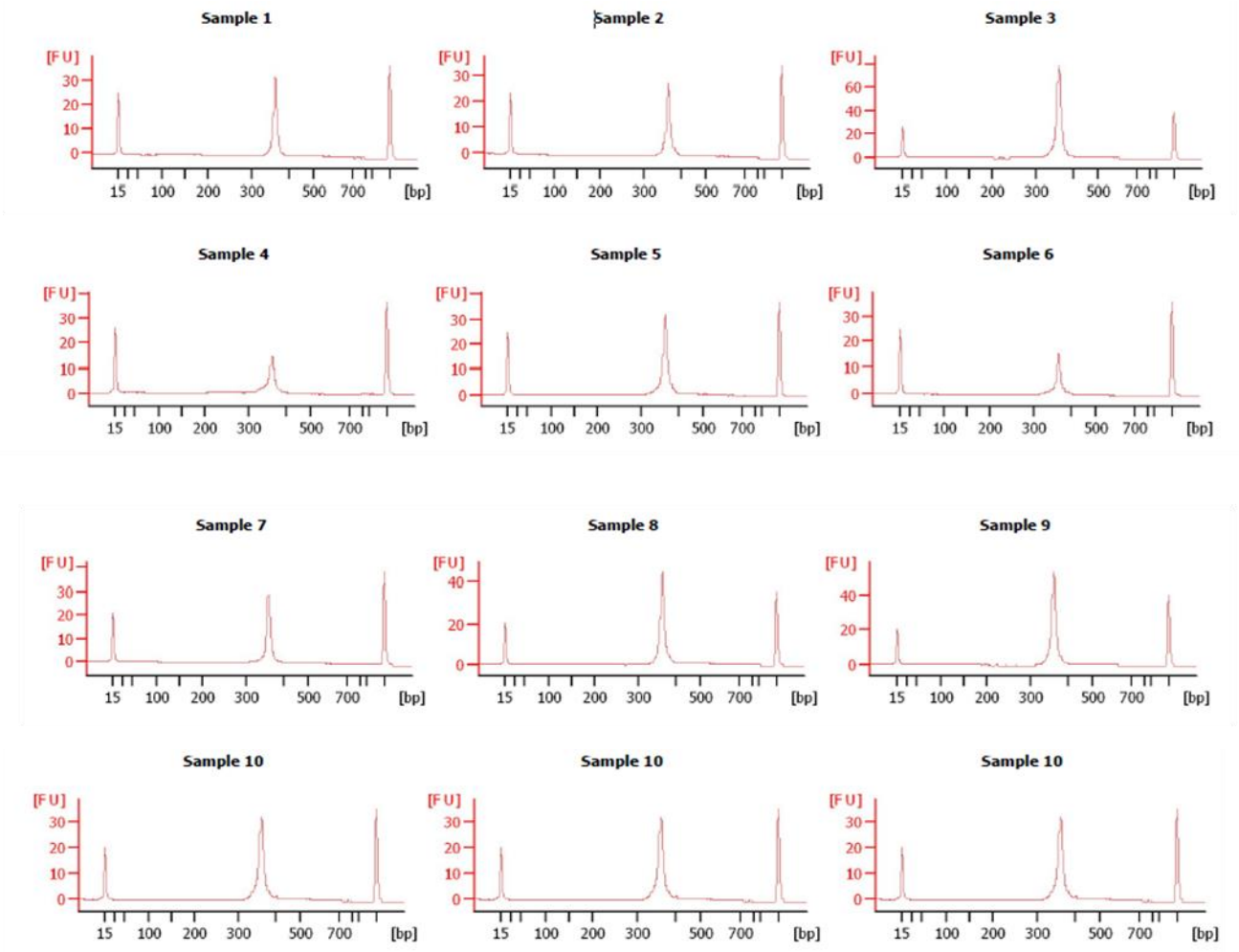

Figure 4.6 Quality assessment of the barcoded product on the Bioanalyzer. Amplified CRISPR amplicons were checked for the quality using bioanalyzer gel electrophoresis. No sample showed any contamination of secondary peak.

To determine whether the CRISPR-based screens were successful, changes in essential genes and nonessential genes between timepoints as described in shRNA screens section. that sgRNAs targeting essential genes were reduced while sgRNAs targeting nonessential genes remained the same between these time points, indicating that the successful **(Figure 4.7)**. The GTelo-/GTelo+ CRSIPR screen identified 470 potential SDL hits and HTelo-/HTelo+ CRISPR screen identified 313 genes to be essential in hTERT-High cell.

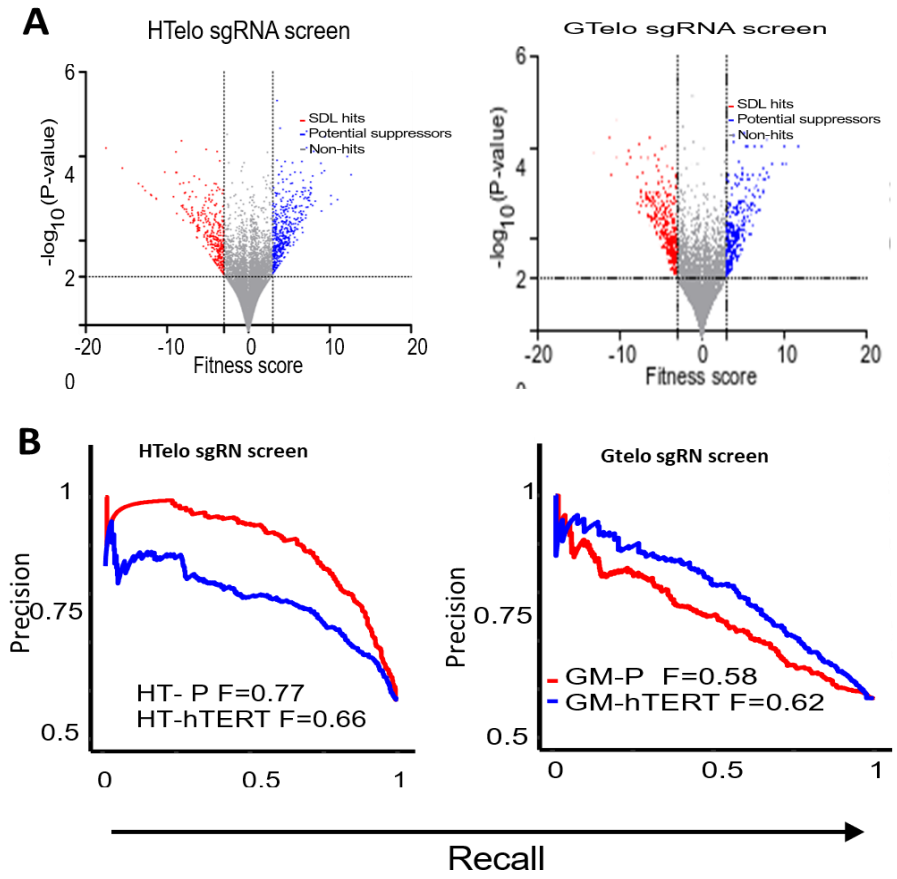

Figure 4.7 CRISPR screen analysis for SDL hits Telomerase. (A) Volcano plot of the genome-wide pooled screens in two isogenic models by two different methods. The x-axis represents the fitness score that identifies the SDL hits (red dots) on the left and potential suppressors (blue dots) **(B)** Precision-recall analysis of the telomerase genome-wide screens. The y-axis shows the significance of these hits. Precision-recall curve evaluating the quality of the screen as described in HART et al 2013. Higher F-measure, lower is the error rate.

4.4 Analysis of screening results.

Identification of the top hit genes from each screen by ranking genes identified as lethal to hTERT overexpressing cell lines and not the parental cells was done using p-value for each pair of cells. In total, the four screens generated 2763 candidate targets that can be used to target telomerase overexpressing tumors. As in **(Figure 4.14)** GTelo shRNA-based screens have suggested 829 candidates, 470 GTelo CRISR, 1278 HTelo *sh*RNA screen and 313 candidate hits

in HTelo-CRISPR screen. Most of these candidate genes scored in only one of the three screens. Poor overlap between the shRNA and CRISPR/Cas9 screens as mentioned in body of publications (Evers et al., 2014) (Mohr et al., 2014). Only 25 genes overlapped between the HTelo shRNA and CRISPR/Cas9, while 37 genes scored overlapping between GTelo shRNA and CRISPR/Cas9. Only12 genes scored in three screens and no candidate gene scored in all four screens.

Using Ingenuity Pathway Analyses, Cellular interaction network of identified hits and their cellular localization as shown in **(Figure4.8).** Nodes indicated the identified targets from each screen. Nodes colors illustrate the primary function of the identified hits. Red lines illustrating the interactions. Clearly, SDL hits related to different biological processes. For example, several hTERT SDL hits to be associated with mitochondria, spliceosome complex or translation initiation complex. To determine which pathway in being overrepresented, pathway enrichment analyses of hTERT SDL hits identified was used. Pathway enrichment analysis revealed hits involved in components of RNA processing and ribosome assembly and signal transduction. **(Figure4.9).** Interestingly, consistent with some of the non-canonical functions of hTERT, enrichment of genes involved in cellular processes such as cell cycle regulation and protein autophosphorylation were also found to be enriched in hTERT SDL hits. Given that telomere replication requires specific helicases and repair proteins, it is interesting to note that several such components (MCM5, POLA2), apart from components of the shelterin/ telomerase ribonucleoprotein complex (TINF2, , DKC1), and several transcriptional regulators of telomerase (MYC, MXD3) are identified as SDL hits. These enrichment analyses increased confidence in several SDL hits identified in CRISPR/shRNA screens.

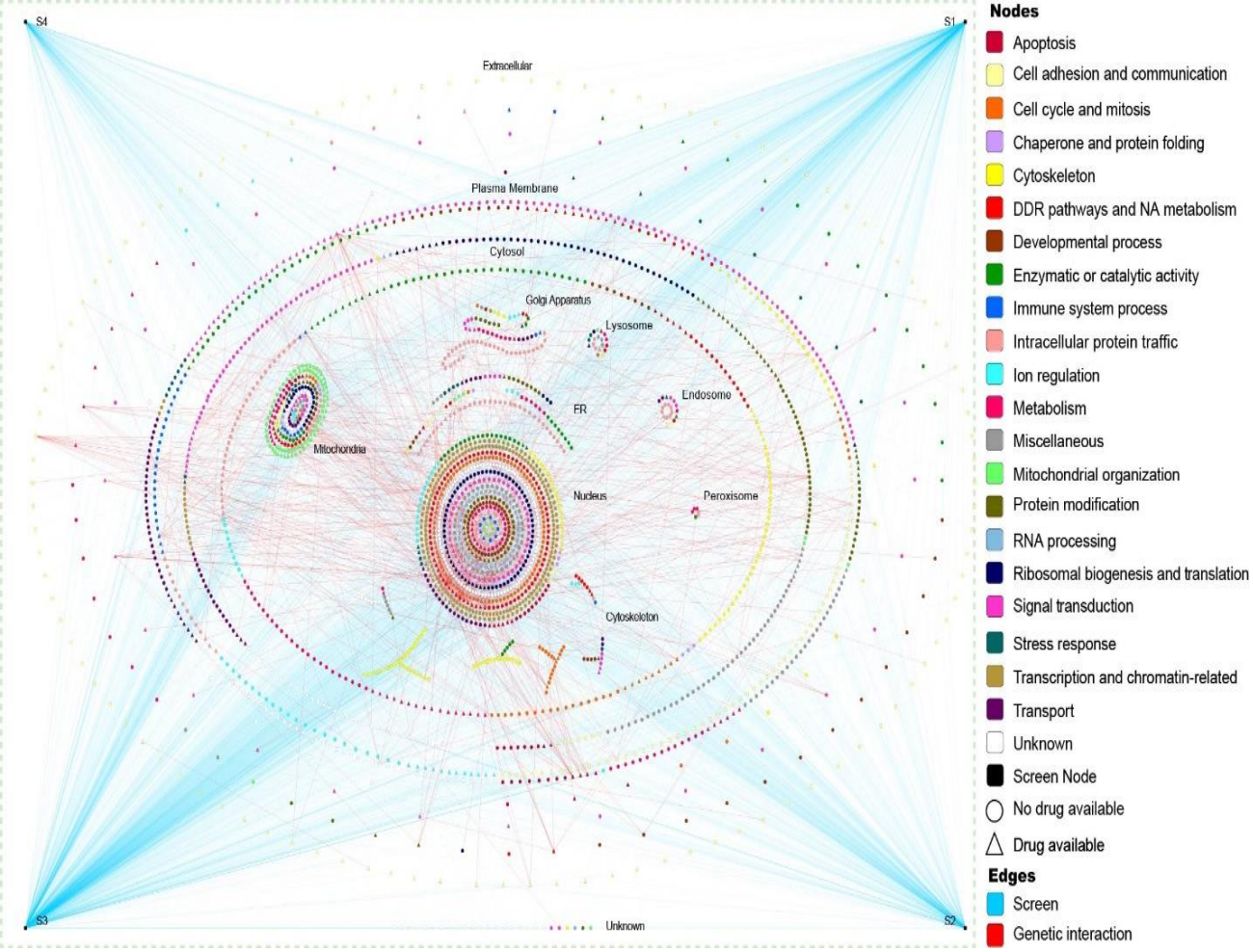

Figure4.8 SDL interactions of hTERT. Cystoscope representation of the hits arranged based on cellular compartments. The four screens are placed in the four corners with the SDL genes identified in each of them represented as nodes connected in blue edges. The nodes are color-coded based on the Gene Ontology slim terms. The red edges are interaction derived from ingenuity pathway analyses. Many nuclear and mitochondrial genes are found to have extensive interactions.

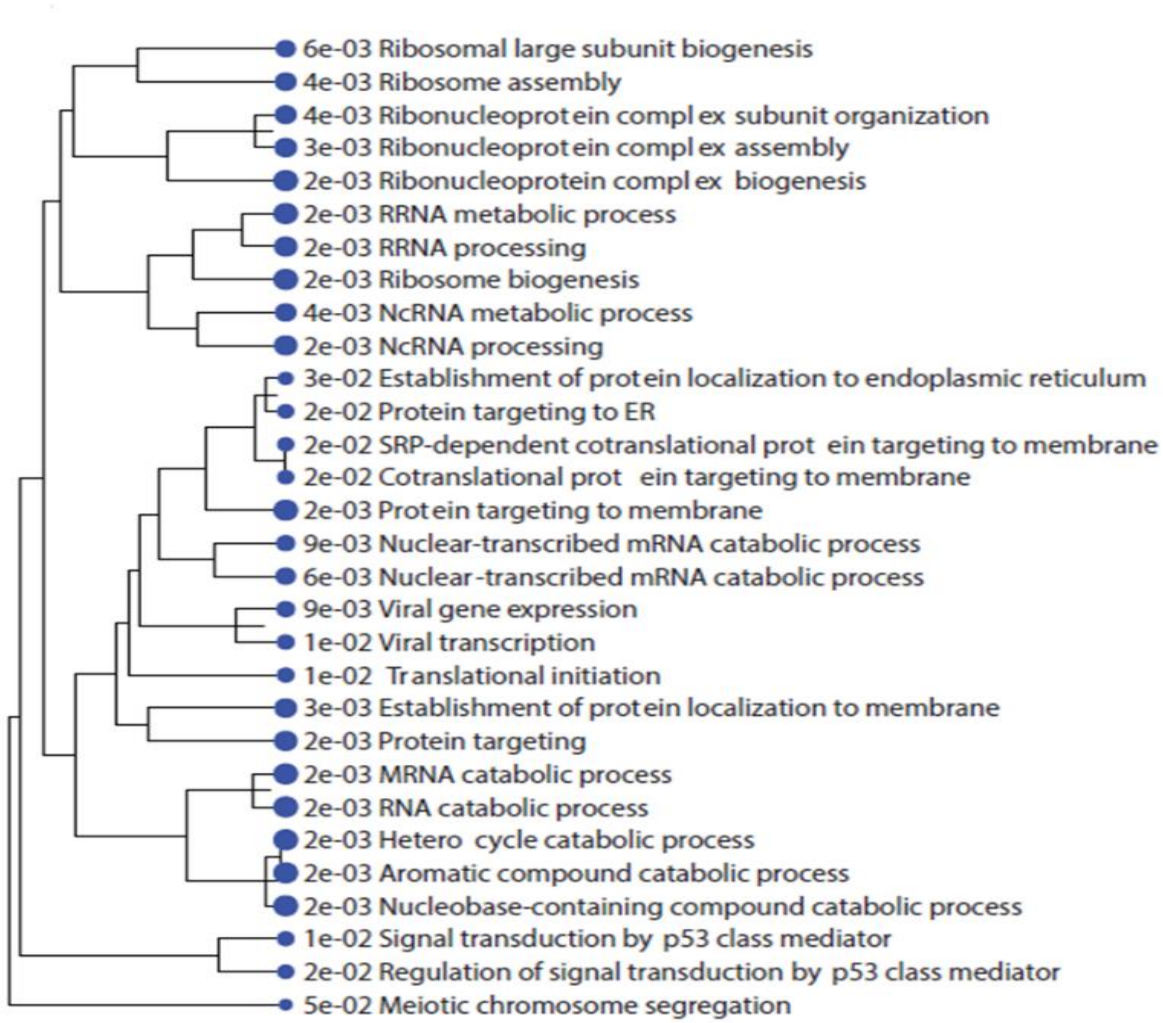

Figure 4. 9 Pathway enrichment analysis of hTERT SDL hits. Dendrogram of the Reactome pathways that are significantly overrepresented in hTERT SDL hits. P-Values indicate pathway is overrepresented.

Next, we looked for chemical inhibitors for the identified hits. Few of our SDL hits had chemical inhibitors, and we used drug response data from the cancerRXgene database (https://www.cancerrxgene.org). We looked for cell lines in which these inhibitors have been tested in and segregated these cell lines based on hTERT levels. Accordingly, we tested these inhibitors in GTelo-/GTelo+ cells using automated microscopy Incucyte® S3 and Incucyte® Base

Analysis Software was used to calculate cell percentage of confluency every 24 hours. Differences in cells confluency between treated cells and the control and between the isogenic cell lines were used to confirm chemical inhibitor effectiveness toward hTERT. We found inhibitors of the top validated hits suppress growth in hTERT-^{high} cells but not hTERT-^{low} cells **(Figure.4.9)**, confirming the potential to identify therapeutically relevant targets that can target telomerase overexpressing tumors.

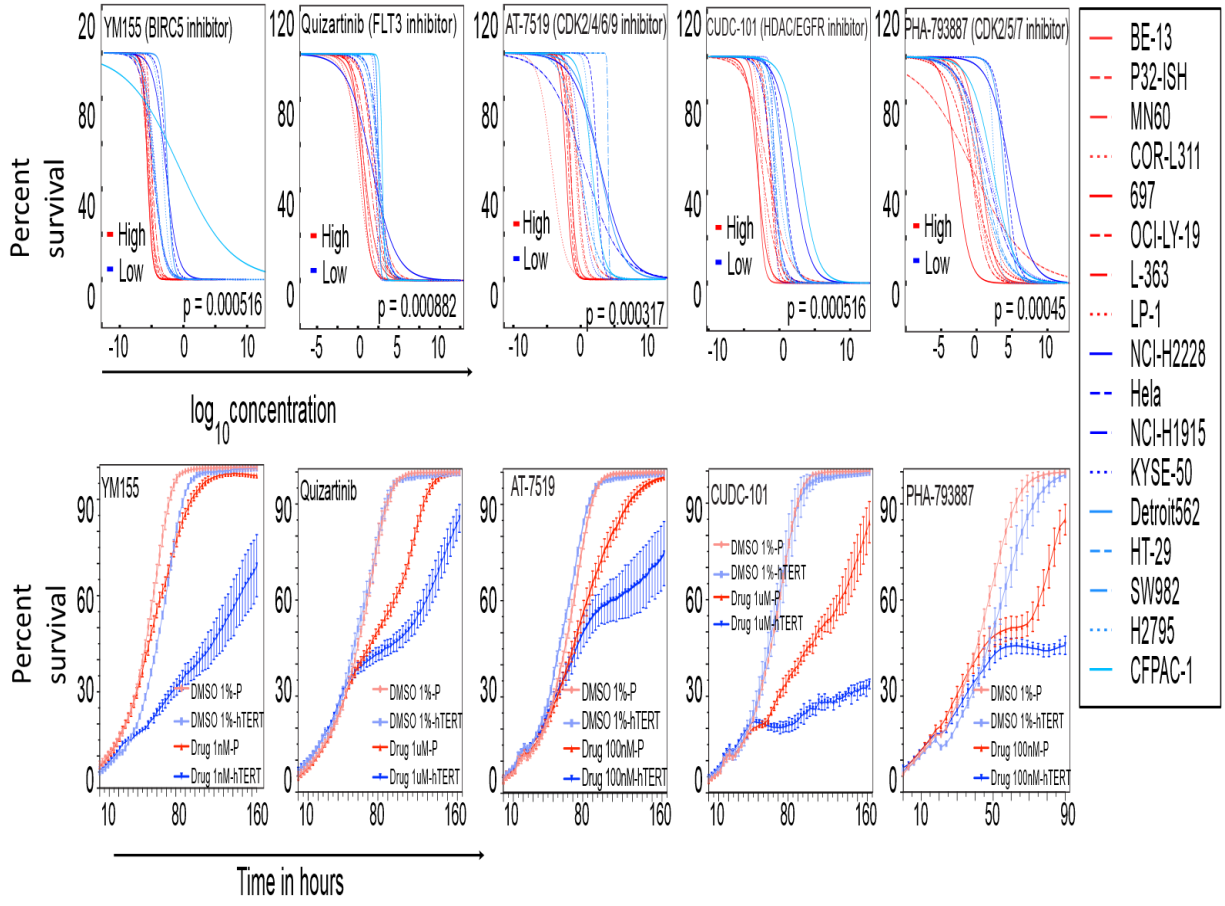

Figure 4. 10 Chemical inhibitors found from cancerRXgene database. The top panel represent chemical inhibitors found in the database. The column on the right represent the cell lines in which these inhibitors were tested in. bottom panel represent testing in GTelo-/GTelo+ cell lines.

4.5 Prioritizing Synthetic Dosage Lethal Interactions Computationally

Telomerase SDL screens yielded at total of 2763 potential hits. Validating large number of SDL hits is labor-intensive. Therefore, we adopted four strategies to prioritize hits. First, we rationalized, those SDL hits that are differentially upregulated with hTERT overexpression, may reflect a co-regulatory mechanism that becomes essential within the $hTERT^{high}$ cells. To test this possibility, the question asked was how many of the SDL hits are co-upregulated with hTERT across 33 different cancers using patient data from The Cancer Genome Atlas (https://portal.gdc.cancer.gov). We tested the usefulness of this approach for the GTelo-/GTelo+ screen and identified 17 co-upregulated genes that, when knocked down, selectively decreased the proliferation of $hTERT^{high}$ cells compared to $hTERT^{low}$ cells **(Figure.4.12).** Results show 12 of 17 genes validated in GTelo-/GTelo+). While genome-wide screens are notorious for false positives and ~25 to 40% of the hits alone get validated, successful validation of 17 out of 17 proved the efficiency of this strategy. Therefore, this approach was applied across all screens and prioritized 46 genes that was included in the final number of genes to be validated. The second approach adopted to select potential hits was by using data from previous publications that have identified essential genes across multiple cancer cell lines(Cowley et al., 2014; Marcotte et al., 2012; McDonald et al., 2017; Meyers et al., 2017).We categorized all cell lines used in these studies based on hTERT expression. Then we looked for how many genes from our list became essential $hTERT^{high}$ (top 10%) and those that are naturally $hTERT^{low}$ (bottom 10%). This approach identified additional 47 potential genes for further validation. Additionally, we used data published from two studies to find genes that are upregulated upon hTERT inhibition (Hu et al., 2012; Lafferty-Whyte et al., 2009). This approach identified 82 genes in our hit list that we included for the next step validation. **(Figure 4.13A).**

The fourth approach used a previously published data mining pipeline called DAISY to identify clinically relevant SDL hits (Jerby-Arnon et al., 2014). Briefly, patients were grouped into 'naturally-occurring SDL interactions' and 'no SDL interactions' categories based on expression levels of hTERT and the potential hTERT SDL hits **(Figure 4.13B)**. Accordingly, we found 21 SDL hits within the 'naturally-occurring SDL interaction' category that were selected for further validation **(Figure 4.13C).** Finally, we selected 30 SDL hits that overlapped in any two of the CRISPR/Cas9 and shRNA screens. Overall, we prioritized 212 SDL hits (13 were picked by multiple approaches and 46+47+82+21+30-13 = 212) for further validation studies. however, cloning of 25 sgRNAs for some of these genes failed, our final focus was on validating 187 (212-25=187) selected hits **(Figure 4.14)(Table A.1).**

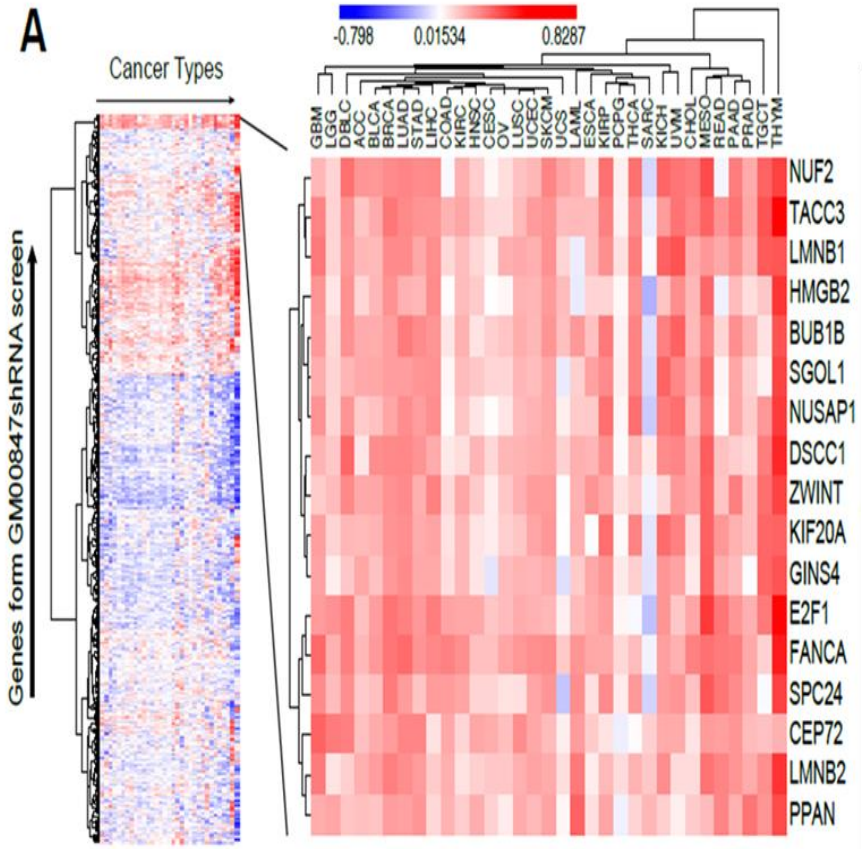

Figure 4.11. Correlation cluster gram for expression of hTERT with expression of each screen hit across 33 cancer types.

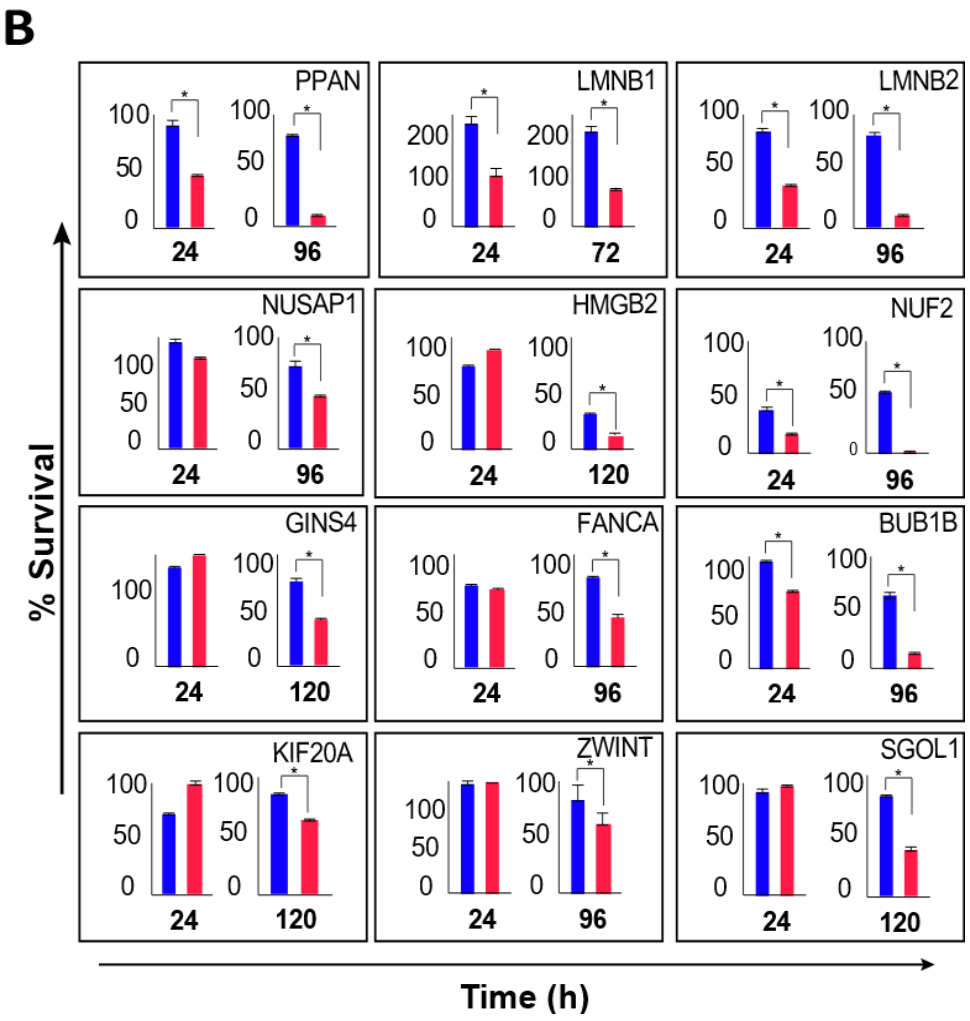

Figure 4.12 Proliferation assay of SDL hits. GTelo-/GTelo+ screen and identified 17 co-upregulated genes that, when knocked down, selectively decreased the proliferation of hTERT^{high} cells. Proliferation assay was done in multiple time points and the best two timepoints are represented. GTelo+ are in red and GTelo- are in blue.

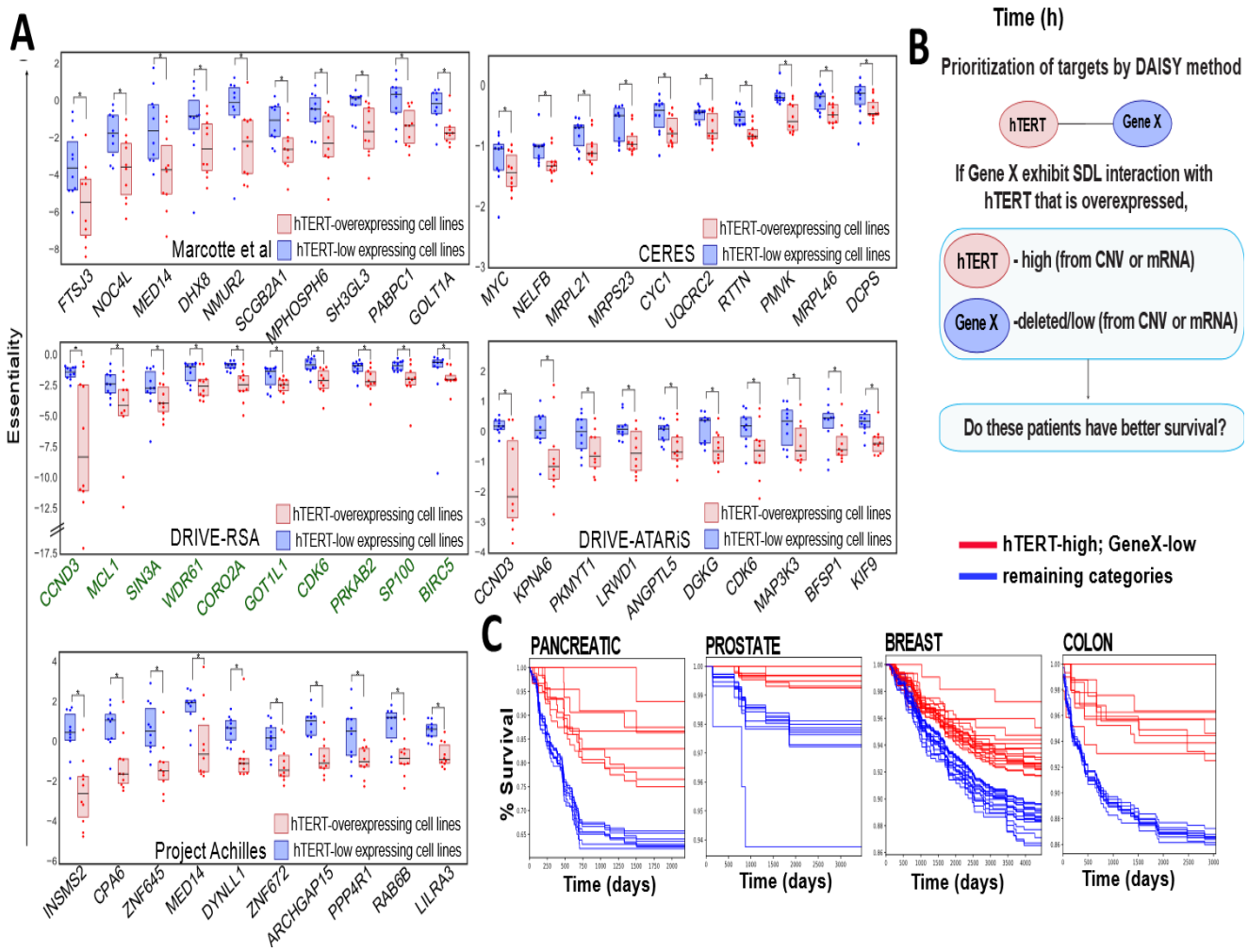

Figure 4.13 Prioritizing Synthetic Dosage Lethal Interactions Computationally. (A) Essentiality score derived from five published studies, where SDL hits are validated. *p<0.01. **(B)** Schematic of the DAISY method for prioritization of SDL hits. **(C)** Kaplan-Meier plots of SDL hits in different cancer types from TCGA. Interestingly, patients with naturally expressing SDL interaction (red) survive better than patients that do not have natural SDL (blue) with log-rank p<0.05.

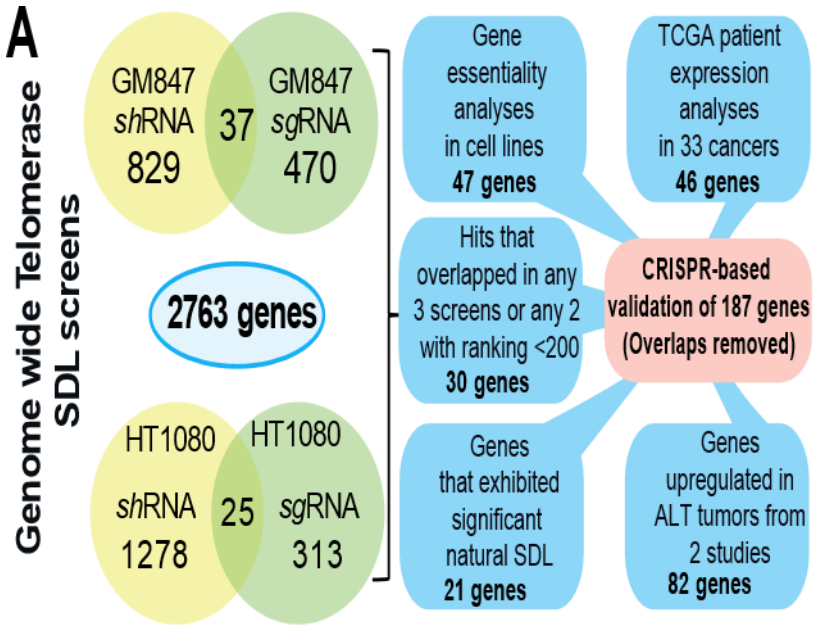

Figure 4.14 Summary of SDL hit prioritization strategy from shRNA screen and CRISPR-Cas9 screen. Graph shows number of hits generated each genome wide screen and the overlap between the screen **(left**). The approaches adopted for hits prioritization and number of hits selected by each approach **(right)**.

4.6 Validation of the selected hTERT SDL hits using an arrayed CRISPR/Cas9 system

The next step after prioritizing the hits was to be validated in the GTelo and HTelo Cas9 model cell lines. To validate 187 SDL hits, sgRNA used were clone individually with two guides targeting specific genes. Non-targeting sgRNA was used as a control (NTC). We chose to validate the hits in the same GTelo-/GTelo+ and HTelo-/HTelo+ cells that were used for screening, because we expected that this gene-by gene interrogation in the same cells will reconfirm if the SDL hits are truly hTERT-dependent and eliminate any screening-related false positives. Briefly, an equal number of Cas9 expressing cells were seeded in a 96 well plates, followed by transduction with lentiviruses expressing individual sgRNAs targeting one of 187 SDL hits in each transduction.

After 24 hours of transduction, Fresh media with selection antibiotic was added and the plates were imaged for 6-8 days in S3-IncuCyte® platform and cells were counted to confirm true SDL hits. Incucyte® Base Analysis Software was used to calculate cell confluency every 24 hrs. Differences in cells confluency between *sg*RNA targeting individual gene and non targeting *sg*RNA control and between the isogenic cell lines were used to confirm true SDL hits. Experiments were terminated once the non- targeting control became confluent. For each cell line.

20 out of the 187 SDL hits were robustly validated by the CRISPR/Cas9 strategy in both isogenic models **(Figure 4.15).** In addition, 17 SDL hits got validated in GTelo-/GTelo+ cells but not in HTelo-/HTelo+ cells and 5 SDL hits got validated in HTelo-/HTelo+ but not in GTelo-/GTelo+ cells. Some of the targets among the validated hits include the checkpoint kinase gene (CHEK1). It has been shown previously that ATR-CHEK1 pathway inhibition induces replicative stress in hTERT overexpressing ovarian caner cells(Gralewska et al., 2020). Another successfully validated hit is LMNB1which part on nuclear envelop. LMNB1 depletion has been shown to have a role in cellular aging and affecting telomere length(Dreesen et al., 2013). Additionally, BIRC5 is was one of the successfully validated hit and the chemical inhibitor YM155 showed consistent result with the genetic validation. Overall, our CRISPR arrayed screen identified 42 hits that significant reduced cell growth of $hTERT^{high}$ cells.

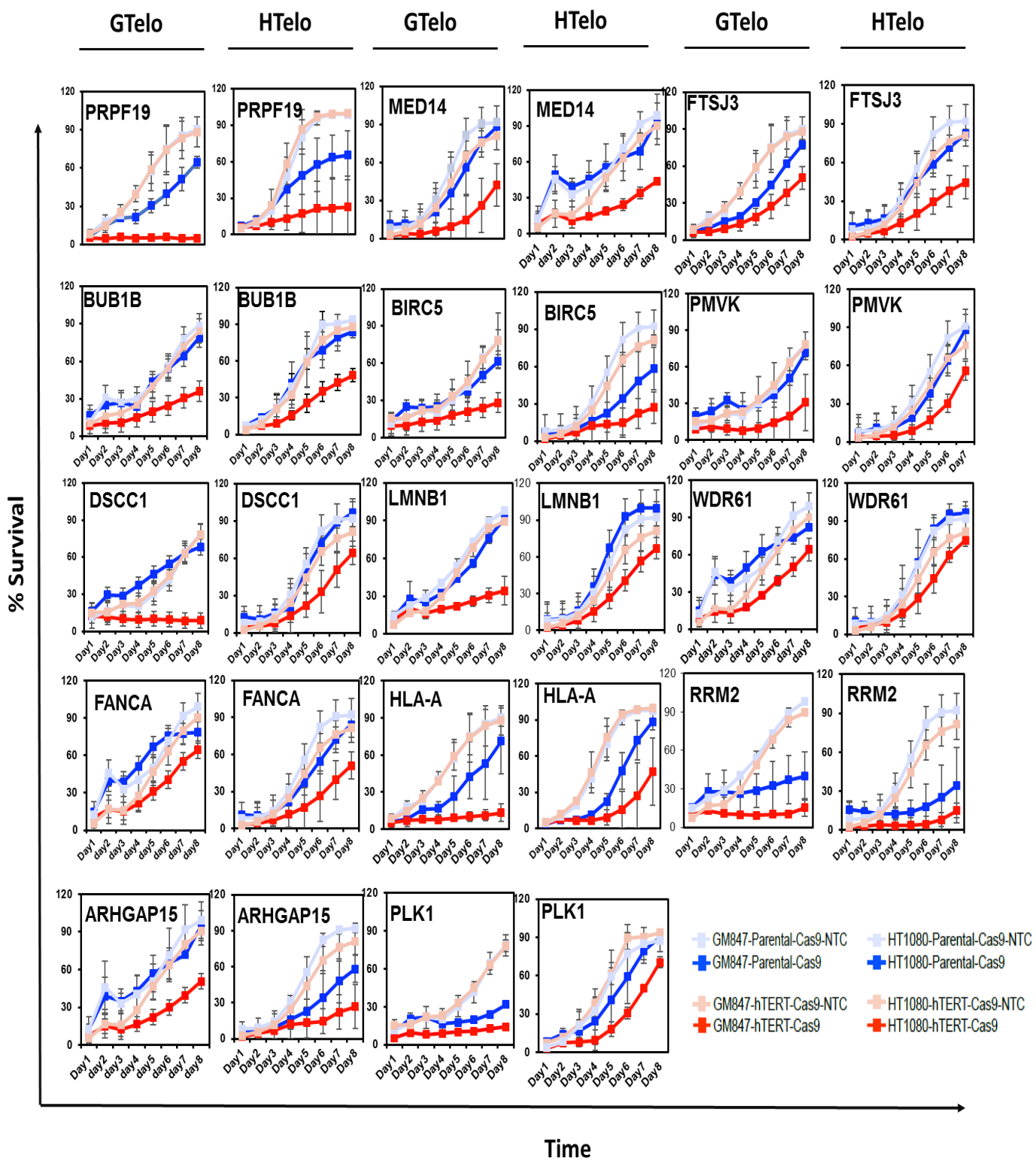
GTelo
HTelo
GTelo
HTelo
GTelo
HTelo
PRPF19
PRPF19
MED14
MED14
FTSJ3
FTSJ3
BUB1B
BUB1B
BIRC5
BIRC5
PMVK
PMVK
DSCC1
DSCC1
LMNB1
LMNB1
WDR61
WDR61
FANCA
FANCA
HLA-A
HLA-A
RRM2
RRM2
ARHGAP15
ARHGAP15
PLK1
PLK1
% Survival
Time
GM847-Parental-Cas9-NTC
GM847-Parental-Cas9
HT1080-Parental-Cas9-NTC
HT1080-Parental-Cas9
GM847-hTERT-Cas9-NTC
GM847-hTERT-Cas9
HT1080-hTERT-Cas9-NTC
HT1080-hTERT-Cas9

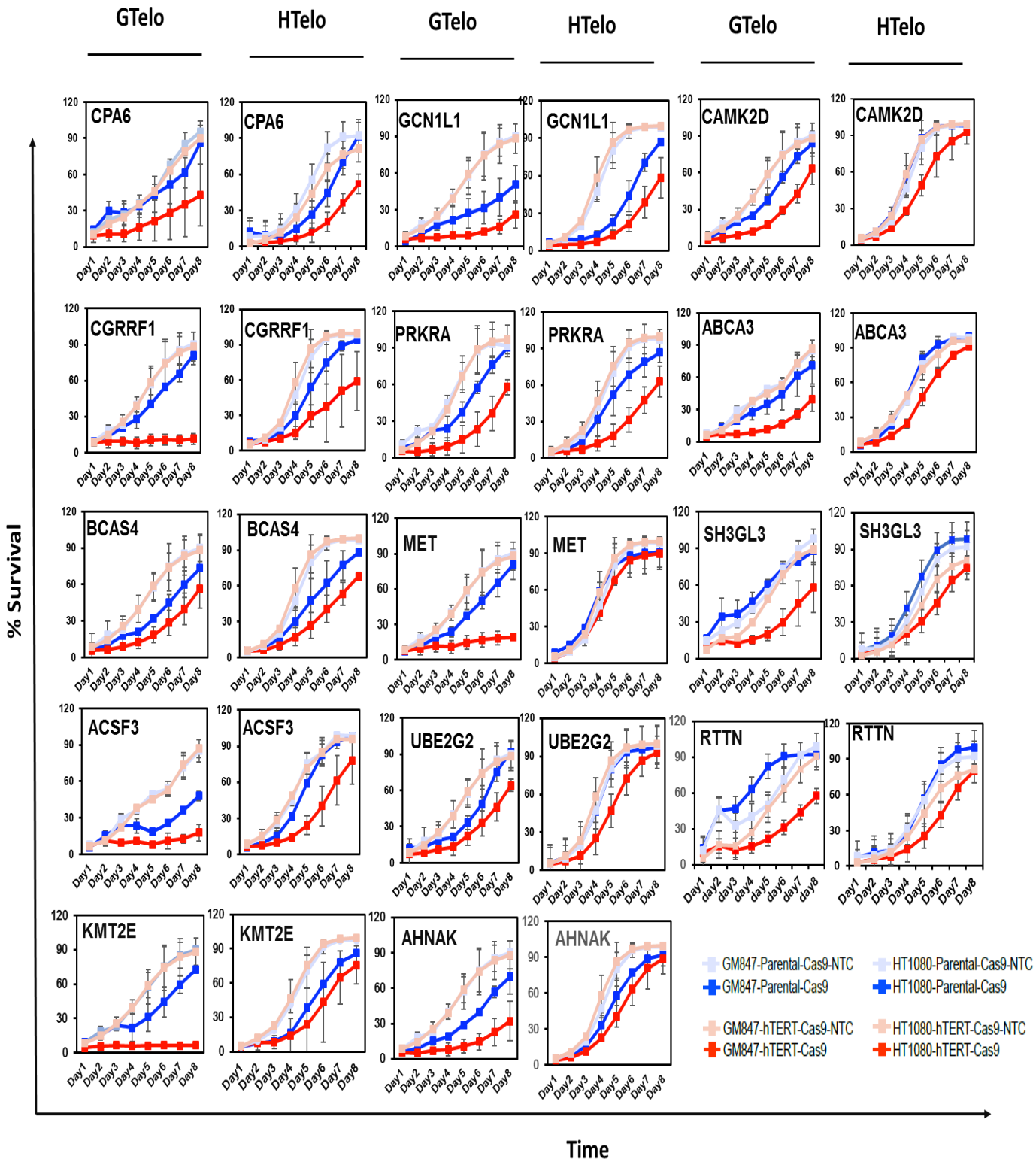
GTelo
HTelo
GTelo
HTelo
GTelo
HTelo
CPA6
CPA6
GCN1L1
GCN1L1
CAMK2D
CAMK2D
CGRRF1
CGRRF1
PRKRA
PRKRA
ABCA3
ABCA3
BCAS4
BCAS4
MET
MET
SH3GL3
SH3GL3
ACSF3
ACSF3
UBE2G2
UBE2G2
RTTN
RTTN
KMT2E
KMT2E
AHNAK
AHNAK
% Survival
Time
Day1 Day2 Day3 Day4 Day5 Day6 Day7 Day8
GM847-Parental-Cas9-NTC
GM847-Parental-Cas9
HT1080-Parental-Cas9-NTC
HT1080-Parental-Cas9
GM847-hTERT-Cas9-NTC
GM847-hTERT-Cas9
HT1080-hTERT-Cas9-NTC
HT1080-hTERT-Cas9

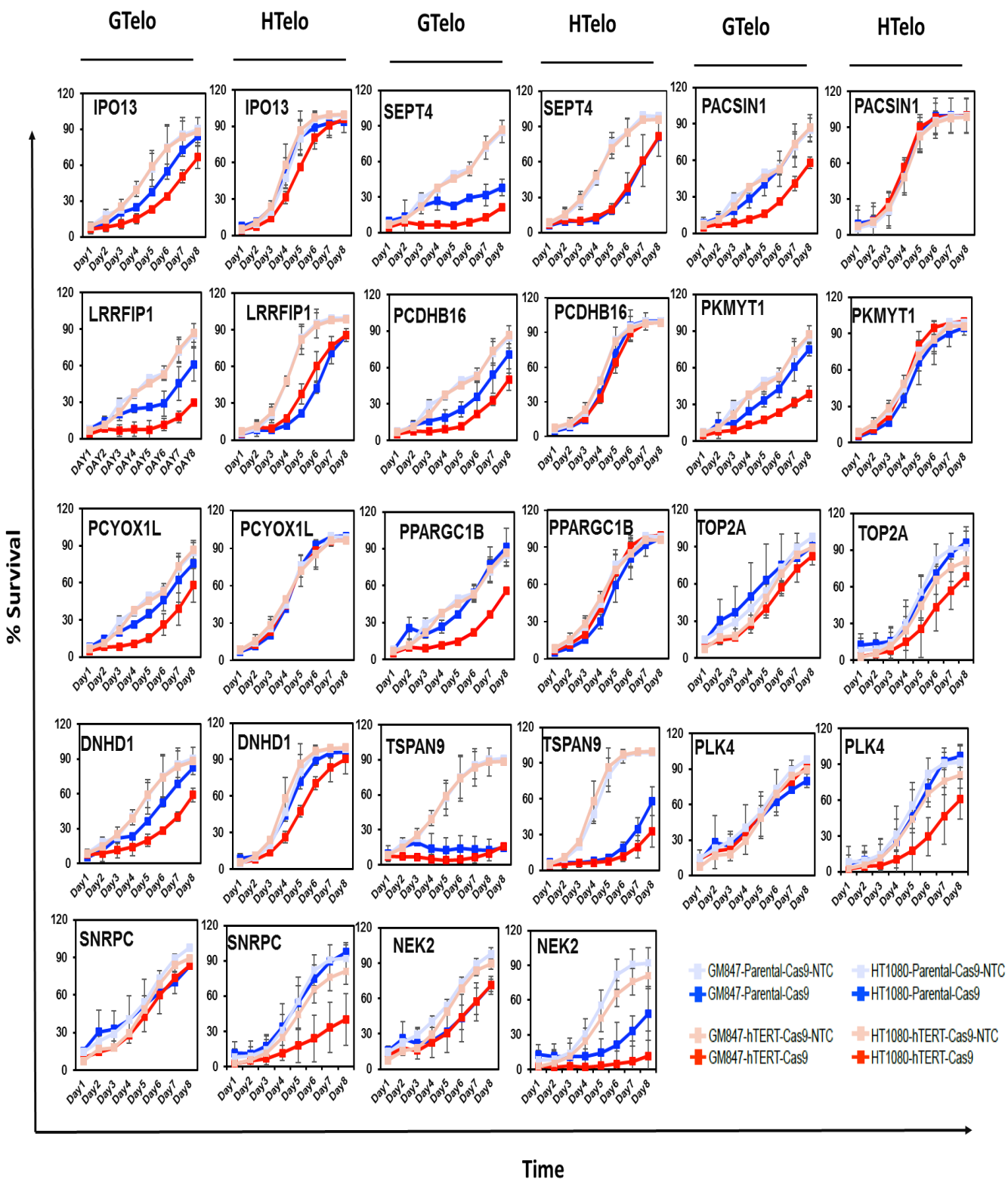
GTelo
HTelo
GTelo
HTelo
GTelo
HTelo
IPO13
IPO13
SEPT4
SEPT4
PACSIN1
PACSIN1
LRRFIP1
LRRFIP1
PCDHB16
PCDHB16
PKMYT1
PKMYT1
PCYOX1L
PCYOX1L
PPARGC1B
PPARGC1B
TOP2A
TOP2A
DNHD1
DNHD1
TSPAN9
TSPAN9
PLK4
PLK4
SNRPC
SNRPC
NEK2
NEK2
% Survival
Time
GM847-Parental-Cas9-NTC
GM847-Parental-Cas9
HT1080-Parental-Cas9-NTC
HT1080-Parental-Cas9
GM847-hTERT-Cas9-NTC
GM847-hTERT-Cas9
HT1080-hTERT-Cas9-NTC
HT1080-hTERT-Cas9

Figure 4.15. Validation of the SDL hits in two independent isogenic models that express Cas9 are represented. 42 genes decreased cell confluency by 30 % or more in at least one of the cell hTERT -High compared to hTERT-Low cell lines over a period of 8 days until the non-targeting control is confluent.

4.7 Cleavage products were observed for all isolated clones indicating a successful editing event.

To completely exclude the involvement of potential off-target effects of *sg*RNA, genome editing assay was carried on all 42 hits the were validated in the model cell lines using the CRISPR/Cas9-based system **(Figure 4.16).** CRISPR/Cas9 utilizes guide RNAs which direct Cas9 to the gene of interest for cleavage. Because Cas9 only cuts the individual gene of interest, this allows for effective knockout, with little off-target effect. To this end, GTelo cells were transduced with a construct containing sgRNA targeting individual gene. The knockouts were collected, and the assay was conducted as in method section (3.12 Genome editing). Efficiency of genome editing varied between knockouts since all of them showing mixed population rather than clean knockouts.

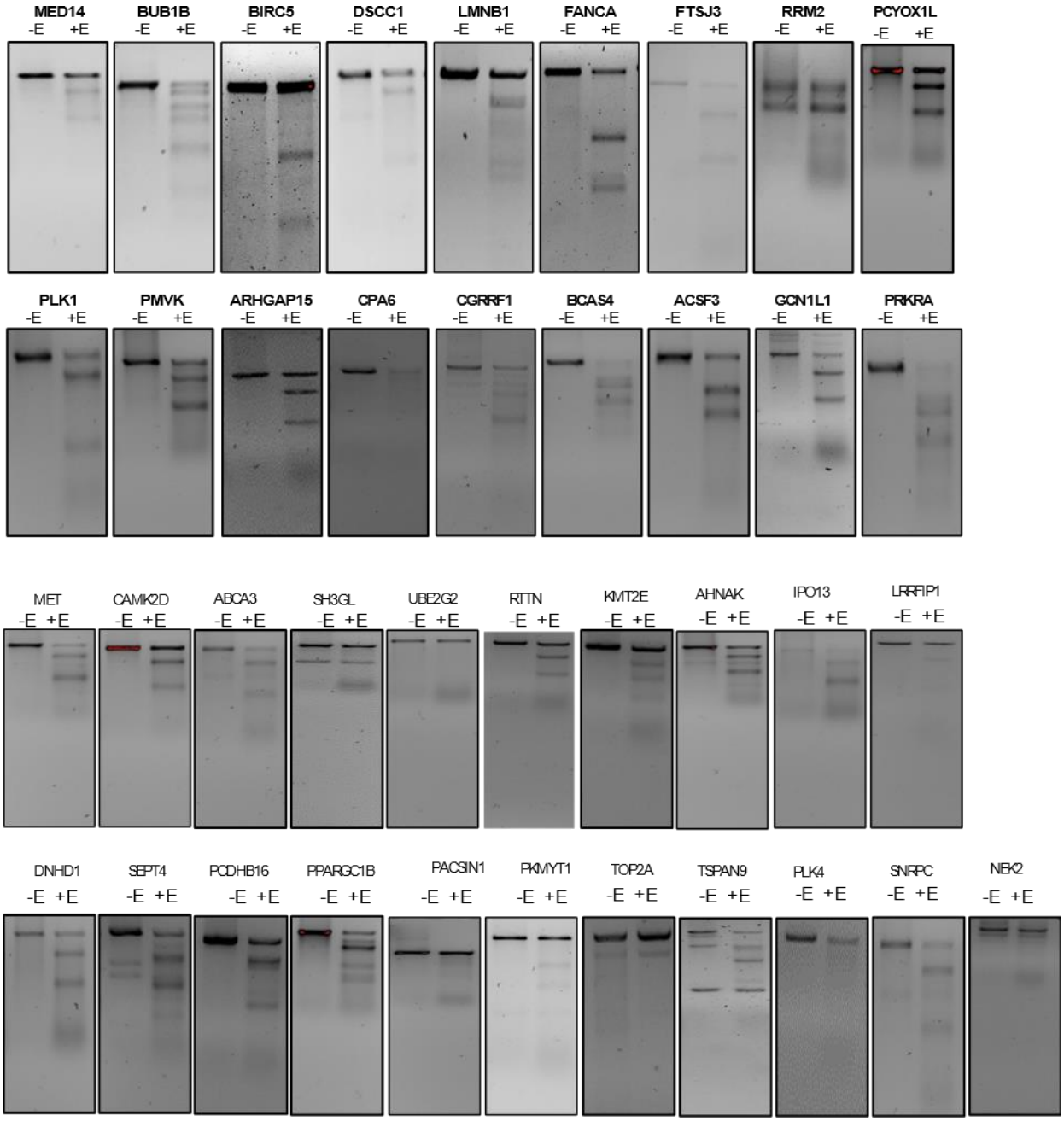

Figure 4.16. Confirmation of cleavage by CRISPR/Cas9 in GTelo-Cas. Confirmation of cleavage by CRISPR/Cas9 in GTelo-Cas cells for the 42 validated SDL hits. Cells were transduced with lentiviral particles containing two sgRNAs targeting individual hits, followed by the cleavage assay. The cleaved bands are shown in the lanes with endonuclease.

4.8 Tissue-agnostic validation the hTERT SDL hits by CRISPR/Cas9 system using individually cloned sgRNAs.

Identifying hTERT SDL interactions was done in an isogenic background using engineered cell lines A constitutively expressing hTERT for modelling hTERT overexpression **(Figure 4.1).** To further eliminate cell line effect of the validates hits, further validation across multiple cell lines was done. The 42 validated SDL hits were further validate using the same arrayed CRISPR-based strategy in cell lines that naturally overexpress hTERT. As telomerase has been known to be overexpressed in practically all cancers, we used the CCLE database (http://www.broadinstitute.org/ccle/home), and identified cell lines, representing multiple tumor types, that naturally overexpress hTERT **(Figure 4.17).** The selection was based on the availability of the cell lines. We chose at least two different cell lines for each type of malignancy, so that any individual cell line specific effects would be eliminated. hTERT expression and protein levels were confirmed in these cell lines. The final cell line are cells of breast (MDA-MB-231 and HCC70), colon (HCT15 and DLD1), pancreas (MiaPaCa2 and ASPC1), ovarian (ES-2 and SKOV3) and prostate (LnCaP and 22RV1) cancer origins. After that, we constructed Cas9-expressing stable cell lines **(Figure 4.18)** and Cas9-expression was confirmed by western blot.

Cas9 Expressing cells were seeded at a density of 2000 cell per in 96 well plates. Cells were transduced with individual sgRNAs targeting the 42 SDL hits and monitored for 6-8 days using the S3-IncuCyte® platform. Incucyte® Base Analysis Software was used to calculate cell confluency every 24 hrs. Hits that showed a difference of at least 30% compered to non-targeting control was count as a hit.

This arrayed screen in multiple cancer cell lines showed preferential lethality in most of the Cas-positive hTERT-overexpressing cancer cell **(Figure 4.19).** We looked at the genes that showed consistent effect across cell lines. This yielded 13 SDL gene knockouts that caused

lethality and our observations suggest that these 13 genes could be a target of choice for eliminating hTERT-high cancer cells.

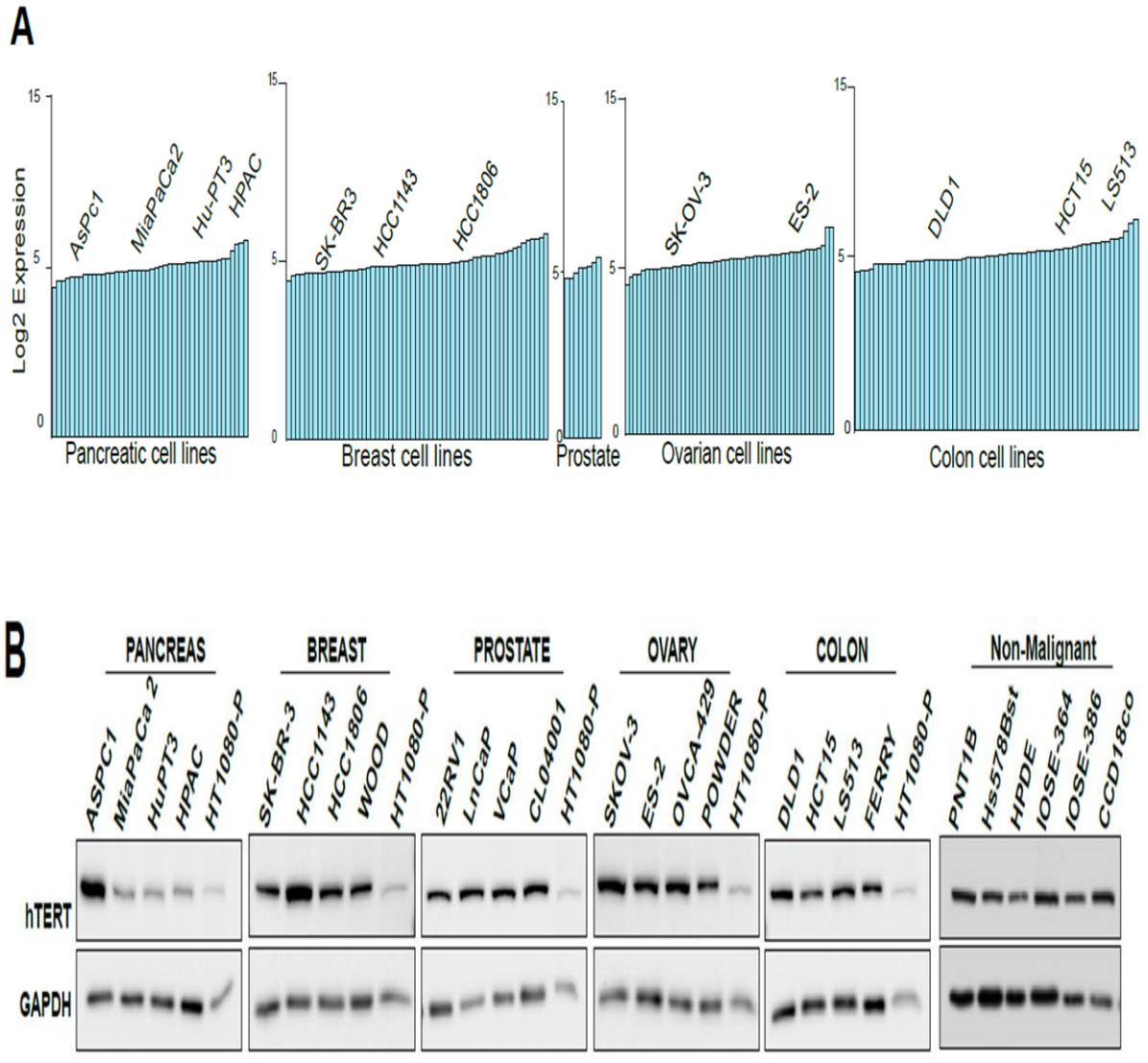

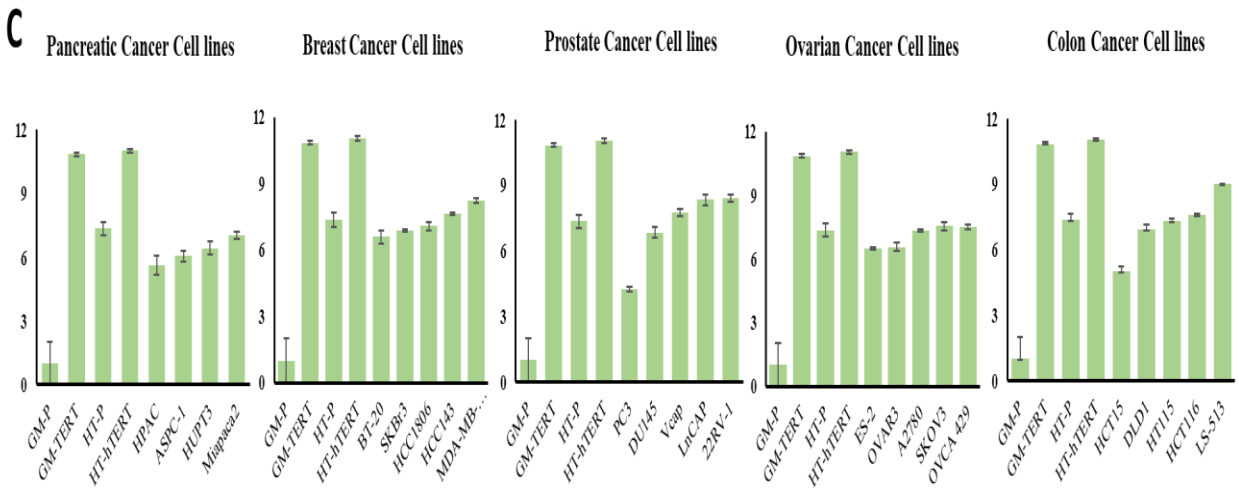

Figure 4.17.hTERT naturally over expressing cell lines. (A). qRT-PCR for cell lines that naturally overexpress hTERT from different tissue type obtained from CCLE database (http://www.broadinstitute.org/ccle/home)**.(B)** Western blot using anti-hTERT antibody for the cell lines selected from the CCLE database. **(C).** qRT-PCR for the showing fold change in hTERT for the selected cell lines.

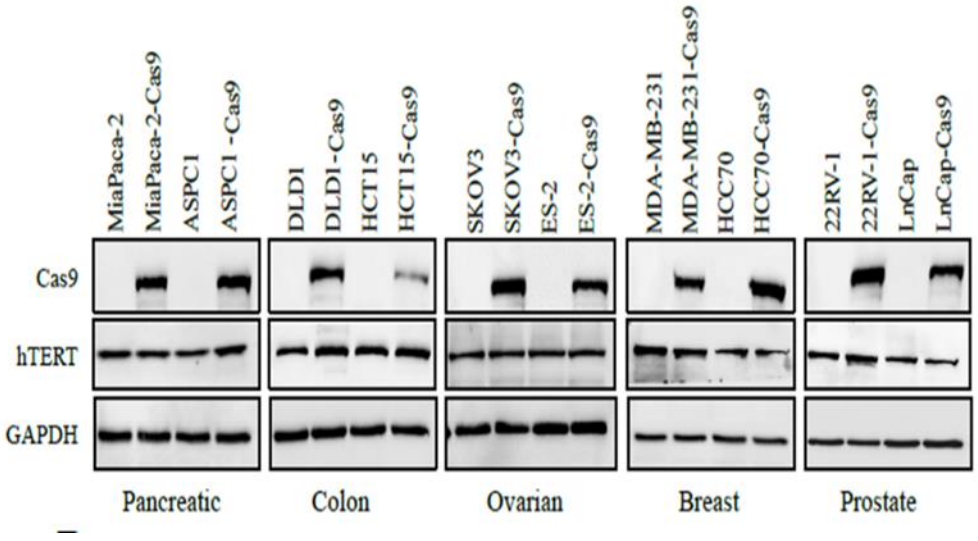

Figure 4.18 Cas9 and hTERT levels for two cell lines for each tissue type selected to validate the 42 hits.

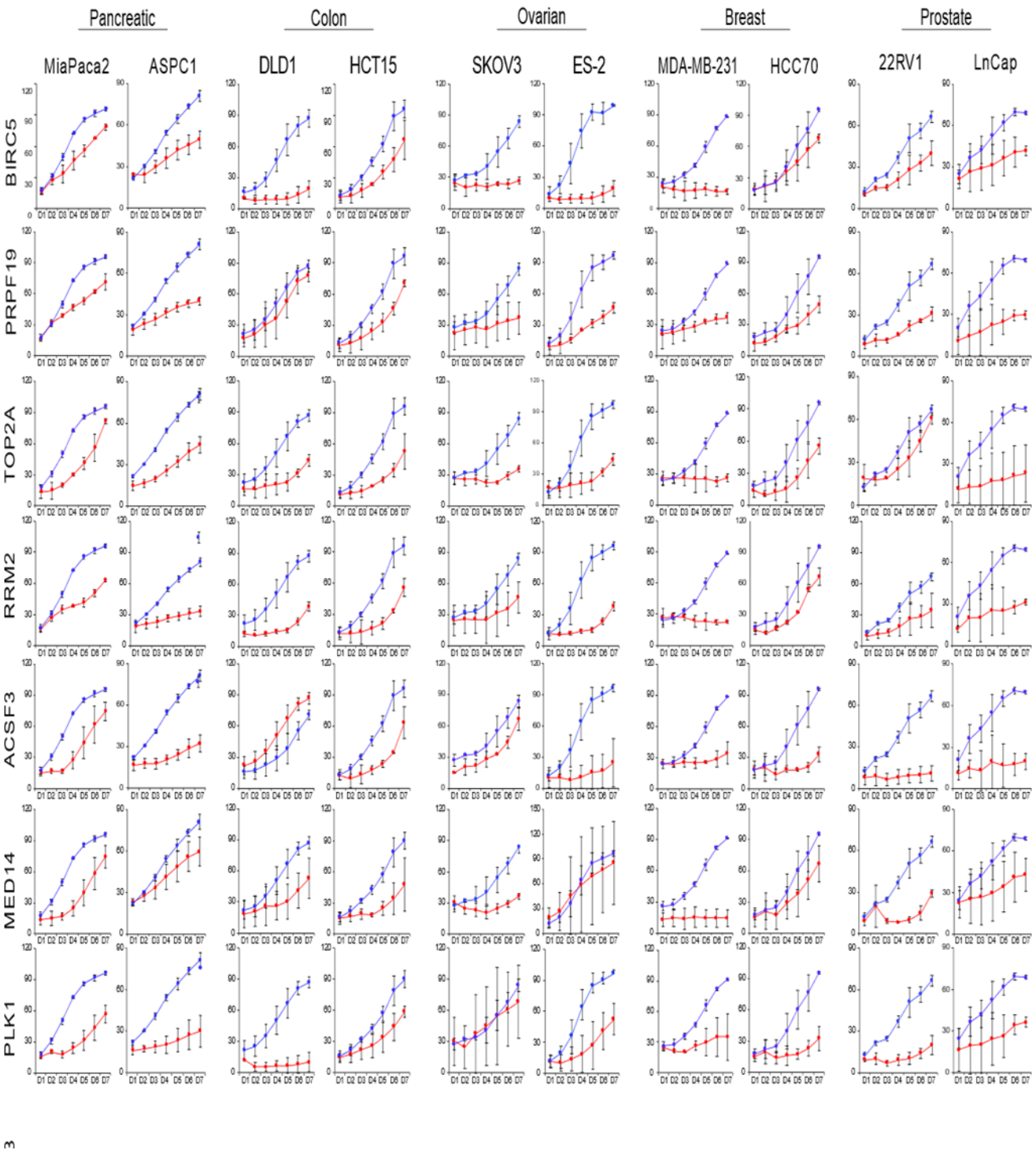
Pancreatic
Colon
Ovarian
Breast
Prostate
MiaPaca2
ASPC1
DLD1
HCT15
SKOV3
ES-2
MDA-MB-231
HCC70
22RV1
LnCap
BIRC5
PRPF19
TOP2A
RRM2
ACSF3
MED14
PLK1
D1 D2 D3 D4 D5 D6 D7

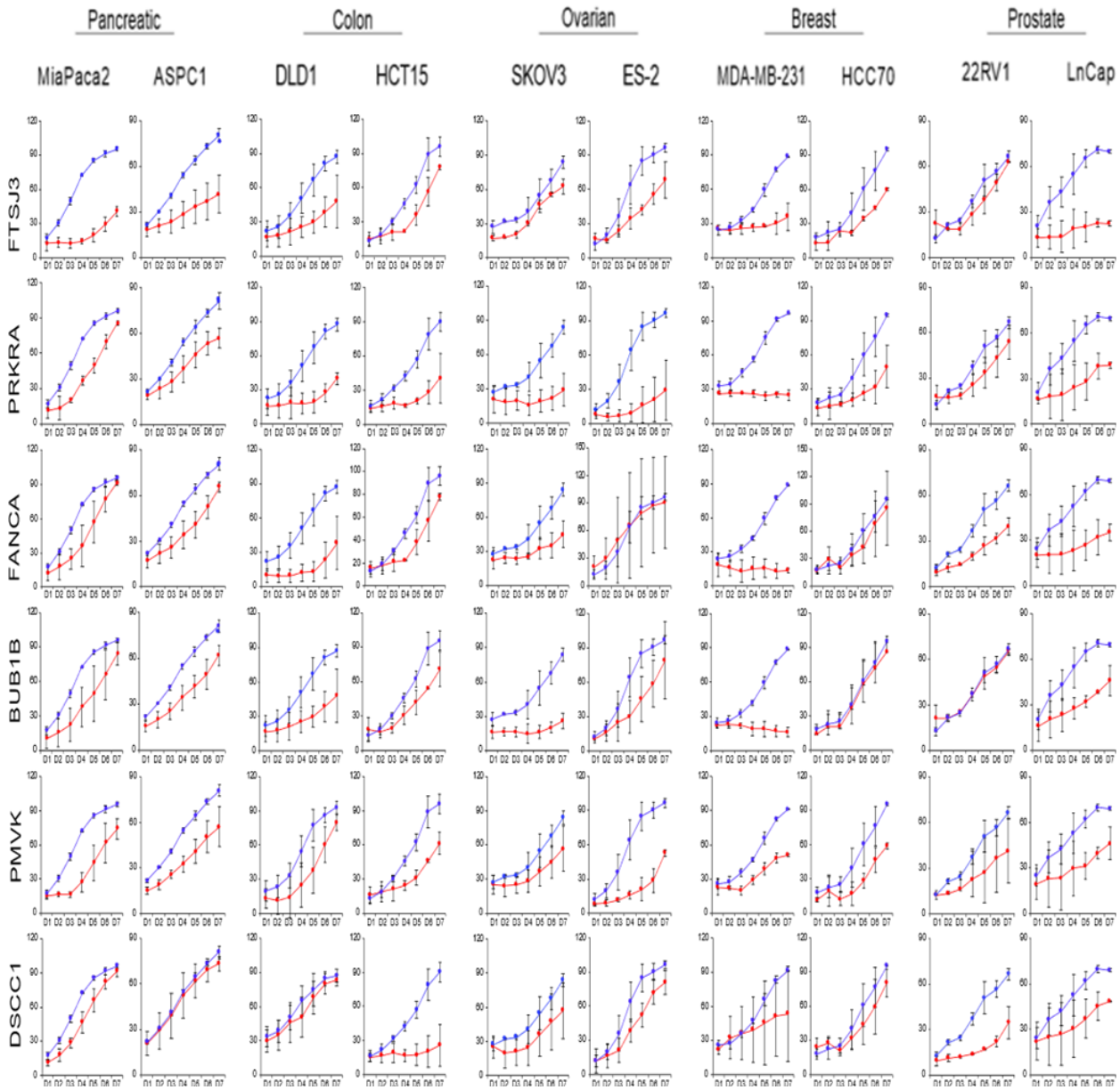

Figure 4.19. SDL hits validation in hTERT naturally expressing cell lines. Top 13 hits validated in naturally hTERT overexpressing cell lines across five different tissue types using CRISPR/Cas9 technology. The red is the gene of interest and the blue is the non-targeting control.

Gene	ASPC1	MiaPaCa2	22Rv1	LnCaP	MDA-231	HCC70	ES2	SKOV3	DLD1	HCT15
FTSJ3	39.19	54.97	6.31	47.25	52.77	21.60	28.39	15.16	39.09	12.65
PLK1	51.33	39.53	46.67	32.60	56.33	56.00	37.06	15.99	76.75	31.02
RRM2	47.69	32.70	32.35	38.00	66.29	52.00	58.27	37.21	48.83	39.89
PRPF19	41.11	24.57	35.88	39.70	52.03	45.70	49.98	47.16	8.38	25.86
MED14	21.55	21.56	37.48	30.40	76.64	28.40	11.35	47.55	34.19	42.61
ACSF3	48.91	21.33	55.61	49.76	53.90	63.80	71.99	17.51	16.31	32.62
ARHGAP15	15.67	18.31	18.54	34.02	14.59	-1.30	31.92	15.32	9.60	4.66
BIRC5	31.40	17.38	26.33	23.80	72.37	27.50	79.72	57.00	67.81	29.59
SEPT4	11.67	16.87	0.88	13.40	56.75	8.80	8.09	28.87	4.15	6.92
TOP2A	36.44	14.19	5.80	46.50	61.96	40.30	52.97	48.29	43.52	43.07
PLK4	12.78	13.22	5.04	33.00	3.76	4.90	44.26	15.72	2.60	3.34
BUB1B	19.25	11.73	4.91	23.30	72.46	9.20	17.45	57.77	5.97	24.91
PRKRA	24.45	10.22	7.34	30.70	71.62	45.50	67.39	54.87	47.47	49.19
ABCA3	5.61	9.66	5.73	38.38	9.37	1.30	14.46	-2.38	10.66	5.69
PKMYT1	28.80	9.49	42.46	20.88	8.56	0.00	11.63	9.93	-7.45	1.78
SNRPC	9.77	7.28	20.73	29.70	32.50	2.80	20.18	12.29	-4.84	-4.43
BCAS4	16.53	6.63	31.38	29.20	54.87	16.00	28.88	13.69	-1.37	7.93
CAMK2D	17.21	6.36	21.42	18.30	14.98	13.40	3.05	1.55	10.07	3.67
PPARGC1B	5.80	5.68	15.22	37.10	8.50	-1.70	14.63	9.22	-2.78	-7.95
PCDHB16	12.31	4.81	15.22	14.20	58.74	-0.20	0.68	44.28	29.41	8.25
FANCA	16.91	4.67	26.74	37.50	74.95	8.80	8.17	39.33	49.07	13.72
LMNB1	3.89	4.28	19.03	23.04	9.65	1.10	0.40	-2.36	8.25	-2.37
DSCC1	10.14	4.00	32.16	21.90	37.81	12.00	15.98	27.04	3.96	64.08
CGRRF1	15.02	3.65	15.90	13.70	45.34	9.10	7.95	45.95	33.08	16.58
PMVK	18.21	3.62	25.40	22.90	40.02	36.70	43.59	27.43	13.34	18.49
IPO13	15.34	3.17	9.67	16.40	4.27	0.90	13.10	13.43	-5.40	0.13
AHNAK	8.02	2.74	9.90	32.09	10.20	1.30	1.16	6.13	8.01	2.61
PCYOX1L	1.35	2.52	13.58	28.59	1.43	-5.40	12.53	-5.74	10.16	4.37
LRRFIP1	18.70	2.08	15.61	31.40	-2.31	7.90	14.89	10.79	1.81	-9.01
TSPAN9	2.81	1.28	9.41	25.46	7.63	7.90	16.50	4.08	3.01	7.09
GCN1L1	10.05	0.99	9.82	27.14	14.91	15.60	3.64	-5.91	4.93	4.72
WDR61	5.89	0.34	-0.19	28.00	19.15	1.60	5.56	18.90	-2.66	-2.95
SH3GL3	6.14	0.16	5.62	9.30	10.42	-3.00	-0.01	7.18	2.32	-4.45
UBE2G2	11.98	0.12	3.21	28.75	17.64	4.30	8.17	3.80	-0.91	1.73
KMT2E	2.11	-0.19	-5.61	9.90	7.76	-3.20	1.86	9.08	-3.67	-4.03
MET	13.36	-0.49	5.80	39.21	6.46	31.00	14.32	-1.10	0.10	-6.46
DNHD1	5.36	-0.59	5.89	8.00	12.62	-1.70	6.67	-0.91	-6.84	-6.13
HLA-A	8.84	-0.67	1.76	31.27	3.20	12.00	13.96	8.54	0.75	12.84
PACSIN1	0.67	-0.95	14.42	12.20	8.62	0.20	13.99	10.06	-3.73	-7.01
NEK2	-1.82	-1.68	8.89	8.80	-0.40	-0.90	6.71	2.85	1.07	8.55
RTTN	5.14	-2.04	-3.60	9.30	0.49	-4.20	10.35	2.34	5.97	-4.54
CPA6	8.00	-6.76	11.94	10.14	10.18	2.60	6.13	2.04	3.76	-4.74

Figure 4.17 Heatmap of the SDL hits in multiple tissue type with the difference in growth percentage. Hits were ranked in descending order based on how many cell lines the show growth suppression.

4.9 Investigating the canonical and non-canonical functions of hTERT from the hTERT SDL hits

In addition to its role in telomere maintenance, body of publication describe the non-canonical roles for telomerase (Lai et al., 2007; Martinez and Blasco, 2011; Roake and Artandi, 2020; Saretzki, 2014; Segal-Bendirdjian and Geli, 2019). We next tested if the identified SDL hits affect canonical functions of telomere maintenance. Therefore, we examined the three-dimensional nuclear-telomeric architecture defined by telomere number, size, and frequency of

telomeric aggregates after knocking out the SDL hit. We used MiaPaCa-2 cells that naturally overexpress hTERT, individually knocked out each of the 13 SDL hits. We investigate the 3D nuclear telomeric architecture using 3D Q-FISH with the telomere PNA probe was performed and TeloView^{TM} software was applied for the analyses. this single celled quantitative approach is a powerful tool to link the functionality of individual SDL hit to the canonical role of hTERT. At least 30 nuclei were analyzed for each knockout. Following the Knockout of the 13 SDL hits, we evaluated the total number of telomere signals, which corresponds to the number of telomeres in each cell. Cancer cells commonly exhibit both an altered number of telomeres per cell and a decrease in telomere length compared to normal cells. We found the knockouts of seven of the 13 SDL hits (FTSJ3, PLK1, DSCC1, FANCA, TOP2A, BUB1B and ACSF3) showed significant changes in their 3D nuclear telomere organization when compared to the non-targeting control (NTC). Representative images of the 3D telomere organization in NTC and in FTSJ3, PLK1, DSCC1, FANCA, TOP2A, and in BUB1B KOs (top row) with the 3D nuclei (blue) and the 3D telomere (red) organization (bottom row) are shown in **(Figure 4.20).** The quantitative analysis from 60 single cell of each knockout showed that FTS3 and BUB1B decreased telomere intensity and while PLK1 and FANCA knockouts showed increased in the total telomere intensity.

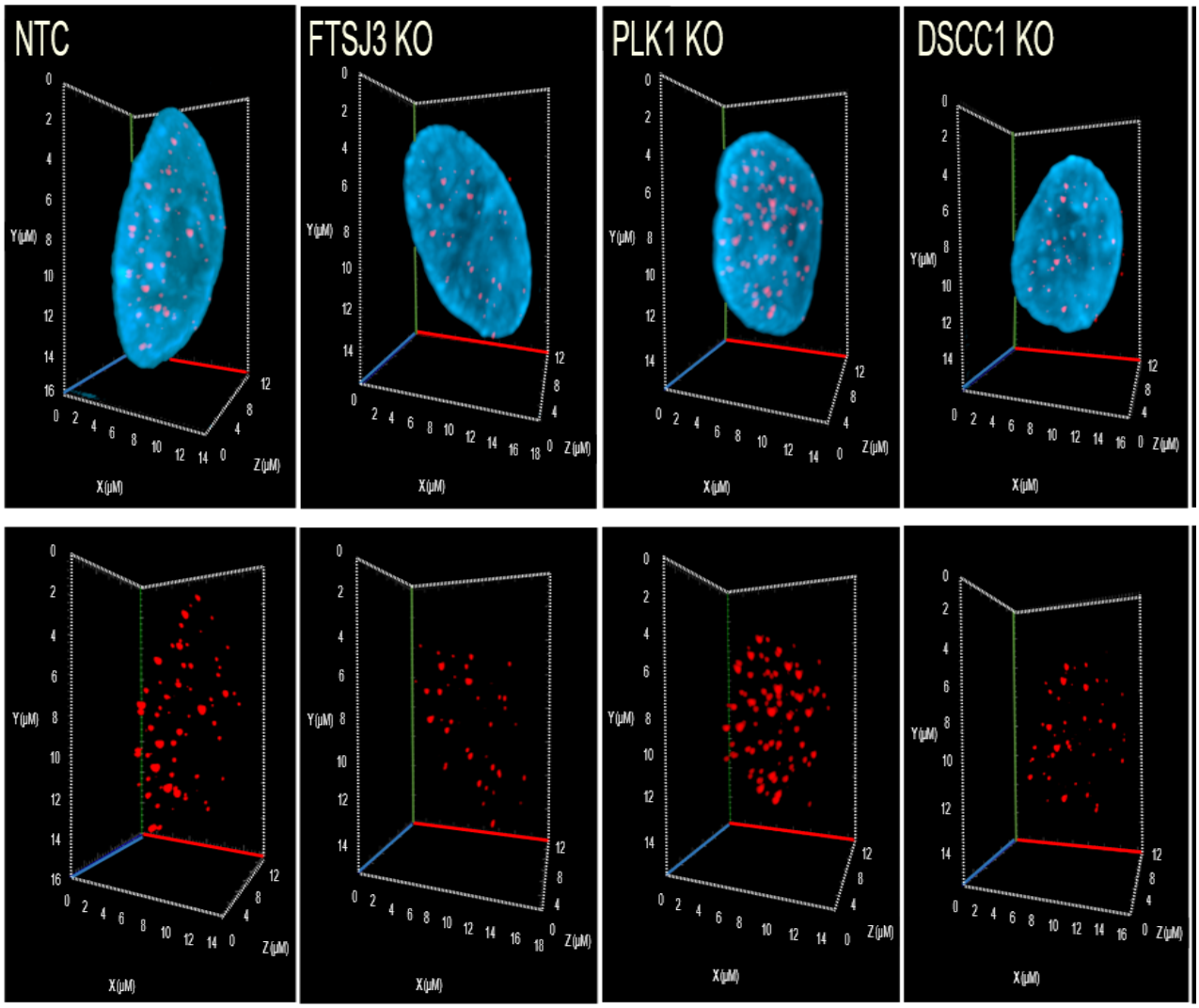
NTC
FTSJ3 KO
PLK1 KO
DSCC1 KO
Y (µM)
X (µM)
Z (µM)

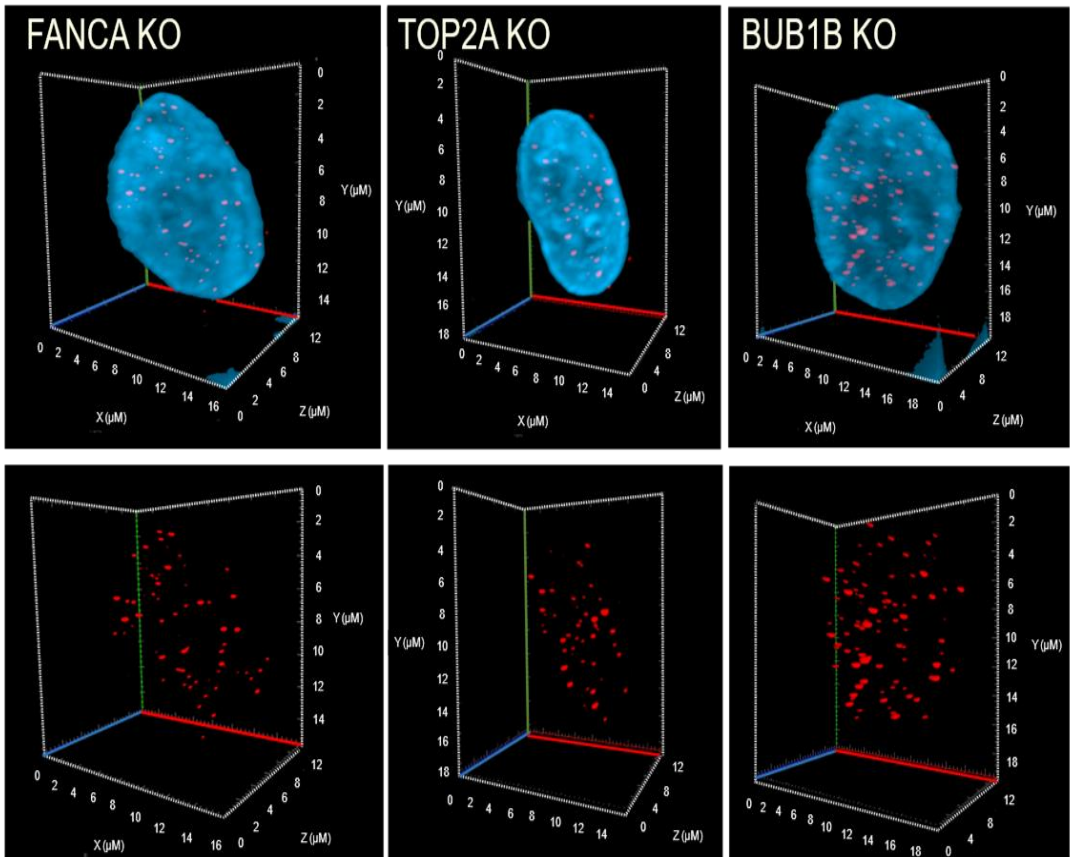

Figure 4.20 Investigating the canonical role of hTERT by 3D analyses of telomeres using TeloView. 3D nuclear telomere distribution (red) within the counterstained nucleus (blue) for SDL genes whose loss-of function affects telomeres are shown in the top panel. The bottom panel represents spatial representation of the telomeres.

Quantitative imaging and analysis using TeloView (Vermolen et al., 2005) allowed for the detailed analysis of telomere parameters and allowed us to determine significant 3D changes that included, but were not identical for individual targets, the total number of telomere signals detected, the nuclear volume and the total number of aggregates. The heterogeneity of the telomeric signals and their intensities (length) is indicated in the graphs shown in (**Figure 4.21)** for predicted canonical (blue) and non-canonical (red) targets, while **(Figure 4.22)** summarizes

box blots for respective 3D telomere markers measured in these experiments for canonical and non-canonical targets respectively. **Figure 4.21** summarizes the numbers of short or long telomeres found.

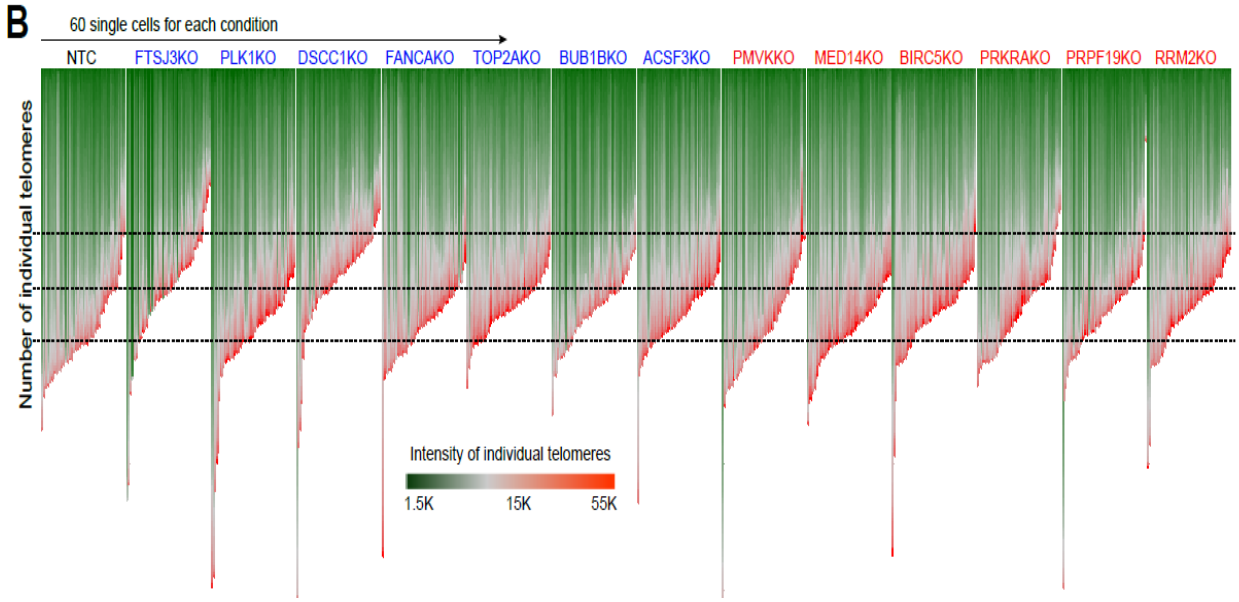

Figure 4.21 Gradient scale representation of the number of telomeres and their corresponding intensities (a measure of telomere length) gathered from 60 random cells in each of the selected 13 SDL genes knock outs.

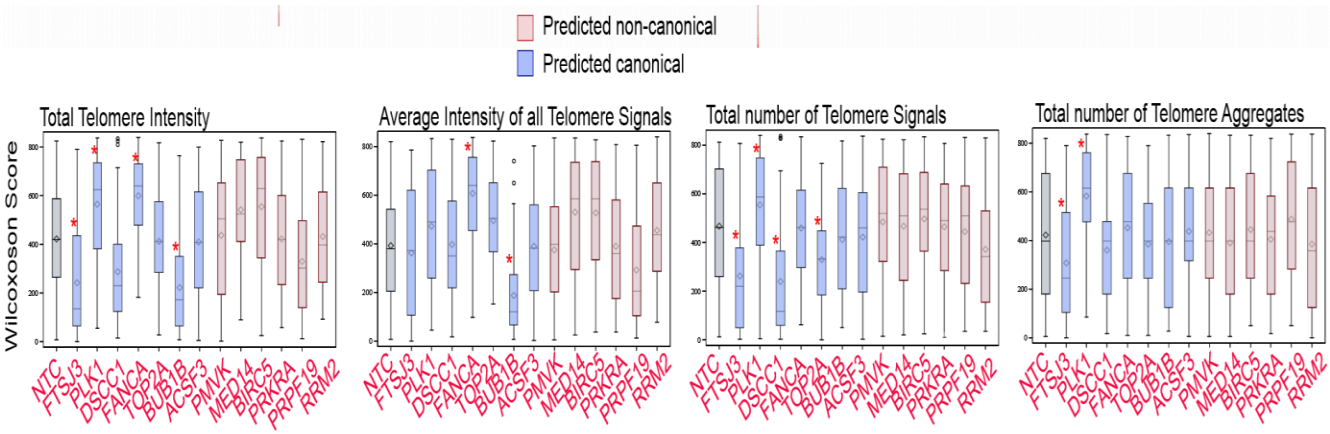

Figure 4.22 Quantitative measurements of telomere-specific parameters for all the 13 SDL hits to investigate their role in canonical and non-canonical functions of hTERT.

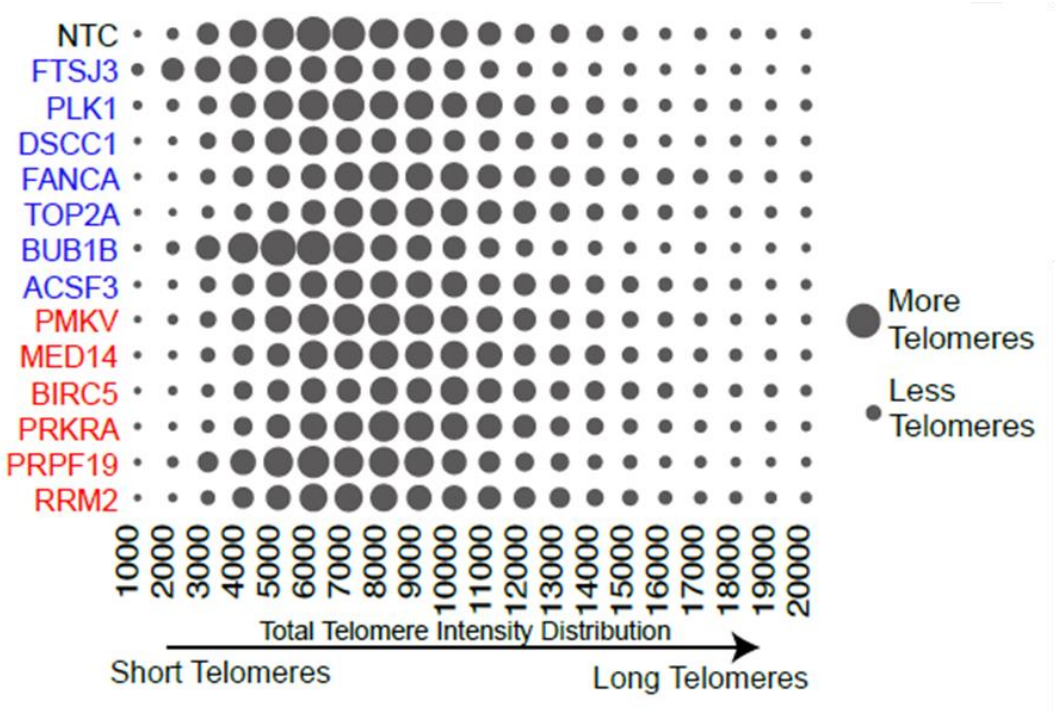

Figure 4.23 Dot plot representation of total intensity data that represents telomere length from single cells. The predicted canonical SDL hits (blue) show more short telomeres with low intensity (short telomeres), while the SDL hits in (red) show less short telomer.

4.10 SDL hits effect on TERT Expression and telomerase activity.

It is well established that the main mechanism involved in telomere maintenance is the enzyme telomerase (Kim et al., 1994). Since some of the identified SDL hits showed an effect on Telomere length, and our predication showed genes (FTSJ3,PLK1,DSCC1,FANCA,TOP2A,BUB1B,ACSF3) could be involved in canonical function of telomerase, we then asked whether these hits could regulate telomerase activity in MiaPaca2 cells. To test this, A TRAP assay was performed to measure telomerase activity **(Figure 24.4).** The results show reduction in telomerase activity in five of the seven SDL knockouts (PLK1, DSCC1, FANCA, TOP2A, and ACSF3). These results are in agreement with Teloview analyses confirming that these SDL hits may affect canonical functions of hTERT. However, BUB1B and

FTSJ3 did not affect the telomerase activity, suggesting that there affects on telomeric integrity may be due to other mechanism not related telomerase. Interestingly, hTERT protein levels were not significantly affected in any of these models **(Figure 4.25)**, suggesting the holoenzyme may be affected.

Overall, these data predict that at least five of the selected SDL hits may be involved in the canonical hTERT action and six of the SDL hits may be associated with non-canonical hTERT functions that are yet to be explored.

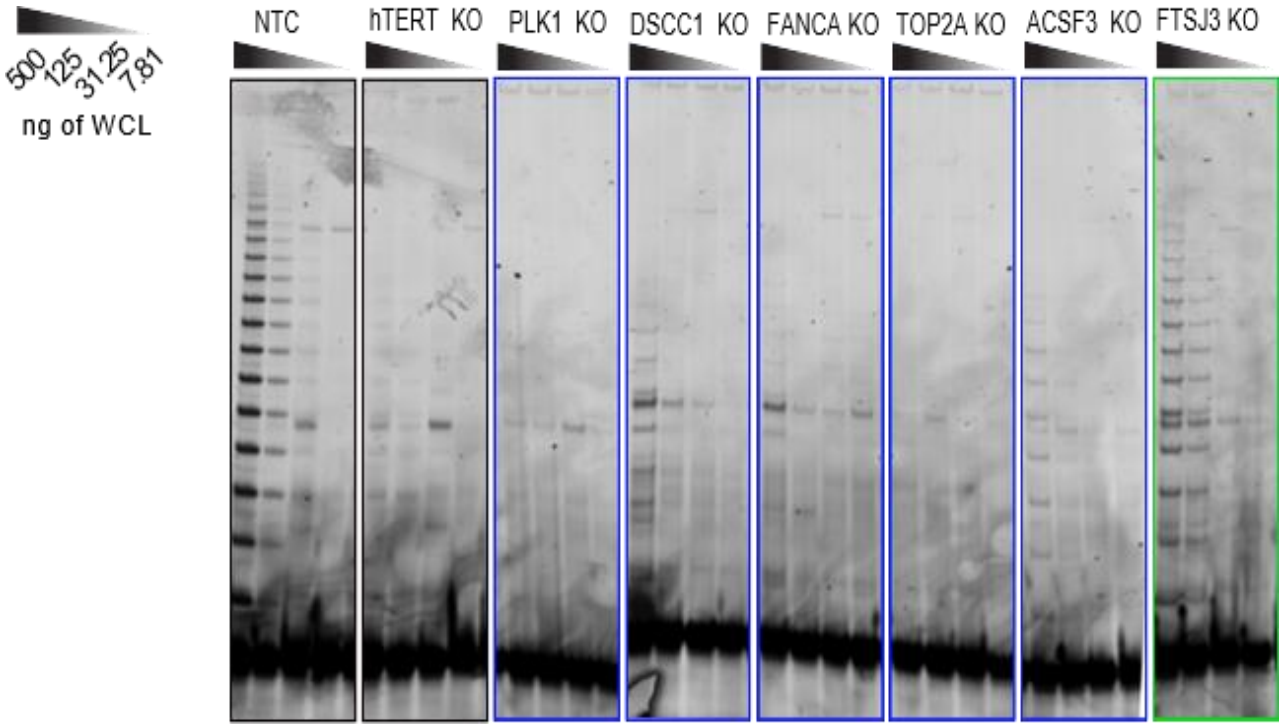

Figure 4.24. Telomerase activity. TRAP assay for the 7 hits predicated from Teloview to be associated with canonical function of hTERT.

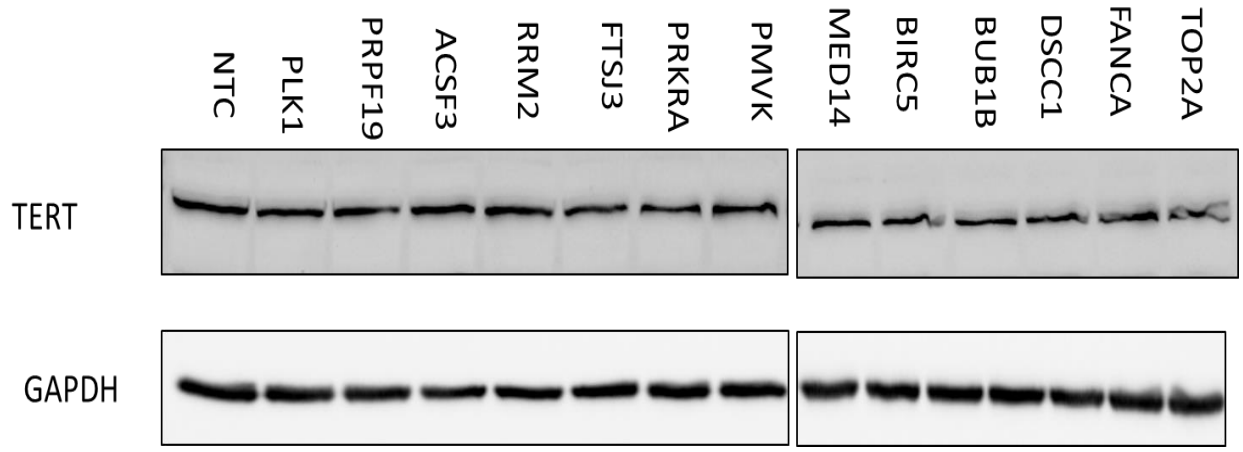

Figure 4.25 Western blot of hTERT for the Knockouts in Miapaca2-Cas cells.

4.11 Tumor-agnostic in vivo validation of the hTERT SDL hits in multiple cancer models

Three of SDL hits identified from the validation in cell lines in different cancer models were also assessed in primary pancreatic cells (FTSJ3, MED14 and PRPF19). We chose these genes because these gene caused the highest suppression of the growth in almost all the naturally hTERT-overexpressing cell lines as ranked in **Figure 4.17.** While PLK1 was also another top candidate, this SDL hit is also considered to have effects on non-malignant models and is generally deemed to be essential. As controls, we considered non-malignant cells that were not immortalized by telomerase overexpression and represented different tissue types, including HPDE-H6c7 (pancreatic cells immortalized by HPV16 E6/E7 gene expression(Furukawa et al., 1996), BPH-1, NHPrE1, BHPrE1 (primary prostate epithelial cells immortalized with SV40 large T antigen) (Hayward et al., 1995)Hs578Bst (breast epithelial cells)(Hackett et al., 1977), and CCD-18Co (intestinal epithelial cells). Unfortunately, all these non-malignant cells had high expression of

hTERT **(Figure 4.26)** figure shows high level of hTERT expression in non-malignant cell lines. Therefore, we chose a primary pancreatic cell line that had low/minimal expression of hTERT (PaCaDD135) and two additional hTERThigh primary pancreatic cell lines (PaCaDD161 and PaCaDD137) as controls for our analysis **(Figure 4.27)**. We used individual shRNA to knock down the expression of FTSJ3, MED14 and PRPF19 and found that their silencing suppressed the proliferation of hTERThigh primary pancreatic cell lines PaCaDD161 and PaCaDD137 but not hTERT-^{low} primary pancreatic cell lines PaCaDD135, with an exception of MED14 silencing in PaCaDD137, where it unexpectedly has not produced a suppressive effect **(Figure 4.28).**

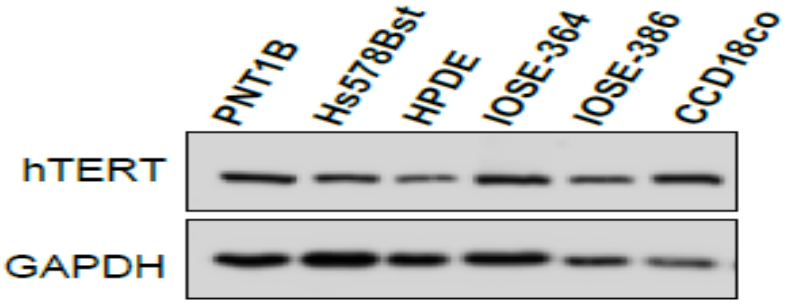

Figure 4.26 Western blot of non-malignant cell lines using anti-hTERT antibody.

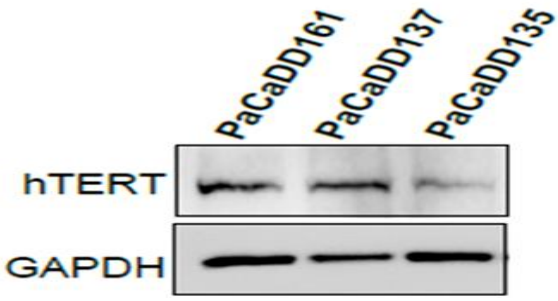

Figure 4. 27 Western blot of primary pancreatic cancer cell lines using anti-hTERT antibody.

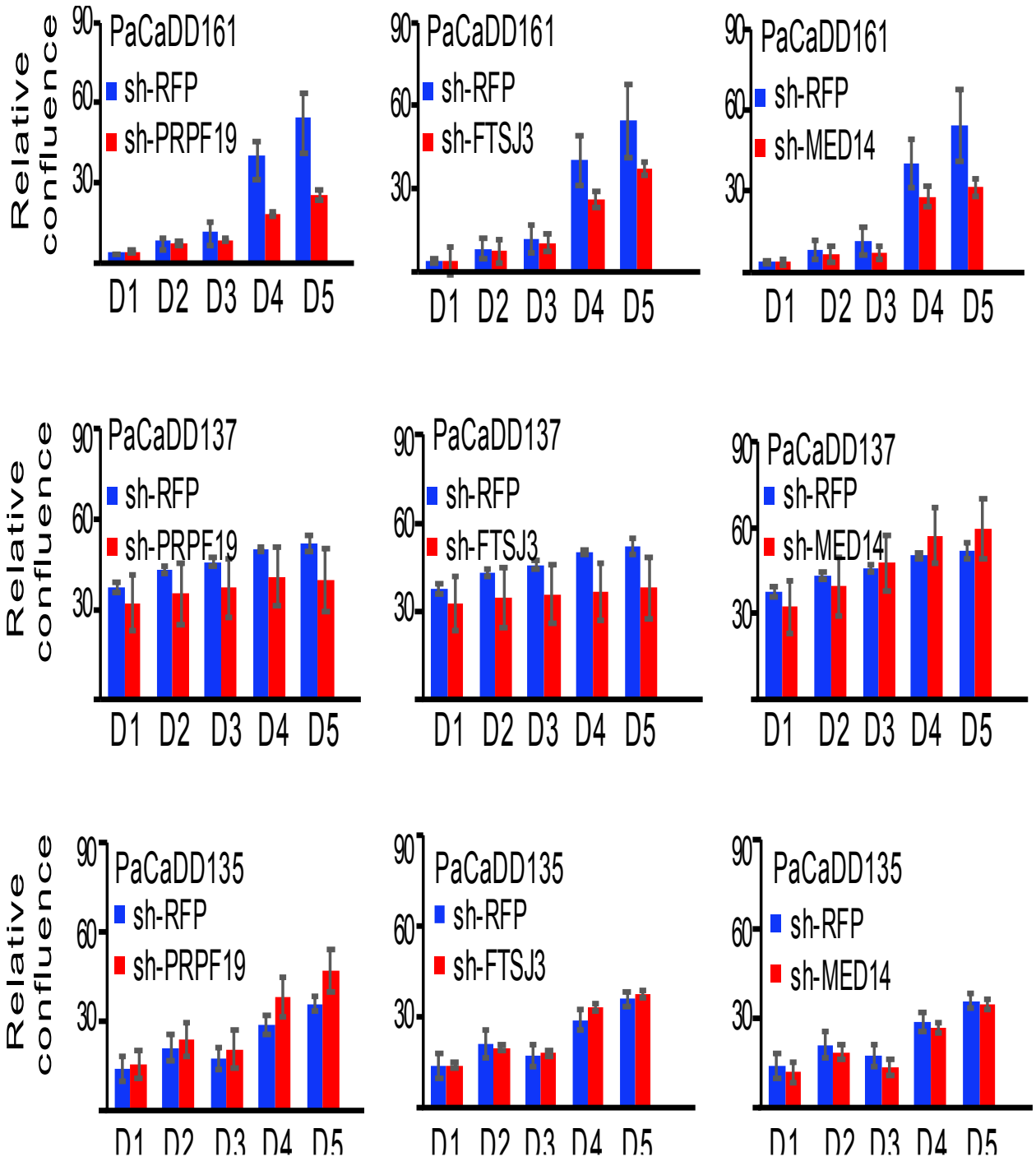

Figure 4.28 Validation of PRPF19, MED14, FTSJ3 in primary pancreatic cancer cell lines using pooled two shRNA targeting each gene compared to non-targeting shRFP as control.

4.12 Validation in animal models

After completing in vitro validation, the most promising SDL targets were selected and tested in appropriate animal model. We further extended our assessment of these three selected SDL interactions into xenograft models representing hTERThigh pancreatic, prostate, breast and ovarian tumors. We validated these three genes in four cell lines that are tumorigenic Miapaca2, ES2 ,22RV1 and HCC70. Tumor were produced in experimental animal model by injecting cell after knocking down each gene invitro shRFP was used as control for each model. Tumors reach detectable size after varying time point depending on the cell line. Measurement of tumor was then carried out until the mice had to be sacrificed in accordance with the guidelines established by the Animal Research Ethics Board. Almost all of three knockouts in all cell lines showed significant reduction in tumor size compared to the shRFP control **(Figure 4.29)**. Experiments were terminated when the shRFP control reaches approximately $1000mm^{3.}$ Tumors were excised and weighed. *in vivo* xenograft experiments showed that loss of FTSJ3, MED14 and PRFP19 could significantly reduce tumor growth all animal models with exception of FTSJ3 in MiaPaCa2 and PRPF19 in HCC70.

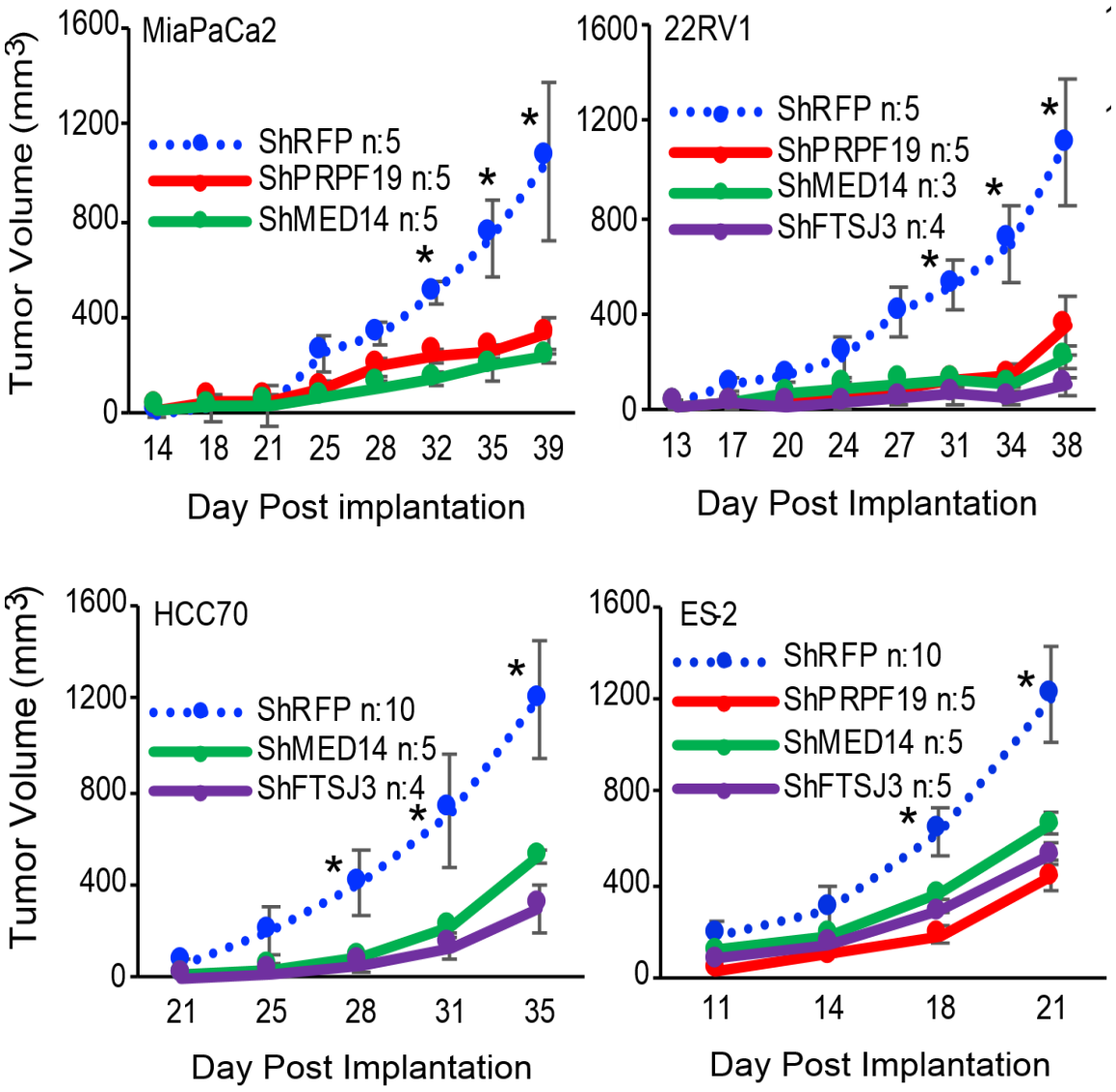

Figure 0.29. **Validation in Xenograft models**. The three hits (PRPF1, MED14, FTSJ3) were validated in xenograft model using 22RV-1, ES2 HCC70, and MiaPaca2.

Chapter 5 Discussion

Telomerase activity is repressed in majority of somatic cells but is overly expressed in majority of tumors. Reactivation of telomerase in malignant cells leads telomere maintenance and infinite proliferative capacity(Ding et al., 2019). Previous studies have shown that telomerase inhibitors often have a long lag phase before critical telomere shortening(Goldblatt et al., 2009). In addition, telomerase inhibitors can induce alternative lengthening of telomeres(Queisser et al., 2013). This indicates that tumor cells can use adaptive ways to evade cell death induced by telomerase inhibitors. Considering canonical and non canonical function of hTERT, questions arise with the use of anti-telomerase therapy, if their effect is due to downregulation or inhibition, does the effect is mimics hTERT downregulation, or is the effect supposed to inhibit telomerase as holoenzyme?

The aim of this study was to find genetic targets that fulfill SDL concept in telomerase overexpressing tumors. To achieve this aim, we performed genome wide pooled shRNA and CRISPR screen. This is the first study ever to investigate SDL in telomerase overexpression context. Our strategy to identify SDL hits of hTERT relies on the level of hTERT expression since this parameter is crucial for maintaining telomerase activity (Cong et al., 2002b; Kyo et al., 2008; MacNeil et al., 2016b). Significant differences in hTERT expression and telomerase activity between malignant and benign cells, suggest that hTERT expression critical in the development and progression of human cancer. Moreover, we believe that our approach based on expression levels captures SDL interactions based on both canonical and non-canonical functions of hTERT, since hTERT overexpression not only assures high telomerase activity, but also is essential for some of its non-canonical responses. Investigation of SDL interactions in this study is not limited to hTERT, but also the components of active telomerase holoenzyme. We aimed to

investigate the SDL interaction that may act to decrease expression hTERT, assembly of the holoenzyme and / or activity of the holoenzyme.

To comprehensively identify SDL interactions of hTERT, a strong model system was required. The isogenic cell line system used in this study offer a defined genetic background that can aid in identifying mutation specific vulnerabilities. In our isogenic cell line model, The HTelo-/+ model represent high and low TERT which is dependent on TERT(Cristofari and Lingner, 2006). HT1080 is a super-telomerase' which demonstrated massive telomerase activity and had by co-overexpression of TERC and TERT(Farooqi et al., 2018). while GTelo-/+ model is and ALT based model(Fleisig and Wong, 2012). The differences in hTERT expression between the isogenic cell lines as well as the activity **(Figure 4.1)** clearly showing our isogenic model embrace high and low TERT concept.

High-throughput genome wide screens have become powerful tools for studying a wide variety of biological processes. Applications of ShRNA screening together with CRISPR-Cas9 screening enabled us to identified sets of targets a required for growth inhibition in hTERT-^{High} but not hTERT-^{low}. shRNA reduces gene expression at the mRNA level, while CRISPR completely and silences the gene at the DNA level. limitations of High-Throughput Genetic Screening silencing method are that it suffers from high off-target effects. These targets result in phenotypes the is irrelevant to the gene of interest. Due to poor overlap between the two screen and difference false negative results. We took the two approaches as complementary to each other in finding SDL hits without giving and advantage of one technology over the other, we conduct genome wide screens to identify essential genes when gene function is reduced or lost.

To increase the reliability of the readouts we used multiple time points instead of start and end point where the dropouts must show consistent pattern to be scored as positive in each screen.

Additionally, using robust metrics described previously(Hart et al., 2014b) allowed identification of shRNA or sgRNAs that are depleted from the final cell population.

We identify 2763 potential hits at a level of genome-wide with significance as hTERT SDL at FDR < 0.05. As expected, shRNA screen scored more hits than CRISPR screens. ablating gene function with CRISPR will eliminate all essential genes. Several of which SDL hits are already known to be related to telomeres and/or telomerase. For example, loss of BIRC5 has been shown to reduce telomerase activity (Li et al., 2019).Similarly, binding of the shelterin component TRF1 to the telomeres have been shown to be dependent on PLK1 phosphorylation(Chen et al., 2020; Huang et al., 2015). In the same manner, it is not surprising to see the spindle assembly checkpoint protein BUB1B, as an SDL hit, as unprotected telomeres has been shown to activate spindle assembly checkpoint (Chen et al., 2020). and some of these checkpoint proteins were also shown to regulate telomere replication (19). Because this is the first study ever to look for hTERT SDL genes, we were unable to comparing our findings with others.

Clustering our SDL genes via cellular component analyses confirmed some relevance of hits with telomer and telomerase. our screens network analysis highlighted pathways and complexes related to nucleus, mitochondria, cell surface protein and signalling pathways. Enrichment of biological processes, including ribosome biogenesis, rRNA processing, rRNA metabolic process, translation initiation, ribonucleoprotein complex biogenesis, and RNA processing. Among the synthetic dosage lethal genes, there was a strong enrichment for genes involved in ribosomal biogenesis, which it not surprising since telomerase has been shown to affect ribosomal maturation as a part of its noncanonical function(Gonzalez et al., 2014). In addition, successfully validating chemical inhibitors of some of the targets in our list show that SDL that are more robust, and hence

more likely to be reproduced in follow up studies. Taken together our screens has identified genes that are strongly connected to telomerase.

Because genetic screens are notorious for false positive, experimental validation of the identified hits was required. However, validation of high number of hits is labour intensive. By validating tops hits from each screen, we may miss some of potential hits that can be a promising therapeutic target. Therefore, we used different strategies to select potential hits from the final list. Gene prioritization was based multiple unique approaches that enabled unbiased selection of genes for validation. Integration of publicly available databases combined with bioinformatic analysis.

To find more novel interactors, we utilized data bases such as Project Achilles and TCGA to prioritize SDL targets for subsequent validation. We believe that the computational approaches we employed to prioritize the final number of hits to be validated produced more robust SDL hits that can be potential therapeutic targets. Prioritization strategies reduced the number of hits to be validation to 187 after removing the hits were identified by multiple approaches.

Although both shRNA and CRISPR/Cas9 screen are unbiased approaches, false positives and false negatives results are very common. Experimental validation is still required to confirm any interactions. Validation in the model's cell lines aimed to identify cell-line specific interactions from the true SDL interactions. This extensive validation of 187 SDL narrowed down the number of the hits to for the next step validation. Indeed difference between the two screen technologies exist with CRISPT/Cas9 being more robust and specific than shRNA(Joung et al., 2017b). Consequently, next step validation was conducted in Cas9 expressing cells. Cas9 knockouts has been shown to have a lower false-negative and high reproducibility rates than shRNA(Joung et al., 2017b). Arrayed well-by-well screens allows more phenotypical changes observation rather than dropout number of reads. sgRNAs in the library was prepare in a way contain two sgRNAs

per gene. Our imaging system is based on monitoring cell confluency over time. Therefore, there is no or minimal false positive in our approaches and increase reliability. Minimal variation in the result due to variation in lentivirus concentration in arrayed screen library. 42 gene were successfully validated in model cell lines. These findings suggest that genes are lethal to the cell in the presence of high hTERT (**Figure4.15**). Taking into considerations that validated hits scored in different screen with different platform, more hits could potentially give a promising result. This warrants further validation of the other genes, particularly those with a higher ranking, to identify novel SDL with hTERT.

CRISPR is gene editing technology where CRISPR-associated nuclease9,Cas9, can edit the target DNA sequence complementary to the sgRNA(Sternberg et al., 2014). Cas9 generates precise DSB at target loci which can be repaired via one of the two DBS repair mechanism, homology-directed repair or, more often, nonhomologous end-joining. Although the technology is highly efficient in target editing, off target effects do occur due non-specific binding(2018). Among methods available for detecting genome editing efficiency is the T7 endonuclease(Frock et al., 2015). The enzyme can detects structural deformities in heteroduplexed DNA as a result of edited DNA(Sentmanat et al., 2018). Interrogation of cleaved DNA target by the Cas9 confirm that the phenotype was caused by depletion of a given gen and not due to an off-target effect.

Initial screens were done in isogenic cell lines. We choose cancer cell line panels from five different tissue types to increase the strength of the validated hits and eliminate any cell line specific effect. Experimental validation of potential hTERT SDL hits was done in a multiple cell lines representing five different tissue type. Since only 10-15 percent of tumors do not rely on telomerase for their telomere maintenance(Bryan et al., 1997), it was of great importance to screen for hTERT expression in these cell lines. Selected tissue types Breast, prostate, pancreatic, ovarian

and colon depends on previous report of these tissue express telomerase. Other common tissue types such as osteosarcoma and lung and glioma stem are reported to employ ALT pathway for their telomere maintenance(Deeg et al., 2016). We choose to generate CRISPR/Cas9-stable lines where the Cas9 nuclease has been stably integrated in the genome to minimize transfection efficiency. co-transducing with two lentiviruses is not as efficient. The Cas9 nucleases have emerged as a new genetic perturbation technology with high efficiency to precisely recognizing and cleaving DNA target. The CRISPR based validations to look at essentiality of the hTERT SDL hits in hTERT-^{high} model was chosen because shRNA knockdown may take longer time to produce effect. Cell lines from different tissue types responded differently to each knockdown as show in (**Figure4.16)** Efficiency of knockouts vary differently as LOF mutations can depend on the copy number of each gene. For example, DLD-1 cell line is a pseudodiploid human cell line with the modal chromosome number of 46 while MiaPaCa-2 cell line is a hypotriploid human cell line with modal chromosome number is 61(Source ATCC). Copy number variation of a target gene has great effect in determining the knockout efficiency by CRISPR/Cas system. Moreover, gene deletion might be more sensitive to copy number therefore, variation in copy number between the cell lines can dramatically affect the efficiency of the knockouts. Future studies are required to confirm our findings in these cell lines.

The high-confidence hits, 13 hits were chosen for an in-depth analysis of their roles in hTERT overexpression. **MED14 (**MED14 (Mediator Complex Subunit 14) that plays an essential role in transcription of protein-encoding genes(Lacombe et al., 2013). Mediator complex regulate RNA polymerase II dependent genes(Björklund and Gustafsson, 2004). Additionally, Mediator complex is important for chromatin remodeling as demonstrated to interact with chromatin remolding complex (CHD1)(Kagey et al., 2010). Mediator complex component has been shown

to affect telomeric repeat lengths(Zhu et al., 2011). Our data show that depletion of MED14 inhibit growth in Pan-cancer. However, there is no literature regarding the biological function of MED14 in telomere and telomerase.

We demonstrate that knockdown of **BIRC5** by CRISPR/Cas9 results in a significant reduction of cell viability in almost all tested cell lines.BIRC5 (Baculoviral IAP Repeat Containing 5) also known as Survivin is a member of the inhibitor of apoptosis (IAP) gene family(Martini et al., 2016). The Multitasking protein is ubiquitously expressed during embryonic development suggesting an important role for this protein in embryogenesis(Jiang et al., 2005). Pervious studies have shown that BIRC5 is overexpressed several malignancies and its expression increase telomerase activity(Endoh et al., 2005)

DSCC1 (DNA Replication And Sister Chromatid Cohesion 1) DSCC1 plays an important role in replication, spindle checkpoint and DNA repair is part of a member of alterative replication factor C (RFC) complex (Yamaguchi et al., 2014). Severe sister chromatid cohesion defects were detected upon DSCC1 deletion(Mayer et al., 2001). Additionally, RFC complex plays a crucial role in telomere stability(Gao et al., 2014). Knockdown of RFC component yield shorter telomere than control cells. Moreover, DSCC1 was found to regulated the expression snail genes(Kim et al., 2019), which is essential for telomere maintenance by regulating TERT expression(Mazzolini et al., 2018). Our data shows DSCC1 knockout slows the proliferation of colon cancer and prostate cell lines compared to the control.

BUB1B (BUB1 Mitotic Checkpoint Serine/Threonine Kinase B) is a spindle assembly checkpoint (SAC) that controls chromosome segregation (Chen et al., 2020). Mutations in BUB1B has been linked to the development of multiple tumor types(de Voer et al., 2013; Rio Frio et al., 2010; Wu et al., 2020). Furthermore, BUB1B was identified as one of the main genes in the

glioblastoma(Chen et al., 2020). BUB1B is recruited to kinetochores via BUB3-BUB1 complex forming a functional complex required for cell cycle control(Taylor et al., 1998).The SAC complex is recruited to the telomere via TRF2 during S phase and reduced expression of BUB3 or BUB1 has been reported to cause telomere abnormalities(Li et al., 2018). Additionally, TRF1 co-localization with BUB1B facilitates recruitment of BLM and telomere replication. Taken together, these results indicating a link between telomeres and the mitotic spindle.

TOP2A is topoisomerases Type II that is known to introduce double strand breaks resolving topological problems topological stress during telomere replication. (Nitiss, 2009). Reduction in expression of TOP2A increases telomere damage(Ye et al., 2010). In addition, TOP2A plays a role in the resolution of telomere fragile sites(d'Alcontres et al., 2014).

FANCA belongs to the Fanconi anemia complementation group (FANC). FANCA *i*s the most common FA subtype which plays a role several cellular processes including DNA damage repair(Abbasi and Rasouli, 2017). Additionally, FANCA are involved in telomere sister chromatid exchange (T-SCE) in ALT cells but not in telomerase-expressing cells(Fan et al., 2009).FANCA assembles in the nuclear complex in response to DNA damage(Garcia-Higuera et al., 2001). Mutation in FANCA gene has been associated with increased breast cancer susceptibility(Abbasi and Rasouli, 2017).

Polo-like kinase 1 **(PLK1)** plays a critical role in cell mitotic events(Archambault and Glover, 2009). PLK1 overexpression has been observed in various human tumors(de Cárcer, 2019). Huang et al demonstrated a positive correlation between PLK1 and telomere through increasing telomerase activity (Huang et al., 2015). Their results showed that PLK1 decreases hTERT ubiquitination and hence decreases its degradation. Moreover, PLK1 overexpression

destabilize PINX-TRF1 interaction thereby increasing telomerase recruitment to telomeres (Wang et al., 2010). Taking together, these data suggest strong interaction between PLK1 and telomerase

Pre-MRNA Processing Factor 19 (**PRPF19**) which also knows as Senescence Evasion Factor, is a multifunctional protein that plays a role in DDR(Montecucco and Biamonti, 2013). PRPF19 is responsible for THO/TREX complex recruitment to prevent R-loop formation at telomeric end therefore prevent telomere shortening(Pfeiffer et al., 2013; Yu et al., 2014).

RRM2 (Ribonucleotide Reductase Regulatory Subunit M2) is providing nucleotide pool necessary for DNA synthesis(Yang et al., 2020). Overexpression of the RRM2 promotes malignant transformation carcinogenesis(Shao et al., 2006). Moreover, RRM2 is associated with poor prognosis in breast cancer(Zhang et al., 2014). While there is no available data that connect RRM2 to hTERT, inhibition of RRM2 was reported to induce senescence(Delfarah et al., 2019).

ACSF3 (Acyl-CoA Synthetase Family Member 3) is malonyl-CoA synthetase that coverts malonic acid to malonyl-CoA. malonylation lysine has the same effect as lysine acetylation causing structural change in histone function(Xie et al., 2012). While protein malonylation has not been explored extensively yet, reduction of telomerase activity in ACSF3 knockout could a result of this effect.

Our data revealed that depletion of **FTSJ3** affects cell proliferation. FTSJ3 is RNA 2'-O-Methyltransferase 3 that was identified a potential regulator of breast cancer progression(Manning et al., 2020). The function of this gene has not been studied in cancer. However, 2′-O Methylation of telomerase RNA at specific site was reported to enhance telomerase activity(Huang and Yu, 2010). Further experiments are required to investigate the effect of FTSJ3 on TERC moiety of the enzyme.

PRKRA We found that knockout of PRKRA inhibits cell growth compared to control. PRKRA over regulated in colon adenocarcinomas(Chiosea et al., 2008), Overexpression of PRKRA in ovarian cancer was shown to promote chemoresistance(Hisamatsu et al., 2019). our validation shows significant reduction in growth in ovarian cancer cell lines by PRKRA depletion.) .PRKRA is a cellular protein activator of PKR kinase which binds to double stranded-RNA and impact microRNA maturation(Hisamatsu et al., 2019). regulation of TERT by microRNAs (Farooqi et al., 2018).

Overall, our pan-cancer CRISPR/Cas9 validation has evidently been useful in identifying most promising hTERT SDL targets.

Telomeres consist of a TTAGGG DNA tandem repeats with the associated shelterin. Disturbing the integrity of telomeric structure leads to genomic instability(Jafri et al., 2016). Loss of telomeric repeats or the repeats binding proteins triggers DNA damage response similar to DNA breaks leading to genomic instability (Maciejowski and de Lange, 2017a). As a consequence of telomere loss, chromosome enter a BFB cycle in which fusion of short telomeres occur creating dicentric chromosomes This is followed by breakage of the chromosome during the anaphase.

In this study we examined whether the down regulation of individual 13 genes affected the 3D structure of telomeres. The probe of this kit does not recognize sub telomeric sequences, and in contrast to traditional telomere restriction fragment (TRF) measurements, the DAKO kit, therefore, allows estimation of the telomere length without inclusion of sub telomeres. We used the semi-automated Teloview imaging platform (Vermolen et al., 2005) as it is scalable and, unlike telomere length measurements from aggregate populations, this single cell quantitative and three-dimensional (3D) approach is a powerful tool to link the SDL hits to telomerase and telomeres.

Our observation of increased number of aggregates indicate more chromosome fusion is taking place in some of knockouts (FTSJ3, PLK1, DSCC1, FANCA, TOP2A, BUB1B and ACSF3). Random selection of 60 single cell for analysis to assess telomeric phenotype in each of the 13 knockouts in Miapaca-2 cell line allows for more c. We selected cells randomly with the same experimental conditions and assessed directly the telomeric phenotype and the measurements were averaged across cells to allow the comparison of each parameters across cells as a population. The observation and of the effect are challenging since the degree of knockouts can not be confirmed in this situation. Differences in the 3D nuclear telomeric architecture between reveals the degree of genomic stability induced upon the knockdown of each gene.

Although we did not assess shelterin proteins bound to telomere, it seems reasonable to suppose that the deprotected telomere is resulted from low expression of shelterin component. Insufficient levels of shelterin components, e.g. TRF2 and RAP1, can affect telomeric end integrity at chromosome ends(van Steensel et al., 1998). The abundance of short telomere and aggregates in the knockouts indicate substantial induction of aneuploidy which can inhibit tumorigenesis(Weaver et al., 2007).

Since telomeres maintenance is dependent on telomerase activity, the proposed changed of telomeric structure is further tested using TRAP assay. Our results show significant reduction in telomerase activity of the tested knockout in the same experimental conditions. With FTSJ3 is being an exception, the effect of each of the knockouts where showing significant reduction of telomerase activity compared to the control. A control matching increase of telomerase repeat addition processivity was observed in FTSJ3. In Q-FISH experiment cells were randomly selected while in TRAP assay the entire knockout population was selected.

To clarify how the knockouts affecting the telomerase activity experimental confirmation of TERT expression was required. The results showed no reduction in protein levels of the knockouts. Telomerase activity is strongly correlated with TERT mRNA expression but not with hTERC expression regardless of it′s ubiquitous expression(Schmidt and Cech, 2015). Presumably, the levels of the knockout are sufficient enough to affect the activity. Reduced repeat addition processivity of telomerase was not supported by low expression data. Ablation of telomerase activity with no substantial effect on the protein levels suggest other components of the holoenzyme is could be affected ultimately leading to low activity of the enzyme. The lack of the expected correlation between the expression and activity could be attributed to recruitment of the enzyme to telomeric ends. Telomere proteins including TPP1, which contributes to telomerase recruitment to telomeres and telomere elongation (Zaug et al., 2013). Another possibility that the interaction between TERT and TERC is disrupted by the knockouts. Previous study Blocking the interaction between the hTERT and the chaperon proteins inhibits telomerase assembly therefore decreasing its activity(Holt et al., 1999).

As mentioned above, hTERT is regulated post-transcriptional process is likely to affect the activity of telomerase. Premature translation results in truncated hTERT and dysfunctional telomerase (Yi et al., 2001b).Since full-length hTERT is the limiting factor for the formation of telomerase activity(Wong et al., 2014), another question arises from these results whether these knockouts can create a splice variant of hTERT which lacks the activity but still detected at the protein level. hTERT is spliced into active and inactive forms simultaneously in telomerase positive cells. Alternative variants of hTERT can still bind to hTERC when expressed but lead telomere shortening due to absence of enzymatic activity (Yi et al., 2000). In addition, hTERT low abundancy makes it difficult to detect and quantify accurately(Akıncılar et al., 2015).

For successful translation of SDL hits, extensive validation of the hits is required. In this project we focused mainly in validating the SDL hits in multiple models to eliminate cell line specific effect. In our validation we tired to look for a non-malignant cancer cell line to serve as a control. However, all non-malignant cell lines (figure) have high expression of hTERT. Validation of the top 3 hits in the primary pancreatic cancer cell lines showed that increased our confidence in the identified hits (FTSJ3, MED14 and PRPF19*)* supressed proliferation $hTERT^{high}$ primary pancreatic cell lines PaCaDD161 and PaCaDD137 but not PaCaDD135 which we identified as $hTERT^{low}$ figure(western). with the exception of MED14 silencing in PaCaDD137, where it unexpectedly showed no effect on proliferation suggesting hTERT SDL interactions likely operate in a context-dependent manner. Additionally, we extended our validation of these three selected SDL targets (FTSJ3, MED14 and PRPF19*)* into pancreatic, prostate, breast and ovarian xenograft models. Our data shows significant reduction in tumor growth upon FTSJ3, MED14 and PRPF19 silencing **(Figure 4.29)**. Despite the unexpected for FTSJ3 in breast xenograft model and PRPF19 in ovarian xenograft model, our data reveal the tumor agnostic effects of hTERT SDL relations in multiple types of malignancies. Taken together, our hTERT SDL targets show promising interactions that can be selected for treatment development.

Additional testing for these possibilities is needed to determine the utility of our data for identifying synthetic lethal interactions. Whilst there may be true interactions present in the results, the variability makes the data difficult to interpret with confidence.

Chapter 6: Conclusion and future directions

6.1 Conclusion

Taken into to consideration the overexpression of hTERT in majority of human cancer, telomerase forms a promising target of anti-cancer therapy. UpToDate, aims to identify of novel anti-telomerase inhibitors has not been successful. This project aims to identify new therapeutic target deals with telomerase overexpressing tumors that can be using genetic interaction. Although these genetic interactions are rare, they still provide promising tool to identify novel therapeutic targets. For example, PARP inhibitors Olaparib is the first FDA approved drugs based on synthetic lethality interactions(Gao and Lai, 2018).

We tried to find an SDL interaction with hTERT knowing that hTERT expression closely correlates with telomerase activity in vitro and in vivo. Our method of conducting genetic screen, hits prioritization as well as extensive validation identified target in hTERT overexpressing cancer models. Using genome-wide screening as unbiased technique that allows systematic identification of rare SDL interactions. Even though genetic screens provide a robust tool to identify their interaction, limitations still exist. False positive and false negative interaction are very common in high throughput screening technologies. Our focus was to do extensive validation of the identified targets. In addition to gene by gene validation, we conducted chemical validation for some of the identified targets. This added more confidence in the final gene list obtained from these screens. Another limitation of high throughput screening that most of these screens are conducted in cell lines. The heterogeneous nature of available cell lines makes these identified targets context dependent where a mutation in one cell line may not be present in another cell line. Selecting multiple cell lines selection from different tissue types gave us more advantage in eliminating cell line specific effect. We were able to identify substantial lists of potential SDL interactions. Our

hits selection strategies enable us to select multiple targets for subsequent validation while reaming unbiased. CRISPR is known for its lower susceptibility to systematic off-target effects. Therefore, we validated the computationally prioritized 187 genes using arrayed CRISPR technology. We found 42 hTERT SDL hits to significantly reduce cell growth in the model cell lines. The next round validation round in hTERT naturally overexpressing cell lines for the 42 genes showed some promising targets that were validated in multiple tumor types. The single cell analyses using Teloview followed by TRAP assay showing some of the identified hits affecting the hTERT canonical functions while others maybe affect non canonical functions of hTERT.

6.2 Future directions

This work uncovered new SDL interaction with hTERT. We conducted shRNA and CRISPR SDL screens to uncover target genes of hTERT. With further validation this could be a new systematic approach for finding SDL target genes that can be utilized to develop therapies for telomerase overexpressing tumors. the project predicted specific general mechanisms of the tested targets. These predictions need more investigation to broaden our understanding of the mechanism by which successful design chemical inhibitors. Although we believe that our hit prioritization strategies provide an unbiased way of selection, some other hits can still be used for further validation.

Here we have demonstrated the link between telomerase and the identified gene via extensive validation and their effect on proliferation. Additionally, we highlighted the effect of knockout on telomeric structure and telomerase activity addressing the conical and non canonical function of telomerase. Further investigation of the connection between TERT and these knockouts. This will allow for more understanding whether these targets have a direct interaction on the hTERT or is affecting the function of hTERT. Using strategies such as antibodies or small peptide-based inhibitors can be of great benefit in studying the molecular interactions. Based on our data, the most logical extension of this work involves investigation of the effect of these genes shelterin complex components and component of the holoenzyme. Super-resolution fluorescence imaging can provide more information about localization of shelterin proteins and the overall structure of telomere. Observing telomere structure integrity in studying telomeres dynamics to avoid false positive results. While our work has identified several functionally related factors, further investigation is still required to understand how these targets can be utilized in developing new anti-tumor therapies.

References

(2018). Keep off-target effects in focus. Nature Medicine *24*, 1081-1081.
Abbasi, S., and Rasouli, M. (2017). A rare FANCA gene variation as a breast cancer susceptibility allele in an Iranian population. Molecular medicine reports *15*, 3983-3988.
Akıncılar, S.C., Low, K.C., Liu, C.Y., Yan, T.D., Oji, A., Ikawa, M., Li, S., and Tergaonkar, V. (2015). Quantitative assessment of telomerase components in cancer cell lines. FEBS Lett *589*, 974-984.
Akincilar, S.C., Unal, B., and Tergaonkar, V. (2016). Reactivation of telomerase in cancer. Cellular and molecular life sciences : CMLS *73*, 1659-1670.
Archambault, V., and Glover, D.M. (2009). Polo-like kinases: conservation and divergence in their functions and regulation. Nat Rev Mol Cell Biol *10*, 265-275.
Armanios, M., and Greider, C.W. (2015). Treating Myeloproliferation--On Target or Off? N Engl J Med *373*, 965-966.
Arndt, G.M., and MacKenzie, K.L. (2016a). New prospects for targeting telomerase beyond the telomere. Nat Rev Cancer *16*, 508-524.
Arndt, G.M., and MacKenzie, K.L. (2016b). New prospects for targeting telomerase beyond the telomere. In Nat Rev Cancer (England), pp. 508-524.
Arnoult, N., Schluth-Bolard, C., Letessier, A., Drascovic, I., Bouarich-Bourimi, R., Campisi, J., Kim, S.-H., Boussouar, A., Ottaviani, A., Magdinier, F.*, et al.* (2010). Replication timing of human telomeres is chromosome arm-specific, influenced by subtelomeric structures and connected to nuclear localization. PLoS genetics *6*, e1000920-e1000920.
Artandi, S.E., and DePinho, R.A. (2010). Telomeres and telomerase in cancer. Carcinogenesis *31*, 9-18.
Asai, A., Oshima, Y., Yamamoto, Y., Uochi, T.-a., Kusaka, H., Akinaga, S., Yamashita, Y., Pongracz, K., Pruzan, R., Wunder, E.*, et al.* (2003). A Novel Telomerase Template Antagonist (GRN163) as a Potential Anticancer Agent. Cancer Research *63*, 3931.
Ashworth, A., Lord, C.J., and Reis-Filho, J.S. (2011). Genetic interactions in cancer progression and treatment. Cell *145*, 30-38.
Azzalin, C.M., Reichenbach, P., Khoriauli, L., Giulotto, E., and Lingner, J. (2007). Telomeric repeat containing RNA and RNA surveillance factors at mammalian chromosome ends. Science *318*, 798-801.
Bandaria, J.N., Qin, P., Berk, V., Chu, S., and Yildiz, A. (2016). Shelterin Protects Chromosome Ends by Compacting Telomeric Chromatin. Cell *164*, 735-746.
Barrientos, K.S., Kendellen, M.F., Freibaum, B.D., Armbruster, B.N., Etheridge, K.T., and Counter, C.M. (2008). Distinct functions of POT1 at telomeres. Molecular and cellular biology *28*, 5251-5264.
Barthel, F.P., Wei, W., Tang, M., Martinez-Ledesma, E., Hu, X., Amin, S.B., Akdemir, K.C., Seth, S., Song, X., Wang, Q.*, et al.* (2017). Systematic analysis of telomere length and somatic alterations in 31 cancer types. Nat Genet *49*, 349-357.
Baur, J.A., Zou, Y., Shay, J.W., and Wright, W.E. (2001). Telomere position effect in human cells. Science *292*, 2075-2077.
Bechter, O.E., Zou, Y., Walker, W., Wright, W.E., and Shay, J.W. (2004). Telomeric recombination in mismatch repair deficient human colon cancer cells after telomerase inhibition. Cancer Res *64*, 3444-3451.
Bernadotte, A., Mikhelson, V.M., and Spivak, I.M. (2016). Markers of cellular senescence. Telomere shortening as a marker of cellular senescence. Aging *8*, 3-11.
Biffi, G., Tannahill, D., McCafferty, J., and Balasubramanian, S. (2013). Quantitative visualization of DNA G-quadruplex structures in human cells. Nat Chem *5*, 182-186.
Björklund, S., and Gustafsson, C.M. (2004). The mediator complex. Adv Protein Chem *67*, 43-65.
Blackburn, E.H. (1991). Structure and function of telomeres. Nature *350*, 569-573.

Blackburn, E.H. (2001). Switching and signaling at the telomere. Cell *106*, 661-673.
Blackburn, E.H. (2005). Telomeres and telomerase: their mechanisms of action and the effects of altering their functions. FEBS Lett *579*, 859-862.
Blackburn, E.H., and Collins, K. (2011). Telomerase: An RNP Enzyme Synthesizes DNA. Cold Spring Harbor Perspectives in Biology *3*, a003558.
Blakely, K., Ketela, T., and Moffat, J. (2011). Pooled lentiviral shRNA screening for functional genomics in mammalian cells. Methods Mol Biol *781*, 161-182.
Bochman, M.L., Paeschke, K., and Zakian, V.A. (2012). DNA secondary structures: stability and function of G-quadruplex structures. Nat Rev Genet *13*, 770-780.
Bodnar, A.G., Ouellette, M., Frolkis, M., Holt, S.E., Chiu, C.P., Morin, G.B., Harley, C.B., Shay, J.W., Lichtsteiner, S., and Wright, W.E. (1998). Extension of life-span by introduction of telomerase into normal human cells. Science *279*, 349-352.
Boggess, J.F., Zhou, C., Bae-Jump, V.L., Gehrig, P.A., and Whang, Y.E. (2006). Estrogen-receptor-dependent regulation of telomerase activity in human endometrial cancer cell lines. Gynecol Oncol *103*, 417-424.
Boone, C., Bussey, H., and Andrews, B.J. (2007). Exploring genetic interactions and networks with yeast. Nature reviews Genetics *8*, 437-449.
Bryan, T.M., Englezou, A., Dalla-Pozza, L., Dunham, M.A., and Reddel, R.R. (1997). Evidence for an alternative mechanism for maintaining telomere length in human tumors and tumor-derived cell lines. Nat Med *3*, 1271-1274.
Buchner, N., Zschauer, T.C., Lukosz, M., Altschmied, J., and Haendeler, J. (2010). Downregulation of mitochondrial telomerase reverse transcriptase induced by H2O2 is Src kinase dependent. Exp Gerontol *45*, 558-562.
Burger, A.M., Dai, F., Schultes, C.M., Reszka, A.P., Moore, M.J., Double, J.A., and Neidle, S. (2005). The G-quadruplex-interactive molecule BRACO-19 inhibits tumor growth, consistent with telomere targeting and interference with telomerase function. Cancer Res *65*, 1489-1496.
Buseman, C.M., Wright, W.E., and Shay, J.W. (2012). Is telomerase a viable target in cancer? Mutat Res *730*, 90-97.
Cao, Y., Bryan, T.M., and Reddel, R.R. (2008). Increased copy number of the TERT and TERC telomerase subunit genes in cancer cells. Cancer Sci *99*, 1092-1099.
Cao, Z., Huang, C.C., and Tan, W. (2006). Nuclease resistance of telomere-like oligonucleotides monitored in live cells by fluorescence anisotropy imaging. Anal Chem *78*, 1478-1484.
Cesare, A.J., and Reddel, R.R. (2008). Telomere uncapping and alternative lengthening of telomeres. Mech Ageing Dev *129*, 99-108.
Chai, W., Du, Q., Shay, J.W., and Wright, W.E. (2006). Human telomeres have different overhang sizes at leading versus lagging strands. Mol Cell *21*, 427-435.
Chang, J.T., Lu, Y.C., Chen, Y.J., Tseng, C.P., Chen, Y.L., Fang, C.W., and Cheng, A.J. (2006). hTERT phosphorylation by PKC is essential for telomerase holoprotein integrity and enzyme activity in head neck cancer cells. British journal of cancer *94*, 870-878.
Chen, L.Y., Redon, S., and Lingner, J. (2012). The human CST complex is a terminator of telomerase activity. Nature *488*, 540-544.
Chen, W., Chen, S.M., Yu, Y., Xiao, B.K., Huang, Z.W., and Tao, Z.Z. (2010). Telomerase inhibition alters telomere maintenance mechanisms in laryngeal squamous carcinoma cells. J Laryngol Otol *124*, 778-783.
Chen, X., Pan, Y., Yan, M., Bao, G., and Sun, X. (2020). Identification of potential crucial genes and molecular mechanisms in glioblastoma multiforme by bioinformatics analysis. Molecular medicine reports *22*, 859-869.

Chiosea, S., Acquafondata, M., Luo, J., Kuan, S., and Seethala, R. (2008). DICER1 and PRKRA in Colon Adenocarcinoma. Biomarker insights *3*, 253-258.
Chow, T.T., Zhao, Y., Mak, S.S., Shay, J.W., and Wright, W.E. (2012). Early and late steps in telomere overhang processing in normal human cells: the position of the final RNA primer drives telomere shortening. Genes Dev *26*, 1167-1178.
Chu, H.-P., Cifuentes-Rojas, C., Kesner, B., Aeby, E., Lee, H.-G., Wei, C., Oh, H.J., Boukhali, M., Haas, W., and Lee, J.T. (2017). TERRA RNA Antagonizes ATRX and Protects Telomeres. Cell *170*, 86-101.e116.
Chung, J., Khadka, P., and Chung, I.K. (2012a). Nuclear import of hTERT requires a bipartite nuclear localization signal and Akt-mediated phosphorylation. J Cell Sci *125*, 2684-2697.
Chung, J., Khadka, P., and Chung, I.K. (2012b). Nuclear import of hTERT requires a bipartite nuclear localization signal and Akt-mediated phosphorylation. Journal of Cell Science *125*, 2684.
Cimprich, K.A., and Cortez, D. (2008). ATR: an essential regulator of genome integrity. Nat Rev Mol Cell Biol *9*, 616-627.
Colgin, L.M., Wilkinson, C., Englezou, A., Kilian, A., Robinson, M.O., and Reddel, R.R. (2000). The hTERTalpha splice variant is a dominant negative inhibitor of telomerase activity. Neoplasia *2*, 426-432.
Cong, Y., and Shay, J.W. (2008). Actions of human telomerase beyond telomeres. Cell Res *18*, 725-732.
Cong, Y.-S., Wright, W.E., and Shay, J.W. (2002a). Human Telomerase and Its Regulation. Microbiology and Molecular Biology Reviews *66*, 407-425.
Cong, Y.S., Wright, W.E., and Shay, J.W. (2002b). Human telomerase and its regulation. Microbiol Mol Biol Rev *66*, 407-425, table of contents.
Cortez, D., Guntuku, S., Qin, J., and Elledge, S.J. (2001). ATR and ATRIP: partners in checkpoint signaling. Science *294*, 1713-1716.
Court, R., Chapman, L., Fairall, L., and Rhodes, D. (2005). How the human telomeric proteins TRF1 and TRF2 recognize telomeric DNA: a view from high-resolution crystal structures. EMBO Rep *6*, 39-45.
Cowley, G.S., Weir, B.A., Vazquez, F., Tamayo, P., Scott, J.A., Rusin, S., East-Seletsky, A., Ali, L.D., Gerath, W.F., Pantel, S.E.*, et al.* (2014). Parallel genome-scale loss of function screens in 216 cancer cell lines for the identification of context-specific genetic dependencies. Sci Data *1*, 140035.
Crabbe, L., Cesare, A.J., Kasuboski, J.M., Fitzpatrick, J.A.J., and Karlseder, J. (2012). Human telomeres are tethered to the nuclear envelope during postmitotic nuclear assembly. Cell reports *2*, 1521-1529.
Cristofari, G., and Lingner, J. (2006). Telomere length homeostasis requires that telomerase levels are limiting. Embo j *25*, 565-574.
d'Alcontres, M.S., Palacios, J.A., Mejias, D., and Blasco, M.A. (2014). TopoIIα prevents telomere fragility and formation of ultra thin DNA bridges during mitosis through TRF1-dependent binding to telomeres. Cell cycle (Georgetown, Tex) *13*, 1463-1481.
Daniali, L., Benetos, A., Susser, E., Kark, J.D., Labat, C., Kimura, M., Desai, K., Granick, M., and Aviv, A. (2013). Telomeres shorten at equivalent rates in somatic tissues of adults. Nat Commun *4*, 1597.
de Cárcer, G. (2019). The Mitotic Cancer Target Polo-Like Kinase 1: Oncogene or Tumor Suppressor? Genes *10*, 208.
de Lange, T. (2004). T-loops and the origin of telomeres. Nat Rev Mol Cell Biol *5*, 323-329.
de Lange, T. (2005). Shelterin: the protein complex that shapes and safeguards human telomeres. Genes Dev *19*, 2100-2110.
De Lange, T. (2005). Telomere-related genome instability in cancer. Cold Spring Harb Symp Quant Biol *70*, 197-204.
de Lange, T. (2009). How telomeres solve the end-protection problem. Science *326*, 948-952.
de Lange, T. (2018). Shelterin-Mediated Telomere Protection. Annu Rev Genet *52*, 223-247.
De Vitis, M., Berardinelli, F., and Sgura, A. (2018). Telomere Length Maintenance in Cancer: At the Crossroad between Telomerase and Alternative Lengthening of Telomeres (ALT). International journal of molecular sciences *19*, 606.

de Voer, R.M., Geurts van Kessel, A., Weren, R.D., Ligtenberg, M.J., Smeets, D., Fu, L., Vreede, L., Kamping, E.J., Verwiel, E.T., Hahn, M.M.*, et al.* (2013). Germline mutations in the spindle assembly checkpoint genes BUB1 and BUB3 are risk factors for colorectal cancer. Gastroenterology *145*, 544-547.
Deeg, K.I., Chung, I., Bauer, C., and Rippe, K. (2016). Cancer Cells with Alternative Lengthening of Telomeres Do Not Display a General Hypersensitivity to ATR Inhibition. Frontiers in oncology *6*, 186-186.
Delfarah, A., Parrish, S., Junge, J.A., Yang, J., Seo, F., Li, S., Mac, J., Wang, P., Fraser, S.E., and Graham, N.A. (2019). Inhibition of nucleotide synthesis promotes replicative senescence of human mammary epithelial cells. J Biol Chem *294*, 10564-10578.
Denchi, E.L., and de Lange, T. (2007). Protection of telomeres through independent control of ATM and ATR by TRF2 and POT1. Nature *448*, 1068.
Dey, A., and Chakrabarti, K. (2018). Current Perspectives of Telomerase Structure and Function in Eukaryotes with Emerging Views on Telomerase in Human Parasites. International journal of molecular sciences *19*, 333.
Dimitrova, N., Chen, Y.C., Spector, D.L., and de Lange, T. (2008). 53BP1 promotes non-homologous end joining of telomeres by increasing chromatin mobility. Nature *456*, 524-528.
Ding, X., Cheng, J., Pang, Q., Wei, X., Zhang, X., Wang, P., Yuan, Z., and Qian, D. (2019). BIBR1532, a Selective Telomerase Inhibitor, Enhances Radiosensitivity of Non-Small Cell Lung Cancer Through Increasing Telomere Dysfunction and ATM/CHK1 Inhibition. International Journal of Radiation Oncology*Biology*Physics *105*, 861-874.
Dixon, J.R., Selvaraj, S., Yue, F., Kim, A., Li, Y., Shen, Y., Hu, M., Liu, J.S., and Ren, B. (2012). Topological domains in mammalian genomes identified by analysis of chromatin interactions. Nature *485*, 376-380.
Doksani, Y., Wu, J.Y., de Lange, T., and Zhuang, X. (2013). Super-resolution fluorescence imaging of telomeres reveals TRF2-dependent T-loop formation. Cell *155*, 345-356.
Dreesen, O., Ong, P.F., Chojnowski, A., and Colman, A. (2013). The contrasting roles of lamin B1 in cellular aging and human disease. Nucleus *4*, 283-290.
Egan, E.D., and Collins, K. (2012). Biogenesis of telomerase ribonucleoproteins. RNA (New York, NY) *18*, 1747-1759.
Endoh, T., Tsuji, N., Asanuma, K., Yagihashi, A., and Watanabe, N. (2005). Survivin enhances telomerase activity via up-regulation of specificity protein 1- and c-Myc-mediated human telomerase reverse transcriptase gene transcription. Exp Cell Res *305*, 300-311.
Evers, B., Bernards, R., and Beijersbergen, R.L. (2014). The Good, the Bad, and the Ugly: in search of gold standards for assessing functional genetic screen quality. Mol Syst Biol *10*, 738.
Fan, Q., Zhang, F., Barrett, B., Ren, K., and Andreassen, P.R. (2009). A role for monoubiquitinated FANCD2 at telomeres in ALT cells. Nucleic Acids Res *37*, 1740-1754.
Farooqi, A.A., Mansoor, Q., Alaaeddine, N., and Xu, B. (2018). MicroRNA Regulation of Telomerase Reverse Transcriptase (TERT): Micro Machines Pull Strings of Papier-Mâché Puppets. International journal of molecular sciences *19*, 1051.
Fasching, C.L. (2018). Telomere length measurement as a clinical biomarker of aging and disease. Crit Rev Clin Lab Sci *55*, 443-465.
Feng, J., Funk, W.D., Wang, S.S., Weinrich, S.L., Avilion, A.A., Chiu, C.P., Adams, R.R., Chang, E., Allsopp, R.C., Yu, J.*, et al.* (1995). The RNA component of human telomerase. Science *269*, 1236-1241.
Ferreira, M.G., and Cooper, J.P. (2004). Two modes of DNA double-strand break repair are reciprocally regulated through the fission yeast cell cycle. Genes & development *18*, 2249-2254.
Fleisig, H.B., and Wong, J.M.Y. (2012). Telomerase promotes efficient cell cycle kinetics and confers growth advantage to telomerase-negative transformed human cells. Oncogene *31*, 954-965.
Frock, R.L., Hu, J., Meyers, R.M., Ho, Y.-J., Kii, E., and Alt, F.W. (2015). Genome-wide detection of DNA double-stranded breaks induced by engineered nucleases. Nature biotechnology *33*, 179-186.

Frohnert, C., Hutten, S., Walde, S., Nath, A., and Kehlenbach, R.H. (2014). Importin 7 and Nup358 promote nuclear import of the protein component of human telomerase. PLoS One *9*, e88887.
Furukawa, T., Duguid, W.P., Rosenberg, L., Viallet, J., Galloway, D.A., and Tsao, M.S. (1996). Long-term culture and immortalization of epithelial cells from normal adult human pancreatic ducts transfected by the E6E7 gene of human papilloma virus 16. Am J Pathol *148*, 1763-1770.
Gao, H., Moss, D.L., Parke, C., Tatum, D., and Lustig, A.J. (2014). The Ctf18RFC clamp loader is essential for telomere stability in telomerase-negative and mre11 mutant alleles. PLoS One *9*, e88633.
Gao, S., and Lai, L. (2018). Synthetic lethality in drug development: the dawn is coming. Future Medicinal Chemistry *10*, 2129-2132.
Garcia-Higuera, I., Taniguchi, T., Ganesan, S., Meyn, M.S., Timmers, C., Hejna, J., Grompe, M., and D'Andrea, A.D. (2001). Interaction of the Fanconi Anemia Proteins and BRCA1 in a Common Pathway. Molecular Cell *7*, 249-262.
Ghosh, A., Saginc, G., Leow, S.C., Khattar, E., Shin, E.M., Yan, T.D., Wong, M., Zhang, Z., Li, G., Sung, W.K.*, et al.* (2012). Telomerase directly regulates NF-kappaB-dependent transcription. Nat Cell Biol *14*, 1270-1281.
Giardini, M.A., Segatto, M., da Silva, M.S., Nunes, V.S., and Cano, M.I.N. (2014). Chapter One - Telomere and Telomerase Biology. In Progress in Molecular Biology and Translational Science, R.T. Calado, ed. (Academic Press), pp. 1-40.
Gobbini, E., Trovesi, C., Cassani, C., and Longhese, M.P. (2014). Telomere uncapping at the crossroad between cell cycle arrest and carcinogenesis. Molecular & cellular oncology *1*, e29901-e29901.
Goldblatt, E.M., Gentry, E.R., Fox, M.J., Gryaznov, S.M., Shen, C., and Herbert, B.S. (2009). The telomerase template antagonist GRN163L alters MDA-MB-231 breast cancer cell morphology, inhibits growth, and augments the effects of paclitaxel. Mol Cancer Ther *8*, 2027-2035.
Gomez, D.L.M., Armando, R.G., Cerrudo, C.S., Ghiringhelli, P.D., and Gomez, D.E. (2016). Telomerase as a Cancer Target. Development of New Molecules. Current topics in medicinal chemistry *16*, 2432-2440.
Gong, Y., and de Lange, T. (2010). A Shld1-controlled POT1a provides support for repression of ATR signaling at telomeres through RPA exclusion. Mol Cell *40*, 377-387.
Gonzalez, O.G., Assfalg, R., Koch, S., Schelling, A., Meena, J.K., Kraus, J., Lechel, A., Katz, S.-F., Benes, V., Scharffetter-Kochanek, K.*, et al.* (2014). Telomerase stimulates ribosomal DNA transcription under hyperproliferative conditions. Nature Communications *5*, 4599.
Gonzalez-Suarez, I., Redwood, A.B., Perkins, S.M., Vermolen, B., Lichtensztejin, D., Grotsky, D.A., Morgado-Palacin, L., Gapud, E.J., Sleckman, B.P., Sullivan, T.*, et al.* (2009). Novel roles for A-type lamins in telomere biology and the DNA damage response pathway. Embo j *28*, 2414-2427.
Gonzalo, S., and Eissenberg, J.C. (2016). Tying up loose ends: telomeres, genomic instability and lamins. Current opinion in genetics & development *37*, 109-118.
Gottschling, D.E., Aparicio, O.M., Billington, B.L., and Zakian, V.A. (1990). Position effect at S. cerevisiae telomeres: reversible repression of Pol II transcription. Cell *63*, 751-762.
Gralewska, P., Gajek, A., Marczak, A., and Rogalska, A. (2020). Participation of the ATR/CHK1 pathway in replicative stress targeted therapy of high-grade ovarian cancer. Journal of Hematology & Oncology *13*, 39.
Greider, C.W., and Blackburn, E.H. (1985). Identification of a specific telomere terminal transferase activity in Tetrahymena extracts. Cell *43*, 405-413.
Griffith, J.D., Comeau, L., Rosenfield, S., Stansel, R.M., Bianchi, A., Moss, H., and de Lange, T. (1999). Mammalian Telomeres End in a Large Duplex Loop. Cell *97*, 503-514.
Grill, S., Tesmer, V.M., and Nandakumar, J. (2018). The N Terminus of the OB Domain of Telomere Protein TPP1 Is Critical for Telomerase Action. Cell reports *22*, 1132-1140.

Guilleret, I., Yan, P., Grange, F., Braunschweig, R., Bosman, F.T., and Benhattar, J. (2002). Hypermethylation of the human telomerase catalytic subunit (hTERT) gene correlates with telomerase activity. Int J Cancer *101*, 335-341.
Haendeler, J., Drose, S., Buchner, N., Jakob, S., Altschmied, J., Goy, C., Spyridopoulos, I., Zeiher, A.M., Brandt, U., and Dimmeler, S. (2009). Mitochondrial telomerase reverse transcriptase binds to and protects mitochondrial DNA and function from damage. Arterioscler Thromb Vasc Biol *29*, 929-935.
Haendeler, J., Hoffmann, J., Brandes, R.P., Zeiher, A.M., and Dimmeler, S. (2003). Hydrogen peroxide triggers nuclear export of telomerase reverse transcriptase via Src kinase family-dependent phosphorylation of tyrosine 707. Mol Cell Biol *23*, 4598-4610.
Hamma, T., and Ferre-D'Amare, A.R. (2010). The box H/ACA ribonucleoprotein complex: interplay of RNA and protein structures in post-transcriptional RNA modification. J Biol Chem *285*, 805-809.
Hanaoka, S., Nagadoi, A., and Nishimura, Y. (2005). Comparison between TRF2 and TRF1 of their telomeric DNA-bound structures and DNA-binding activities. Protein Sci *14*, 119-130.
Harley, C.B. (2008a). Telomerase and cancer therapeutics. Nat Rev Cancer *8*, 167-179.
Harley, C.B. (2008b). Telomerase and cancer therapeutics. Nat Rev Cancer *8*, 167-179.
Hart, T., Brown, K.R., Sircoulomb, F., Rottapel, R., and Moffat, J. (2014a). Measuring error rates in genomic perturbation screens: gold standards for human functional genomics. Molecular systems biology *10*, 733-733.
Hart, T., Brown, K.R., Sircoulomb, F., Rottapel, R., and Moffat, J. (2014b). Measuring error rates in genomic perturbation screens: gold standards for human functional genomics. Mol Syst Biol *10*, 733.
Hayward, S.W., Dahiya, R., Cunha, G.R., Bartek, J., Deshpande, N., and Narayan, P. (1995). Establishment and characterization of an immortalized but non-transformed human prostate epithelial cell line: BPH-1. In Vitro Cell Dev Biol Anim *31*, 14-24.
He, J., Mansouri, A., and Das, S. (2018). Alpha Thalassemia/Mental Retardation Syndrome X-Linked, the Alternative Lengthening of Telomere Phenotype, and Gliomagenesis: Current Understandings and Future Potential. Frontiers in oncology *7*, 322-322.
Hegyi, H. (2015). Enhancer-promoter interaction facilitated by transiently forming G-quadruplexes. Sci Rep *5*, 9165.
Heidenreich, B., and Kumar, R. (2017). TERT promoter mutations in telomere biology. Mutation Research/Reviews in Mutation Research *771*, 15-31.
Hemann, M.T., Strong, M.A., Hao, L.Y., and Greider, C.W. (2001). The shortest telomere, not average telomere length, is critical for cell viability and chromosome stability. Cell *107*, 67-77.
Heselmeyer-Haddad, K., Sommerfeld, K., White, N.M., Chaudhri, N., Morrison, L.E., Palanisamy, N., Wang, Z.Y., Auer, G., Steinberg, W., and Ried, T. (2005). Genomic amplification of the human telomerase gene (TERC) in pap smears predicts the development of cervical cancer. Am J Pathol *166*, 1229-1238.
Hisamatsu, T., McGuire, M., Wu, S.Y., Rupaimoole, R., Pradeep, S., Bayraktar, E., Noh, K., Hu, W., Hansen, J.M., Lyons, Y.*, et al.* (2019). PRKRA/PACT Expression Promotes Chemoresistance of Mucinous Ovarian Cancer. Molecular cancer therapeutics *18*, 162-172.
Hiyama, E., and Hiyama, K. (2007). Telomere and telomerase in stem cells. British journal of cancer *96*, 1020-1024.
Hockemeyer, D., Daniels, J.P., Takai, H., and de Lange, T. (2006). Recent expansion of the telomeric complex in rodents: Two distinct POT1 proteins protect mouse telomeres. Cell *126*, 63-77.
Holt, S.E., Aisner, D.L., Baur, J., Tesmer, V.M., Dy, M., Ouellette, M., Trager, J.B., Morin, G.B., Toft, D.O., Shay, J.W.*, et al.* (1999). Functional requirement of p23 and Hsp90 in telomerase complexes. Genes & development *13*, 817-826.
Hopkins, A.L., and Groom, C.R. (2002). The druggable genome. In Nat Rev Drug Discov (England), pp. 727-730.

Hrdlickova, R., Nehyba, J., and Bose, H.R., Jr. (2012). Alternatively spliced telomerase reverse transcriptase variants lacking telomerase activity stimulate cell proliferation. Mol Cell Biol *32*, 4283-4296.
Hu, J., Hwang, S.S., Liesa, M., Gan, B., Sahin, E., Jaskelioff, M., Ding, Z., Ying, H., Boutin, A.T., Zhang, H.*, et al.* (2012). Antitelomerase therapy provokes ALT and mitochondrial adaptive mechanisms in cancer. Cell *148*, 651-663.
Hu, Y., Shi, G., Zhang, L., Li, F., Jiang, Y., Jiang, S., Ma, W., Zhao, Y., Songyang, Z., and Huang, J. (2016). Switch telomerase to ALT mechanism by inducing telomeric DNA damages and dysfunction of ATRX and DAXX. Sci Rep *6*, 32280.
Huang, C., and Yu, Y.-T. (2010). Targeted 2'-O methylation at a nucleotide within the pseudoknot of telomerase RNA reduces telomerase activity in vivo. Molecular and cellular biology *30*, 4368-4378.
Huang, Y., Sun, L., Liu, N., Wei, Q., Jiang, L., Tong, X., and Ye, X. (2015). Polo-like Kinase 1 (Plk1) Up-regulates Telomerase Activity by Affecting Human Telomerase Reverse Transcriptase (hTERT) Stability. J Biol Chem *290*, 18865-18873.
Hwang, H., Kreig, A., Calvert, J., Lormand, J., Kwon, Y., Daley, J.M., Sung, P., Opresko, P.L., and Myong, S. (2014). Telomeric overhang length determines structural dynamics and accessibility to telomerase and ALT-associated proteins. Structure (London, England : 1993) *22*, 842-853.
Jafri, M.A., Ansari, S.A., Alqahtani, M.H., and Shay, J.W. (2016). Roles of telomeres and telomerase in cancer, and advances in telomerase-targeted therapies. Genome medicine *8*, 69-69.
Jerby-Arnon, L., Pfetzer, N., Waldman, Y.Y., McGarry, L., James, D., Shanks, E., Seashore-Ludlow, B., Weinstock, A., Geiger, T., Clemons, P.A.*, et al.* (2014). Predicting cancer-specific vulnerability via data-driven detection of synthetic lethality. Cell *158*, 1199-1209.
Jiang, Y., de Bruin, A., Caldas, H., Fangusaro, J., Hayes, J., Conway, E.M., Robinson, M.L., and Altura, R.A. (2005). Essential Role for Survivin in Early Brain Development. The Journal of Neuroscience *25*, 6962.
Jie, M.-M., Chang, X., Zeng, S., Liu, C., Liao, G.-B., Wu, Y.-R., Liu, C.-H., Hu, C.-J., Yang, S.-M., and Li, X.-Z. (2019). Diverse regulatory manners of human telomerase reverse transcriptase. Cell Communication and Signaling *17*, 63.
Joung, J., Konermann, S., Gootenberg, J.S., Abudayyeh, O.O., Platt, R.J., Brigham, M.D., Sanjana, N.E., and Zhang, F. (2017a). Genome-scale CRISPR-Cas9 knockout and transcriptional activation screening. Nature Protocols *12*, 828.
Joung, J., Konermann, S., Gootenberg, J.S., Abudayyeh, O.O., Platt, R.J., Brigham, M.D., Sanjana, N.E., and Zhang, F. (2017b). Genome-scale CRISPR-Cas9 knockout and transcriptional activation screening. Nature protocols *12*, 828-863.
Jády, B.E., Richard, P., Bertrand, E., and Kiss, T. (2006). Cell cycle-dependent recruitment of telomerase RNA and Cajal bodies to human telomeres. Molecular biology of the cell *17*, 944-954.
Kagey, M.H., Newman, J.J., Bilodeau, S., Zhan, Y., Orlando, D.A., van Berkum, N.L., Ebmeier, C.C., Goossens, J., Rahl, P.B., Levine, S.S.*, et al.* (2010). Mediator and cohesin connect gene expression and chromatin architecture. Nature *467*, 430-435.
Kaul, Z., Cesare, A.J., Huschtscha, L.I., Neumann, A.A., and Reddel, R.R. (2011). Five dysfunctional telomeres predict onset of senescence in human cells. EMBO Rep *13*, 52-59.
Kaulage, M.H., Maji, B., Pasadi, S., Ali, A., Bhattacharya, S., and Muniyappa, K. (2018). Targeting G-quadruplex DNA structures in the telomere and oncogene promoter regions by benzimidazole–carbazole ligands. European Journal of Medicinal Chemistry *148*, 178-194.
Kharbanda, S., Kumar, V., Dhar, S., Pandey, P., Chen, C., Majumder, P., Yuan, Z.M., Whang, Y., Strauss, W., Pandita, T.K.*, et al.* (2000). Regulation of the hTERT telomerase catalytic subunit by the c-Abl tyrosine kinase. Curr Biol *10*, 568-575.
Khattar, E., and Tergaonkar, V. (2017). Transcriptional Regulation of Telomerase Reverse Transcriptase (TERT) by MYC. Frontiers in cell and developmental biology *5*, 1-1.

Kheirollahi, M. (2013). Telomere, Regulation and Tumorigenesis. In Telomere Territory and Cancer, P. Mehdipour, ed. (Dordrecht: Springer Netherlands), pp. 55-98.
Kim, J.H., Park, S.-M., Kang, M.R., Oh, S.-Y., Lee, T.H., Muller, M.T., and Chung, I.K. (2005). Ubiquitin ligase MKRN1 modulates telomere length homeostasis through a proteolysis of hTERT. Genes & development *19*, 776-781.
Kim, J.T., Cho, H.J., Park, S.Y., Oh, B.M., Hwang, Y.S., Baek, K.E., Lee, Y.H., Kim, H.C., and Lee, H.G. (2019). DNA Replication and Sister Chromatid Cohesion 1 (DSCC1) of the Replication Factor Complex CTF18-RFC is Critical for Colon Cancer Cell Growth. J Cancer *10*, 6142-6153.
Kim, M.Y., Vankayalapati, H., Shin-Ya, K., Wierzba, K., and Hurley, L.H. (2002). Telomestatin, a potent telomerase inhibitor that interacts quite specifically with the human telomeric intramolecular g-quadruplex. J Am Chem Soc *124*, 2098-2099.
Kim, W., Ludlow, A.T., Min, J., Robin, J.D., Stadler, G., Mender, I., Lai, T.-P., Zhang, N., Wright, W.E., and Shay, J.W. (2016). Regulation of the Human Telomerase Gene TERT by Telomere Position Effect-Over Long Distances (TPE-OLD): Implications for Aging and Cancer. PLoS biology *14*, e2000016-e2000016.
Kimura, A., Ohmichi, M., Kawagoe, J., Kyo, S., Mabuchi, S., Takahashi, T., Ohshima, C., Arimoto-Ishida, E., Nishio, Y., Inoue, M*., et al.* (2004). Induction of hTERT expression and phosphorylation by estrogen via Akt cascade in human ovarian cancer cell lines. Oncogene *23*, 4505-4515.
Knecht, H., and Mai, S. (2017). The Use of 3D Telomere FISH for the Characterization of the Nuclear Architecture in EBV-Positive Hodgkin's Lymphoma. Methods Mol Biol *1532*, 93-104.
Konishi, A., and de Lange, T. (2008). Cell cycle control of telomere protection and NHEJ revealed by a ts mutation in the DNA-binding domain of TRF2. Genes Dev *22*, 1221-1230.
Kousholt, A.N., Menzel, T., and Sørensen, C.S. (2012). Pathways for genome integrity in G2 phase of the cell cycle. Biomolecules *2*, 579-607.
Kyo, S., Takakura, M., Fujiwara, T., and Inoue, M. (2008). Understanding and exploiting hTERT promoter regulation for diagnosis and treatment of human cancers. Cancer science *99*, 1528-1538.
Kyo, S., Takakura, M., Taira, T., Kanaya, T., Itoh, H., Yutsudo, M., Ariga, H., and Inoue, M. (2000). Sp1 cooperates with c-Myc to activate transcription of the human telomerase reverse transcriptase gene (hTERT). Nucleic Acids Res *28*, 669-677.
Lacerte, A., Korah, J., Roy, M., Yang, X.J., Lemay, S., and Lebrun, J.J. (2008). Transforming growth factor-beta inhibits telomerase through SMAD3 and E2F transcription factors. Cell Signal *20*, 50-59.
Lacombe, T., Poh, S.L., Barbey, R., and Kuras, L. (2013). Mediator is an intrinsic component of the basal RNA polymerase II machinery in vivo. Nucleic acids research *41*, 9651-9662.
Lai, S.R., Cunningham, A.P., Huynh, V.Q., Andrews, L.G., and Tollefsbol, T.O. (2007). Evidence of extra-telomeric effects of hTERT and its regulation involving a feedback loop. Experimental cell research *313*, 322-330.
Lai, T.-P., Wright, W.E., and Shay, J.W. (2018). Comparison of telomere length measurement methods. Philosophical transactions of the Royal Society of London Series B, Biological sciences *373*, 20160451.
Leao, R., Apolonio, J.D., Lee, D., Figueiredo, A., Tabori, U., and Castelo-Branco, P. (2018). Mechanisms of human telomerase reverse transcriptase (hTERT) regulation: clinical impacts in cancer. J Biomed Sci *25*, 22.
Lee, H.W., Park, T.I., Jang, S.Y., Park, S.Y., Park, W.-J., Jung, S.-J., and Lee, J.-H. (2017). Clinicopathological characteristics of TERT promoter mutation and telomere length in hepatocellular carcinoma. Medicine *96*, e5766-e5766.
Lee, J.H., Khadka, P., Baek, S.H., and Chung, I.K. (2010). CHIP promotes human telomerase reverse transcriptase degradation and negatively regulates telomerase activity. J Biol Chem *285*, 42033-42045.
Lee, J.H., and Paull, T.T. (2005). ATM activation by DNA double-strand breaks through the Mre11-Rad50-Nbs1 complex. Science *308*, 551-554.

Lee, S.K., and Kumar, P. (2009). Conditional RNAi: towards a silent gene therapy. Adv Drug Deliv Rev *61*, 650-664.
Lei, M., Podell, E.R., and Cech, T.R. (2004a). Structure of human POT1 bound to telomeric single-stranded DNA provides a model for chromosome end-protection. Nature Structural &Amp; Molecular Biology *11*, 1223.
Lei, M., Podell, E.R., and Cech, T.R. (2004b). Structure of human POT1 bound to telomeric single-stranded DNA provides a model for chromosome end-protection. Nat Struct Mol Biol *11*, 1223-1229.
Li, F., Aljahdali, I., and Ling, X. (2019). Cancer therapeutics using survivin BIRC5 as a target: what can we do after over two decades of study? J Exp Clin Cancer Res *38*, 368.
Li, F., Kim, H., Ji, Z., Zhang, T., Chen, B., Ge, Y., Hu, Y., Feng, X., Han, X., Xu, H*., et al.* (2018). The BUB3-BUB1 Complex Promotes Telomere DNA Replication. Molecular cell *70*, 395-407.e394.
Li, Y., and Tergaonkar, V. (2014). Noncanonical functions of telomerase: implications in telomerase-targeted cancer therapies. Cancer Res *74*, 1639-1644.
Lipps, H.J., and Rhodes, D. (2009). G-quadruplex structures: in vivo evidence and function. Trends Cell Biol *19*, 414-422.
Listerman, I., Sun, J., Gazzaniga, F.S., Lukas, J.L., and Blackburn, E.H. (2013). The major reverse transcriptase-incompetent splice variant of the human telomerase protein inhibits telomerase activity but protects from apoptosis. Cancer Res *73*, 2817-2828.
Liu, H., Liu, Q., Ge, Y., Zhao, Q., Zheng, X., and Zhao, Y. (2016a). hTERT promotes cell adhesion and migration independent of telomerase activity. Scientific Reports *6*, 22886.
Liu, J.Q., Chen, C.Y., Xue, Y., Hao, Y.H., and Tan, Z. (2010). G-quadruplex hinders translocation of BLM helicase on DNA: a real-time fluorescence spectroscopic unwinding study and comparison with duplex substrates. J Am Chem Soc *132*, 10521-10527.
Liu, N., Ding, D., Hao, W., Yang, F., Wu, X., Wang, M., Xu, X., Ju, Z., Liu, J.-P., Song, Z*., et al.* (2016b). hTERT promotes tumor angiogenesis by activating VEGF via interactions with the Sp1 transcription factor. Nucleic Acids Research *44*, 8693-8703.
Liu, R., and Xing, M. (2016). TERT promoter mutations in thyroid cancer. Endocr Relat Cancer *23*, R143-155.
Liu, X., Wang, Y., Chang, G., Wang, F., Wang, F., and Geng, X. (2017). Alternative Splicing of hTERT Pre-mRNA: A Potential Strategy for the Regulation of Telomerase Activity. International journal of molecular sciences *18*, 567.
Loayza, D., and De Lange, T. (2003). POT1 as a terminal transducer of TRF1 telomere length control. Nature *423*, 1013-1018.
Londono-Vallejo, J.A., DerSarkissian, H., Cazes, L., and Thomas, G. (2001). Differences in telomere length between homologous chromosomes in humans. Nucleic Acids Res *29*, 3164-3171.
Longhese, M.P. (2008). DNA damage response at functional and dysfunctional telomeres. Genes Dev *22*, 125-140.
Lou, Z., Wei, J., Riethman, H., Baur, J.A., Voglauer, R., Shay, J.W., and Wright, W.E. (2009a). Telomere length regulates ISG15 expression in human cells. Aging *1*, 608-621.
Lou, Z., Wei, J., Riethman, H., Baur, J.A., Voglauer, R., Shay, J.W., and Wright, W.E. (2009b). Telomere length regulates ISG15 expression in human cells. Aging (Albany NY) *1*, 608-621.
Lu, W., Zhang, Y., Liu, D., Songyang, Z., and Wan, M. (2013). Telomeres - Structure, Function, and Regulation. Experimental cell research *319*, 133-141.
Luo, B., Cheung, H.W., Subramanian, A., Sharifnia, T., Okamoto, M., Yang, X., Hinkle, G., Boehm, J.S., Beroukhim, R., Weir, B.A*., et al.* (2008). Highly parallel identification of essential genes in cancer cells. Proceedings of the National Academy of Sciences of the United States of America *105*, 20380-20385.
Maciejowski, J., and de Lange, T. (2017a). Telomeres in cancer: tumour suppression and genome instability. Nature reviews Molecular cell biology *18*, 175-186.

Maciejowski, J., and de Lange, T. (2017b). Telomeres in cancer: tumour suppression and genome instability. Nat Rev Mol Cell Biol *18*, 175-186.
MacKenzie, K.L., Franco, S., Naiyer, A.J., May, C., Sadelain, M., Rafii, S., and Moore, M.A. (2002). Multiple stages of malignant transformation of human endothelial cells modelled by co-expression of telomerase reverse transcriptase, SV40 T antigen and oncogenic N-ras. Oncogene *21*, 4200-4211.
MacNeil, D.E., Bensoussan, H.J., and Autexier, C. (2016a). Telomerase Regulation from Beginning to the End. Genes *7*, 64.
MacNeil, D.E., Bensoussan, H.J., and Autexier, C. (2016b). Telomerase Regulation from Beginning to the End. Genes (Basel) *7*.
Maes, L., Van Neste, L., Van Damme, K., Kalala, J.P., De Ridder, L., Bekaert, S., and Cornelissen, M. (2007). Relation between telomerase activity, hTERT and telomere length for intracranial tumours. Oncol Rep *18*, 1571-1576.
Magnenat, L., Tobler, H., and Müller, F. (1999). Developmentally regulated telomerase activity is correlated with chromosomal healing during chromatin diminution in Ascaris suum. Molecular and cellular biology *19*, 3457-3465.
Mali, P., Yang, L., Esvelt, K.M., Aach, J., Guell, M., DiCarlo, J.E., Norville, J.E., and Church, G.M. (2013). RNA-Guided Human Genome Engineering via Cas9. Science (New York, NY) *339*, 823-826.
Manning, M., Jiang, Y., Wang, R., Liu, L., Rode, S., Bonahoom, M., Kim, S., and Yang, Z.-Q. (2020). Pan-cancer analysis of RNA methyltransferases identifies FTSJ3 as a potential regulator of breast cancer progression. RNA biology *17*, 474-486.
Marcotte, R., Brown, K.R., Suarez, F., Sayad, A., Karamboulas, K., Krzyzanowski, P.M., Sircoulomb, F., Medrano, M., Fedyshyn, Y., Koh, J.L.*, et al.* (2012). Essential gene profiles in breast, pancreatic, and ovarian cancer cells. Cancer Discov *2*, 172-189.
Martinez, P., and Blasco, M.A. (2011). Telomeric and extra-telomeric roles for telomerase and the telomere-binding proteins. Nat Rev Cancer *11*, 161-176.
Martinez, P., Thanasoula, M., Munoz, P., Liao, C., Tejera, A., McNees, C., Flores, J.M., Fernandez-Capetillo, O., Tarsounas, M., and Blasco, M.A. (2009). Increased telomere fragility and fusions resulting from TRF1 deficiency lead to degenerative pathologies and increased cancer in mice. Genes Dev *23*, 2060-2075.
Martini, E., Wittkopf, N., Günther, C., Leppkes, M., Okada, H., Watson, Alastair J., Podstawa, E., Backert, I., Amann, K., Neurath, Markus F.*, et al.* (2016). Loss of Survivin in Intestinal Epithelial Progenitor Cells Leads to Mitotic Catastrophe and Breakdown of Gut Immune Homeostasis. Cell Reports *14*, 1062-1073.
Maréchal, A., and Zou, L. DNA damage sensing by the ATM and ATR kinases. Cold Spring Harbor perspectives in biology *5*, a012716.
Mavrogiannou, E., Strati, A., Stathopoulou, A., Tsaroucha, E.G., Kaklamanis, L., and Lianidou, E.S. (2007). Real-time RT-PCR quantification of human telomerase reverse transcriptase splice variants in tumor cell lines and non-small cell lung cancer. Clin Chem *53*, 53-61.
Mayer, M.L., Gygi, S.P., Aebersold, R., and Hieter, P. (2001). Identification of RFC(Ctf18p, Ctf8p, Dcc1p): an alternative RFC complex required for sister chromatid cohesion in S. cerevisiae. Mol Cell *7*, 959-970.
Mazzolini, R., Gonzàlez, N., Garcia-Garijo, A., Millanes-Romero, A., Peiró, S., Smith, S., García de Herreros, A., and Canudas, S. (2018). Snail1 transcription factor controls telomere transcription and integrity. Nucleic acids research *46*, 146-158.
McDonald, E.R., 3rd, de Weck, A., Schlabach, M.R., Billy, E., Mavrakis, K.J., Hoffman, G.R., Belur, D., Castelletti, D., Frias, E., Gampa, K.*, et al.* (2017). Project DRIVE: A Compendium of Cancer Dependencies and Synthetic Lethal Relationships Uncovered by Large-Scale, Deep RNAi Screening. Cell *170*, 577-592 e510.

Meyers, R.M., Bryan, J.G., McFarland, J.M., Weir, B.A., Sizemore, A.E., Xu, H., Dharia, N.V., Montgomery, P.G., Cowley, G.S., Pantel, S*., et al.* (2017). Computational correction of copy number effect improves specificity of CRISPR-Cas9 essentiality screens in cancer cells. Nat Genet *49*, 1779-1784.
Mitchell, J.R., and Collins, K. (2000). Human telomerase activation requires two independent interactions between telomerase RNA and telomerase reverse transcriptase. Mol Cell *6*, 361-371.
Mohr, S.E., Smith, J.A., Shamu, C.E., Neumüller, R.A., and Perrimon, N. (2014). RNAi screening comes of age: improved techniques and complementary approaches. Nature reviews Molecular cell biology *15*, 591-600.
Montecucco, A., and Biamonti, G. (2013). Pre-mRNA processing factors meet the DNA damage response. Frontiers in genetics *4*, 102-102.
Moyzis, R.K., Buckingham, J.M., Cram, L.S., Dani, M., Deaven, L.L., Jones, M.D., Meyne, J., Ratliff, R.L., and Wu, J.R. (1988). A highly conserved repetitive DNA sequence, (TTAGGG)n, present at the telomeres of human chromosomes. Proc Natl Acad Sci U S A *85*, 6622-6626.
Mullenders, J., and Bernards, R. (2009). Loss-of-function genetic screens as a tool to improve the diagnosis and treatment of cancer. Oncogene *28*, 4409-4420.
Muraki, K., Nyhan, K., Han, L., and Murnane, J.P. (2012). Mechanisms of telomere loss and their consequences for chromosome instability. Frontiers in oncology *2*, 135-135.
Murnane, J.P. (2006). Telomeres and chromosome instability. DNA Repair (Amst) *5*, 1082-1092.
Necasova, I., Janouskova, E., Klumpler, T., and Hofr, C. (2017). Basic domain of telomere guardian TRF2 reduces D-loop unwinding whereas Rap1 restores it. Nucleic Acids Res *45*, 12170-12180.
Nijman, S.M.B. (2011). Synthetic lethality: general principles, utility and detection using genetic screens in human cells. FEBS letters *585*, 1-6.
Nitiss, J.L. (2009). DNA topoisomerase II and its growing repertoire of biological functions. Nature reviews Cancer *9*, 327-337.
O'Neil, N.J., Bailey, M.L., and Hieter, P. (2017). Synthetic lethality and cancer. Nature Reviews Genetics *18*, 613.
O'Sullivan, R.J., Arnoult, N., Lackner, D.H., Oganesian, L., Haggblom, C., Corpet, A., Almouzni, G., and Karlseder, J. (2014). Rapid induction of alternative lengthening of telomeres by depletion of the histone chaperone ASF1. Nat Struct Mol Biol *21*, 167-174.
O'Sullivan, R.J., and Karlseder, J. (2010). Telomeres: protecting chromosomes against genome instability. Nat Rev Mol Cell Biol *11*, 171-181.
Oh, W., Lee, E.W., Lee, D., Yang, M.R., Ko, A., Yoon, C.H., Lee, H.W., Bae, Y.S., Choi, C.Y., and Song, J. (2010). Hdm2 negatively regulates telomerase activity by functioning as an E3 ligase of hTERT. Oncogene *29*, 4101.
Ottaviani, A., Schluth-Bolard, C., Rival-Gervier, S., Boussouar, A., Rondier, D., Foerster, A.M., Morere, J., Bauwens, S., Gazzo, S., Callet-Bauchu, E*., et al.* (2009). Identification of a perinuclear positioning element in human subtelomeres that requires A-type lamins and CTCF. The EMBO journal *28*, 2428-2436.
Ozaki, T., and Nakagawara, A. (2011). Role of p53 in Cell Death and Human Cancers. Cancers *3*, 994-1013.
O'Sullivan, R.J., and Karlseder, J. (2010). Telomeres: protecting chromosomes against genome instability. Nature reviews Molecular cell biology *11*, 171-181.
Pagliarini, R., Shao, W., and Sellers, W.R. (2015). Oncogene addiction: pathways of therapeutic response, resistance, and road maps toward a cure. EMBO reports *16*, 280-296.
Palm, W., and de Lange, T. (2008). How shelterin protects mammalian telomeres. Annu Rev Genet *42*, 301-334.
Pascolo, E., Wenz, C., Lingner, J., Hauel, N., Priepke, H., Kauffmann, I., Garin-Chesa, P., Rettig, W.J., Damm, K., and Schnapp, A. (2002). Mechanism of human telomerase inhibition by BIBR1532, a synthetic, non-nucleosidic drug candidate. J Biol Chem *277*, 15566-15572.

Paul, J.M., Toosi, B., Vizeacoumar, F.S., Bhanumathy, K.K., Li, Y., Gerger, C., El Zawily, A., Freywald, T., Anderson, D.H., Mousseau, D.*, et al.* (2016). Targeting synthetic lethality between the SRC kinase and the EPHB6 receptor may benefit cancer treatment. Oncotarget *7*, 50027-50042.
Peifer, M., Hertwig, F., Roels, F., Dreidax, D., Gartlgruber, M., Menon, R., Kramer, A., Roncaioli, J.L., Sand, F., Heuckmann, J.M.*, et al.* (2015). Telomerase activation by genomic rearrangements in high-risk neuroblastoma. Nature *526*, 700-704.
Pfeiffer, V., Crittin, J., Grolimund, L., and Lingner, J. (2013). The THO complex component Thp2 counteracts telomeric R-loops and telomere shortening. The EMBO journal *32*, 2861-2871.
Pilsworth, J.A., Cochrane, D.R., Xia, Z., Aubert, G., Farkkila, A.E.M., Horlings, H.M., Yanagida, S., Yang, W., Lim, J.L.P., Wang, Y.K.*, et al.* (2018). TERT promoter mutation in adult granulosa cell tumor of the ovary. Mod Pathol *31*, 1107-1115.
Podlevsky, J.D., Bley, C.J., Omana, R.V., Qi, X., and Chen, J.J.L. (2008). The telomerase database. Nucleic acids research *36*, D339-D343.
Pombo, A., and Dillon, N. (2015). Three-dimensional genome architecture: players and mechanisms. Nat Rev Mol Cell Biol *16*, 245-257.
Qi, X., Xie, M., Brown, A.F., Bley, C.J., Podlevsky, J.D., and Chen, J.J.L. (2012). RNA/DNA hybrid binding affinity determines telomerase template-translocation efficiency. The EMBO journal *31*, 150-161.
Queisser, A., Heeg, S., Thaler, M., von Werder, A., and Opitz, O.G. (2013). Inhibition of telomerase induces alternative lengthening of telomeres during human esophageal carcinogenesis. Cancer Genet *206*, 374-386.
Rahman, R., Forsyth, N.R., and Cui, W. (2008). Telomeric 3'-overhang length is associated with the size of telomeres. Exp Gerontol *43*, 258-265.
Ramlee, M.K., Wang, J., Toh, W.X., and Li, S. (2016). Transcription Regulation of the Human Telomerase Reverse Transcriptase (hTERT) Gene. Genes (Basel) *7*.
Read, M., Harrison, R.J., Romagnoli, B., Tanious, F.A., Gowan, S.H., Reszka, A.P., Wilson, W.D., Kelland, L.R., and Neidle, S. (2001). Structure-based design of selective and potent G quadruplex-mediated telomerase inhibitors. Proc Natl Acad Sci U S A *98*, 4844-4849.
Reddel, R.R. (2014). Telomere maintenance mechanisms in cancer: clinical implications. Current pharmaceutical design *20*, 6361-6374.
Rhodes, D., and Lipps, H.J. (2015). G-quadruplexes and their regulatory roles in biology. Nucleic Acids Research *43*, 8627-8637.
Rio Frio, T., Lavoie, J., Hamel, N., Geyer, F.C., Kushner, Y.B., Novak, D.J., Wark, L., Capelli, C., Reis-Filho, J.S., Mai, S.*, et al.* (2010). Homozygous BUB1B Mutation and Susceptibility to Gastrointestinal Neoplasia. New England Journal of Medicine *363*, 2628-2637.
Roake, C.M., and Artandi, S.E. (2020). Regulation of human telomerase in homeostasis and disease. Nat Rev Mol Cell Biol.
Robin, J.D., Ludlow, A.T., Batten, K., Gaillard, M.C., Stadler, G., Magdinier, F., Wright, W.E., and Shay, J.W. (2015). SORBS2 transcription is activated by telomere position effect-over long distance upon telomere shortening in muscle cells from patients with facioscapulohumeral dystrophy. Genome Res *25*, 1781-1790.
Robin, J.D., Ludlow, A.T., Batten, K., Magdinier, F., Stadler, G., Wagner, K.R., Shay, J.W., and Wright, W.E. (2014). Telomere position effect: regulation of gene expression with progressive telomere shortening over long distances. Genes & development *28*, 2464-2476.
Roh, J.-I., Sung, Y.H., and Lee, H.-W. (2013). Clinical implications of antitelomeric drugs with respect to the nontelomeric functions of telomerase in cancer. OncoTargets and therapy *6*, 1161-1166.
Ronco, C., Martin, A.R., Demange, L., and Benhida, R. (2016). ATM, ATR, CHK1, CHK2 and WEE1 inhibitors in cancer and cancer stem cells. MedChemComm *8*, 295-319.

Ruckert, F., Aust, D., Bohme, I., Werner, K., Brandt, A., Diamandis, E.P., Krautz, C., Hering, S., Saeger, H.D., Grutzmann, R.*, et al.* (2012). Five primary human pancreatic adenocarcinoma cell lines established by the outgrowth method. J Surg Res *172*, 29-39.
Sabatier, L., Ricoul, M., Pottier, G., and Murnane, J.P. (2005). The loss of a single telomere can result in instability of multiple chromosomes in a human tumor cell line. Mol Cancer Res *3*, 139-150.
Saito, T., Akaike, K., Kurisaki-Arakawa, A., Toda-Ishii, M., Mukaihara, K., Suehara, Y., Takagi, T., Kaneko, K., and Yao, T. (2016). TERT promoter mutations are rare in bone and soft tissue sarcomas of Japanese patients. Molecular and clinical oncology *4*, 61-64.
Salloum, R., Hummel, T.R., Kumar, S.S., Dorris, K., Li, S., Lin, T., Daryani, V.M., Stewart, C.F., Miles, L., Poussaint, T.Y.*, et al.* (2016). A molecular biology and phase II study of imetelstat (GRN163L) in children with recurrent or refractory central nervous system malignancies: a pediatric brain tumor consortium study. Journal of neuro-oncology *129*, 443-451.
Sanjana, N.E., Shalem, O., and Zhang, F. (2014). Improved vectors and genome-wide libraries for CRISPR screening. Nat Methods *11*, 783-784.
Saretzki, G. (2014). Extra-telomeric functions of human telomerase: cancer, mitochondria and oxidative stress. Curr Pharm Des *20*, 6386-6403.
Schmidt, J.C., and Cech, T.R. (2015). Human telomerase: biogenesis, trafficking, recruitment, and activation. Genes & development *29*, 1095-1105.
Schmutz, I., Timashev, L., Xie, W., Patel, D.J., and de Lange, T. (2017). TRF2 binds branched DNA to safeguard telomere integrity. Nat Struct Mol Biol *24*, 734-742.
Schuster, A., Erasimus, H., Fritah, S., Nazarov, P.V., van Dyck, E., Niclou, S.P., and Golebiewska, A. (2018). RNAi/CRISPR Screens: from a Pool to a Valid Hit. Trends Biotechnol.
Schuster, A., Erasimus, H., Fritah, S., Nazarov, P.V., van Dyck, E., Niclou, S.P., and Golebiewska, A. (2019). RNAi/CRISPR Screens: from a Pool to a Valid Hit. Trends in Biotechnology *37*, 38-55.
Segal-Bendirdjian, E., and Geli, V. (2019). Non-canonical Roles of Telomerase: Unraveling the Imbroglio. Front Cell Dev Biol *7*, 332.
Seimiya, H., Sawada, H., Muramatsu, Y., Shimizu, M., Ohko, K., Yamane, K., and Tsuruo, T. (2000). Involvement of 14-3-3 proteins in nuclear localization of telomerase. Embo j *19*, 2652-2661.
Sentmanat, M.F., Peters, S.T., Florian, C.P., Connelly, J.P., and Pruett-Miller, S.M. (2018). A Survey of Validation Strategies for CRISPR-Cas9 Editing. Scientific Reports *8*, 888.
Sexton, A.N., Youmans, D.T., and Collins, K. (2012). Specificity requirements for human telomere protein interaction with telomerase holoenzyme. J Biol Chem *287*, 34455-34464.
Sfeir, A., Kabir, S., van Overbeek, M., Celli, G.B., and de Lange, T. (2010). Loss of Rap1 induces telomere recombination in the absence of NHEJ or a DNA damage signal. Science *327*, 1657-1661.
Sfeir, A., Kosiyatrakul, S.T., Hockemeyer, D., MacRae, S.L., Karlseder, J., Schildkraut, C.L., and de Lange, T. (2009). Mammalian telomeres resemble fragile sites and require TRF1 for efficient replication. Cell *138*, 90-103.
Shalem, O., Sanjana, N.E., Hartenian, E., Shi, X., Scott, D.A., Mikkelsen, T.S., Heckl, D., Ebert, B.L., Root, D.E., Doench, J.G.*, et al.* (2014). Genome-scale CRISPR-Cas9 knockout screening in human cells. Science *343*, 84-87.
Shao, J., Zhou, B., Chu, B., and Yen, Y. (2006). Ribonucleotide reductase inhibitors and future drug design. Curr Cancer Drug Targets *6*, 409-431.
Shats, I., Milyavsky, M., Tang, X., Stambolsky, P., Erez, N., Brosh, R., Kogan, I., Braunstein, I., Tzukerman, M., Ginsberg, D.*, et al.* (2004). p53-dependent down-regulation of telomerase is mediated by p21waf1. J Biol Chem *279*, 50976-50985.
Shay, J.W. (2016). Role of Telomeres and Telomerase in Aging and Cancer. Cancer Discov *6*, 584-593.
Shay, J.W., and Wright, W.E. (2004). Senescence and immortalization: role of telomeres and telomerase. Carcinogenesis *26*, 867-874.

Shay, J.W., and Wright, W.E. (2011). Role of telomeres and telomerase in cancer. Seminars in Cancer Biology *21*, 349-353.
Shay, J.W., and Wright, W.E. (2019). Telomeres and telomerase: three decades of progress. Nat Rev Genet.
Shibuya, H., Hernandez-Hernandez, A., Morimoto, A., Negishi, L., Hoog, C., and Watanabe, Y. (2015). MAJIN Links Telomeric DNA to the Nuclear Membrane by Exchanging Telomere Cap. Cell *163*, 1252-1266.
Shih, I.M., Zhou, W., Goodman, S.N., Lengauer, C., Kinzler, K.W., and Vogelstein, B. (2001). Evidence that genetic instability occurs at an early stage of colorectal tumorigenesis. Cancer Res *61*, 818-822.
Shimoi, T., Yoshida, M., Kitamura, Y., Yoshino, T., Kawachi, A., Shimomura, A., Noguchi, E., Yunokawa, M., Yonemori, K., Shimizu, C*., et al.* (2018). TERT promoter hotspot mutations in breast cancer. Breast Cancer *25*, 292-296.
Shin-ya, K., Wierzba, K., Matsuo, K., Ohtani, T., Yamada, Y., Furihata, K., Hayakawa, Y., and Seto, H. (2001). Telomestatin, a novel telomerase inhibitor from Streptomyces anulatus. J Am Chem Soc *123*, 1262-1263.
Shiotani, B., and Zou, L. (2009). Single-stranded DNA orchestrates an ATM-to-ATR switch at DNA breaks. Mol Cell *33*, 547-558.
Sitaram, R.T., Degerman, S., Ljungberg, B., Andersson, E., Oji, Y., Sugiyama, H., Roos, G., and Li, A. (2010). Wilms' tumour 1 can suppress hTERT gene expression and telomerase activity in clear cell renal cell carcinoma via multiple pathways. British journal of cancer *103*, 1255-1262.
Slijepcevic, P. (2016). Mechanisms of the Evolutionary Chromosome Plasticity: Integrating the 'Centromere-from-Telomere' Hypothesis with Telomere Length Regulation. Cytogenetic and Genome Research *148*, 268-278.
Smith, E.D., Garza-Gongora, A.G., MacQuarrie, K.L., and Kosak, S.T. (2018). Interstitial telomeric loops and implications of the interaction between TRF2 and lamin A/C. Differentiation *102*, 19-26.
Smith, S., Giriat, I., Schmitt, A., and de Lange, T. (1998). Tankyrase, a poly(ADP-ribose) polymerase at human telomeres. Science *282*, 1484-1487.
Smogorzewska, A., and de Lange, T. (2004). Regulation of telomerase by telomeric proteins. Annu Rev Biochem *73*, 177-208.
Stadler, G., Rahimov, F., King, O.D., Chen, J.C.J., Robin, J.D., Wagner, K.R., Shay, J.W., Emerson, C.P., Jr., and Wright, W.E. (2013). Telomere position effect regulates DUX4 in human facioscapulohumeral muscular dystrophy. Nature structural & molecular biology *20*, 671-678.
Stansel, R.M., de Lange, T., and Griffith, J.D. (2001). T-loop assembly in vitro involves binding of TRF2 near the 3' telomeric overhang. Embo j *20*, 5532-5540.
Stephens, P.J., McBride, D.J., Lin, M.L., Varela, I., Pleasance, E.D., Simpson, J.T., Stebbings, L.A., Leroy, C., Edkins, S., Mudie, L.J*., et al.* (2009). Complex landscapes of somatic rearrangement in human breast cancer genomes. Nature *462*, 1005-1010.
Sternberg, S.H., Redding, S., Jinek, M., Greene, E.C., and Doudna, J.A. (2014). DNA interrogation by the CRISPR RNA-guided endonuclease Cas9. Nature *507*, 62-67.
Stewart, S.A., Hahn, W.C., O'Connor, B.F., Banner, E.N., Lundberg, A.S., Modha, P., Mizuno, H., Brooks, M.W., Fleming, M., Zimonjic, D.B*., et al.* (2002). Telomerase contributes to tumorigenesis by a telomere length-independent mechanism. Proc Natl Acad Sci U S A *99*, 12606-12611.
Suda, T., Fujiyama, A., Takimoto, M., Igarashi, M., Kuroiwa, T., Waguri, N., Kawai, H., Mita, Y., and Aoyagi, Y. (2002). Interchromosomal telomere length variation. Biochem Biophys Res Commun *291*, 210-214.
Swift, J., Ivanovska, I.L., Buxboim, A., Harada, T., Dingal, P.C., Pinter, J., Pajerowski, J.D., Spinler, K.R., Shin, J.W., Tewari, M*., et al.* (2013). Nuclear lamin-A scales with tissue stiffness and enhances matrix-directed differentiation. Science *341*, 1240104.

Takai, K.K., Kibe, T., Donigian, J.R., Frescas, D., and de Lange, T. (2011). Telomere protection by TPP1/POT1 requires tethering to TIN2. Mol Cell *44*, 647-659.
Tang, J., Kan, Z.Y., Yao, Y., Wang, Q., Hao, Y.H., and Tan, Z. (2008). G-quadruplex preferentially forms at the very 3' end of vertebrate telomeric DNA. Nucleic Acids Res *36*, 1200-1208.
Tauchi, T., Shin-Ya, K., Sashida, G., Sumi, M., Nakajima, A., Shimamoto, T., Ohyashiki, J.H., and Ohyashiki, K. (2003). Activity of a novel G-quadruplex-interactive telomerase inhibitor, telomestatin (SOT-095), against human leukemia cells: involvement of ATM-dependent DNA damage response pathways. Oncogene *22*, 5338-5347.
Taylor, S.S., Ha, E., and McKeon, F. (1998). The human homologue of Bub3 is required for kinetochore localization of Bub1 and a Mad3/Bub1-related protein kinase. J Cell Biol *142*, 1-11.
Teixeira, M.T., Arneric, M., Sperisen, P., and Lingner, J. (2004a). Telomere length homeostasis is achieved via a switch between telomerase- extendible and -nonextendible states. Cell *117*, 323-335.
Teixeira, M.T., Arneric, M., Sperisen, P., and Lingner, J. (2004b). Telomere Length Homeostasis Is Achieved via a Switch between Telomerase- Extendible and -Nonextendible States. Cell *117*, 323-335.
Thomas, N.E., Edmiston, S.N., Tsai, Y.S., Parker, J.S., Googe, P.B., Busam, K.J., Scott, G.A., Zedek, D.C., Parrish, E.A., Hao, H.*, et al.* (2018). Utility of TERT Promoter Mutations for Cutaneous Primary Melanoma Diagnosis. Am J Dermatopathol.
Tomlinson, R.L., Abreu, E.B., Ziegler, T., Ly, H., Counter, C.M., Terns, R.M., and Terns, M.P. (2008a). Telomerase reverse transcriptase is required for the localization of telomerase RNA to cajal bodies and telomeres in human cancer cells. Mol Biol Cell *19*, 3793-3800.
Tomlinson, R.L., Abreu, E.B., Ziegler, T., Ly, H., Counter, C.M., Terns, R.M., and Terns, M.P. (2008b). Telomerase reverse transcriptase is required for the localization of telomerase RNA to cajal bodies and telomeres in human cancer cells. Molecular biology of the cell *19*, 3793-3800.
Turner, S., Wong, H.P., Rai, J., and Hartshorne, G.M. (2010). Telomere lengths in human oocytes, cleavage stage embryos and blastocysts. Mol Hum Reprod *16*, 685-694.
Ulaner, G.A., Hu, J.-F., Vu, T.H., Giudice, L.C., and Hoffman, A.R. (1998). Telomerase Activity in Human Development Is Regulated by Human Telomerase Reverse Transcriptase (hTERT) Transcription and by Alternate Splicing of hTERT Transcripts. Cancer Research *58*, 4168.
Utsugi, T. (2013). New challenges and inspired answers for anticancer drug discovery and development. Japanese journal of clinical oncology *43*, 945-953.
Uziel, T., Lerenthal, Y., Moyal, L., Andegeko, Y., Mittelman, L., and Shiloh, Y. (2003). Requirement of the MRN complex for ATM activation by DNA damage. Embo j *22*, 5612-5621.
Valentijn, L.J., Koster, J., Zwijnenburg, D.A., Hasselt, N.E., van Sluis, P., Volckmann, R., van Noesel, M.M., George, R.E., Tytgat, G.A., Molenaar, J.J.*, et al.* (2015). TERT rearrangements are frequent in neuroblastoma and identify aggressive tumors. Nat Genet *47*, 1411-1414.
Valls Bautista, C., Pinol Felis, C., Rene Espinet, J.M., Buenestado Garcia, J., and Vinas Salas, J. (2009). Telomerase activity and telomere length in the colorectal polyp-carcinoma sequence. Rev Esp Enferm Dig *101*, 179-186.
Van Ly, D., Low, R.R.J., Frolich, S., Bartolec, T.K., Kafer, G.R., Pickett, H.A., Gaus, K., and Cesare, A.J. (2018). Telomere Loop Dynamics in Chromosome End Protection. Mol Cell *71*, 510-525.e516.
van Steensel, B., Smogorzewska, A., and de Lange, T. (1998). TRF2 protects human telomeres from end-to-end fusions. Cell *92*, 401-413.
Venteicher, A.S., Abreu, E.B., Meng, Z., McCann, K.E., Terns, R.M., Veenstra, T.D., Terns, M.P., and Artandi, S.E. (2009). A human telomerase holoenzyme protein required for Cajal body localization and telomere synthesis. Science (New York, NY) *323*, 644-648.
Vermolen, B.J., Garini, Y., Mai, S., Mougey, V., Fest, T., Chuang, T.C., Chuang, A.Y., Wark, L., and Young, I.T. (2005). Characterizing the three-dimensional organization of telomeres. Cytometry A *67*, 144-150.

Victorelli, S., and Passos, J.F. (2017). Telomeres and Cell Senescence - Size Matters Not. EBioMedicine *21*, 14-20.
Vinagre, J., Almeida, A., Populo, H., Batista, R., Lyra, J., Pinto, V., Coelho, R., Celestino, R., Prazeres, H., Lima, L.*, et al.* (2013). Frequency of TERT promoter mutations in human cancers. Nat Commun *4*, 2185.
Wang, C., Yu, J., Yuan, K., Lan, J., Jin, C., and Huang, H. (2010). Plk1-mediated mitotic phosphorylation of PinX1 regulates its stability. Eur J Cell Biol *89*, 748-756.
Wang, F., Podell, E.R., Zaug, A.J., Yang, Y., Baciu, P., Cech, T.R., and Lei, M. (2007). The POT1-TPP1 telomere complex is a telomerase processivity factor. Nature *445*, 506-510.
Wang, L., Tu, Z., Liu, C., Liu, H., Kaldis, P., Chen, Z., and Li, W. (2018). Dual roles of TRF1 in tethering telomeres to the nuclear envelope and protecting them from fusion during meiosis. Cell Death & Differentiation *25*, 1174-1188.
Wang, S., Su, J.H., Beliveau, B.J., Bintu, B., Moffitt, J.R., Wu, C.T., and Zhuang, X. (2016). Spatial organization of chromatin domains and compartments in single chromosomes. Science *353*, 598-602.
Wang, X., Kam, Z., Carlton, P.M., Xu, L., Sedat, J.W., and Blackburn, E.H. (2008). Rapid telomere motions in live human cells analyzed by highly time-resolved microscopy. Epigenetics & chromatin *1*, 4-4.
Wang, Y., Chen, Y., Chen, J., Wang, L., Nie, L., Long, J., Chang, H., Wu, J., Huang, C., and Lei, M. (2019). The meiotic TERB1-TERB2-MAJIN complex tethers telomeres to the nuclear envelope. Nature Communications *10*, 564.
Weaver, B.A., Silk, A.D., Montagna, C., Verdier-Pinard, P., and Cleveland, D.W. (2007). Aneuploidy acts both oncogenically and as a tumor suppressor. Cancer Cell *11*, 25-36.
Weinstein, I.B., and Joe, A. (2008). Oncogene Addiction. Cancer Research *68*, 3077.
Wente, S.R., and Rout, M.P. (2010). The nuclear pore complex and nuclear transport. Cold Spring Harbor perspectives in biology *2*, a000562-a000562.
Williamson, J.R., Raghuraman, M.K., and Cech, T.R. (1989). Monovalent cation-induced structure of telomeric DNA: the G-quartet model. Cell *59*, 871-880.
Wise, J.L., Crout, R.J., McNeil, D.W., Weyant, R.J., Marazita, M.L., and Wenger, S.L. (2009). Human telomere length correlates to the size of the associated chromosome arm. PloS one *4*, e6013-e6013.
Wojtyla, A., Gladych, M., and Rubis, B. (2011). Human telomerase activity regulation. Molecular biology reports *38*, 3339-3349.
Wong, M.S., Wright, W.E., and Shay, J.W. (2014). Alternative splicing regulation of telomerase: a new paradigm? Trends in genetics : TIG *30*, 430-438.
Wood, A.M., Rendtlew Danielsen, J.M., Lucas, C.A., Rice, E.L., Scalzo, D., Shimi, T., Goldman, R.D., Smith, E.D., Le Beau, M.M., and Kosak, S.T. (2014). TRF2 and lamin A/C interact to facilitate the functional organization of chromosome ends. Nat Commun *5*, 5467.
Wright, W.E., Piatyszek, M.A., Rainey, W.E., Byrd, W., and Shay, J.W. (1996). Telomerase activity in human germline and embryonic tissues and cells. Dev Genet *18*, 173-179.
Wu, J., Lv, Q., Huang, H., Zhu, M., and Meng, D. (2020). Screening and Identification of Key Biomarkers in Inflammatory Breast Cancer Through Integrated Bioinformatic Analyses. Genet Test Mol Biomarkers.
Wu, P., Takai, H., and de Lange, T. (2012). Telomeric 3' overhangs derive from resection by Exo1 and Apollo and fill-in by POT1b-associated CST. Cell *150*, 39-52.
Xi, L., and Cech, T.R. (2014). Inventory of telomerase components in human cells reveals multiple subpopulations of hTR and hTERT. Nucleic Acids Res *42*, 8565-8577.
Xi, P., Zhou, L., Wang, M., Liu, J.P., and Cong, Y.S. (2013). Serine/threonine-protein phosphatase 2A physically interacts with human telomerase reverse transcriptase hTERT and regulates its subcellular distribution. J Cell Biochem *114*, 409-417.
Xie, Z., Dai, J., Dai, L., Tan, M., Cheng, Z., Wu, Y., Boeke, J.D., and Zhao, Y. (2012). Lysine succinylation and lysine malonylation in histones. Molecular & cellular proteomics : MCP *11*, 100-107.

Xin, H., Liu, D., Wan, M., Safari, A., Kim, H., Sun, W., O'Connor, M.S., and Songyang, Z. (2007). TPP1 is a homologue of ciliate TEBP-β and interacts with POT1 to recruit telomerase. Nature *445*, 559.
Xu, D., Dwyer, J., Li, H., Duan, W., and Liu, J.P. (2008). Ets2 maintains hTERT gene expression and breast cancer cell proliferation by interacting with c-Myc. J Biol Chem *283*, 23567-23580.
Xu, Y., and Goldkorn, A. (2016). Telomere and Telomerase Therapeutics in Cancer. Genes *7*, 22.
Xue, Y., Li, L., Zhang, D., Wu, K., Chen, Y., Zeng, J., Wang, X., and He, D. (2011). Twisted epithelial-to-mesenchymal transition promotes progression of surviving bladder cancer T24 cells with hTERT-dysfunction. PLoS One *6*, e27748.
Yamaguchi, K., Yamaguchi, R., Takahashi, N., Ikenoue, T., Fujii, T., Shinozaki, M., Tsurita, G., Hata, K., Niida, A., Imoto, S*., et al.* (2014). Overexpression of cohesion establishment factor DSCC1 through E2F in colorectal cancer. PloS one *9*, e85750-e85750.
Yang, P.-M., Lin, L.-S., and Liu, T.-P. (2020). Sorafenib Inhibits Ribonucleotide Reductase Regulatory Subunit M2 (RRM2) in Hepatocellular Carcinoma Cells. Biomolecules *10*, 117.
Ye, J., Lenain, C., Bauwens, S., Rizzo, A., Saint-Léger, A., Poulet, A., Benarroch, D., Magdinier, F., Morere, J., Amiard, S*., et al.* (2010). TRF2 and Apollo Cooperate with Topoisomerase 2α to Protect Human Telomeres from Replicative Damage. Cell *142*, 230-242.
Ye, J.Z., Donigian, J.R., van Overbeek, M., Loayza, D., Luo, Y., Krutchinsky, A.N., Chait, B.T., and de Lange, T. (2004). TIN2 binds TRF1 and TRF2 simultaneously and stabilizes the TRF2 complex on telomeres. J Biol Chem *279*, 47264-47271.
Yi, X., Shay, J.W., and Wright, W.E. (2001a). Quantitation of telomerase components and hTERT mRNA splicing patterns in immortal human cells. Nucleic Acids Research *29*, 4818-4825.
Yi, X., Shay, J.W., and Wright, W.E. (2001b). Quantitation of telomerase components and hTERT mRNA splicing patterns in immortal human cells. Nucleic Acids Res *29*, 4818-4825.
Yi, X., White, D.M., Aisner, D.L., Baur, J.A., Wright, W.E., and Shay, J.W. (2000). An Alternate Splicing Variant of the Human Telomerase Catalytic Subunit Inhibits Telomerase Activity. Neoplasia *2*, 433-440.
Yu, T.-Y., Kao, Y.-w., and Lin, J.-J. (2014). Telomeric transcripts stimulate telomere recombination to suppress senescence in cells lacking telomerase. Proceedings of the National Academy of Sciences of the United States of America *111*, 3377-3382.
Zaug, A.J., Crary, S.M., Jesse Fioravanti, M., Campbell, K., and Cech, T.R. (2013). Many disease-associated variants of hTERT retain high telomerase enzymatic activity. Nucleic acids research *41*, 8969-8978.
Zhang, A., Zheng, C., Hou, M., Lindvall, C., Wallin, K.L., Angstrom, T., Yang, X., Hellstrom, A.C., Blennow, E., Bjorkholm, M*., et al.* (2002). Amplification of the telomerase reverse transcriptase (hTERT) gene in cervical carcinomas. Genes Chromosomes Cancer *34*, 269-275.
Zhang, H., Liu, X., Warden, C.D., Huang, Y., Loera, S., Xue, L., Zhang, S., Chu, P., Zheng, S., and Yen, Y. (2014). Prognostic and therapeutic significance of ribonucleotide reductase small subunit M2 in estrogen-negative breast cancers. BMC cancer *14*, 664-664.
Zhao, Y., Sfeir, A.J., Zou, Y., Buseman, C.M., Chow, T.T., Shay, J.W., and Wright, W.E. (2009). Telomere Extension Occurs at Most Chromosome Ends and Is Uncoupled from Fill-In in Human Cancer Cells. Cell *138*, 463-475.
Zhu, J., Zhao, Y., and Wang, S. (2010). Chromatin and epigenetic regulation of the telomerase reverse transcriptase gene. Protein Cell *1*, 22-32.
Zhu, X., Han, W., Xue, W., Zou, Y., Xie, C., Du, J., and Jin, G. (2016). The association between telomere length and cancer risk in population studies. Scientific reports *6*, 22243-22243.
Zhu, X., Liu, B., Carlsten, J.O.P., Beve, J., Nyström, T., Myers, L.C., and Gustafsson, C.M. (2011). Mediator Influences Telomeric Silencing and Cellular Life Span. Molecular and Cellular Biology *31*, 2413.
Zou, Y., Sfeir, A., Gryaznov, S.M., Shay, J.W., and Wright, W.E. (2004). Does a sentinel or a subset of short telomeres determine replicative senescence? Molecular biology of the cell *15*, 3709-3718.

APPENDICES

Table A.1 list of prioritized SDL genes

number	Gene	GeneID
1	E2F1	1869
2	COL6A1	1291
3	POLA2	23649
4	FANCA	2175
5	LMNB1	4001
6	PABPC1	26986
7	MPHOSPH6	10200
8	WDR61	80349
9	PMVK	10654
10	FTSJ3	117246
11	DSCC1	79075
12	PKMYT1	9088
13	BIRC5	332
14	WDR20	91833
15	SELPLG	6404
16	PLEKHF1	79156
17	SPRY1	10252
18	GP5	2814
19	MAP1LC3B	81631
20	SAV1	60485
21	ALS2CL	259173
22	ABCC2	1244
23	CARD11	84433

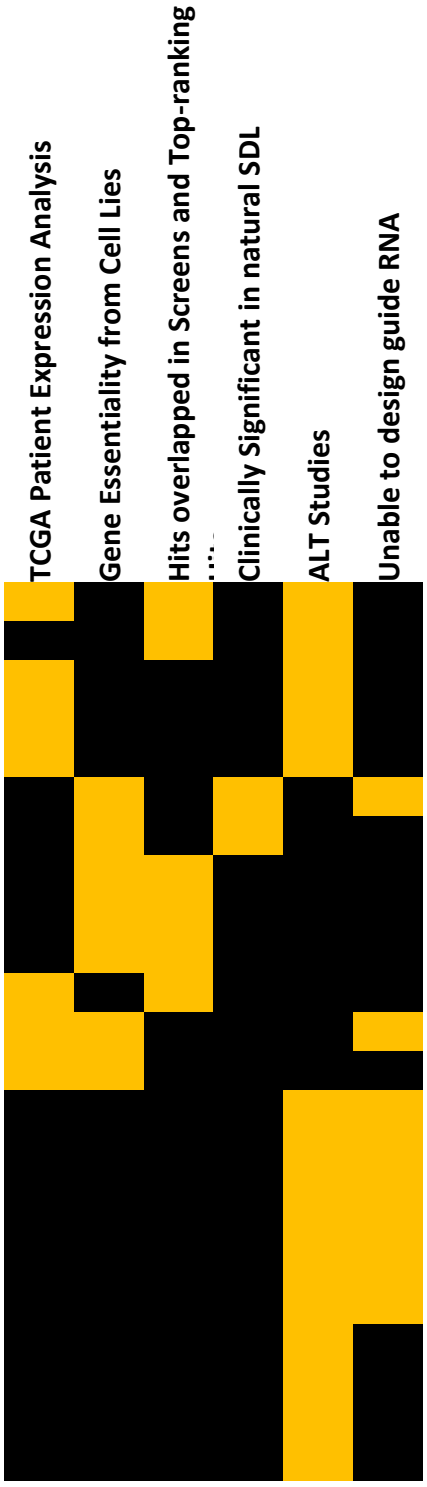

24	TNK1	8711	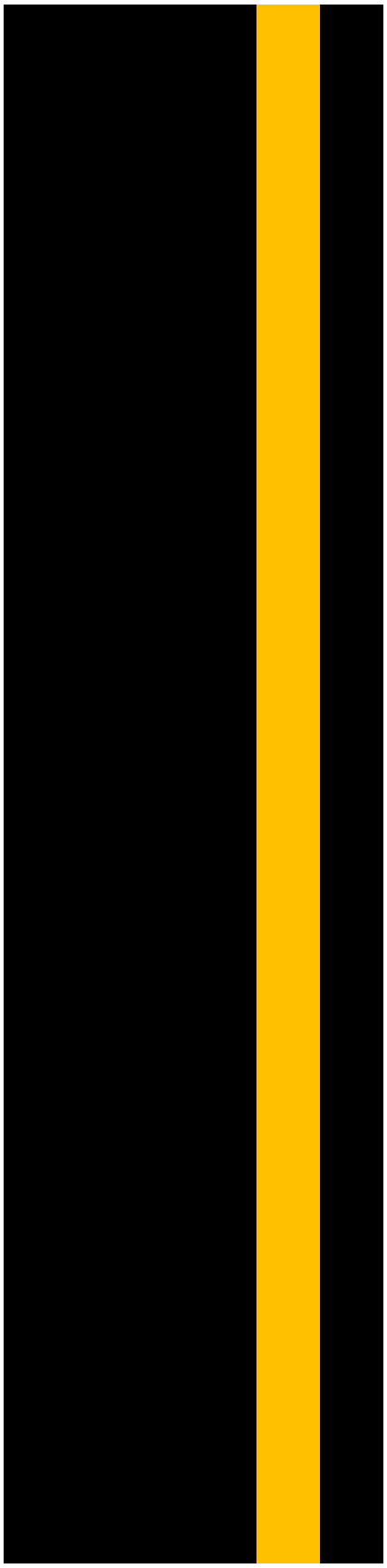
25	KLK8	11202	
26	NOS1	4842	
27	CEACAM4	1089	
28	BTK	695	
29	EPC1	80314	
30	PCYOX1L	78991	
31	TRIB2	28951	
32	PRKAR2B	5577	
33	ABCA3	21	
34	PRRT1	80863	
35	ADCK2	90956	
36	NOB1	28987	
37	OSBPL1A	114876	
38	SEPT4	5414	
39	GNB1L	54584	
40	BAMBI	25805	
41	CD8B	926	
42	ATP1B1	481	
43	PSTPIP2	9050	
44	MYO1F	4542	
45	CBX8	57332	
46	HAUS1	115106	
47	ATRNL1	26033	
48	PCDHB16	57717	
49	PACSIN1	29993	
50	TFB1M	51106	
51	REM2	161253	
52	PTRH1	138428	
53	FMNL2	114793	
54	SMC3	9126	
55	TEX14	56155	
56	MSX2	4488	
57	PPARGC1B	133522	
58	LRRFIP1	9208	
59	TAF7	6879	
60	ACSF3	197322	
61	CUZD1	50624	
62	ACTN1	87	
63	MET	4233	
64	OXSR1	9943	
65	EPS8	2059	
66	AHNAK	79026	
67	CD40	958	

68	PRKCDBP	112464
69	LAMP2	3920
70	PCDHB7	56129
71	COL16A1	1307
72	MATN2	4147
73	TRIM16	10626
74	STC2	8614
75	TSPAN9	10867
76	PRKD1	5587
77	CAMK2D	817
78	C10orf25	220979
79	NRN1	51299
80	SMPD3	55512
81	HLA-B	3106
82	HLA-A	3105
83	ERCC2	2068
84	UPP1	7378
85	GALNT10	55568
86	AP4S1	11154
87	ENO2	2026
88	FBLN5	10516
89	DYNC1H1	1778
90	CGRRF1	10668
91	AMIGO2	347902
92	VDAC1	7416
93	RSL24D1	51187
94	TMEM68	137695
95	GOLGA8A	23015
96	RNF26	79102
97	TUBA4A	7277
98	EIF5B	9669
99	FAM208B	54906
100	SEC63	11231
101	PRKRA	8575
102	RSRC1	51319
103	KLK6	5653
104	TNFRSF21	27242
105	GTF3C2	2976
106	UBE2G2	7327
107	PIGA	5277
108	BCAS4	55653
109	DNHD1	144132
110	APOC1	341
111	C12orf44	60673

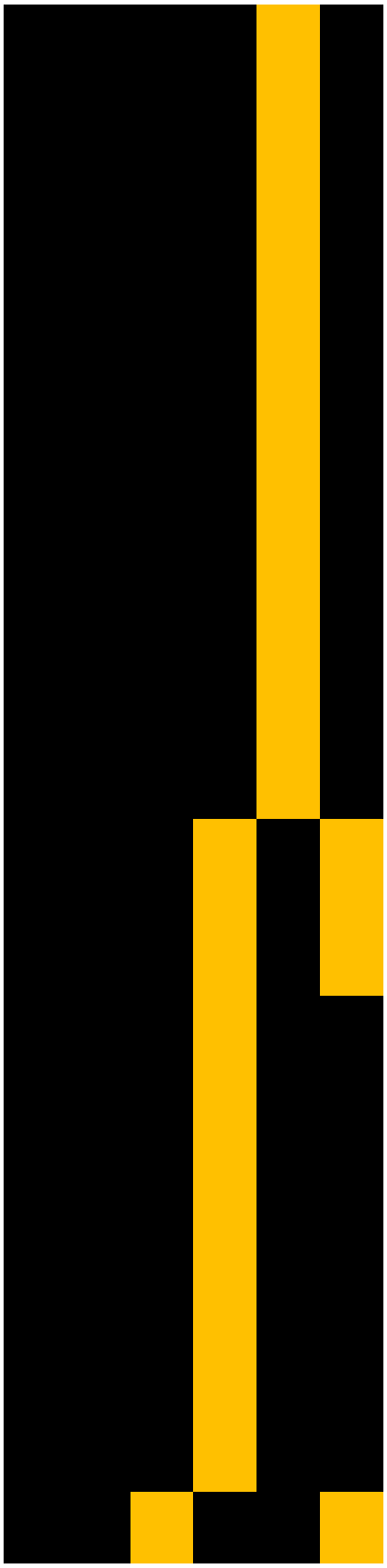

112	ZNF530	348327
113	ZNF295	49854
114	IPO13	9670
115	RPS24	6229
116	PRPF19	27339
117	PHF5A	84844
118	FGFR1	2260
119	LIMK1	3984
120	B3GALNT2	148789
121	SYK	6850
122	ZMYND19	116225
123	R3HDML	140902
124	MLL5/KMT2E	55904
125	PRMT1	3276
126	C18orf26/DYNAP	284254
127	NID2	22795
128	ZBTB47	92999
129	GCN1L1	10985
130	PFDN2	5202
131	ARHGEF4	50649
132	AK7	122481
133	KEL	3792
134	MYC	4609
135	CCND3	896
136	DYNLL1	8655
137	ZNF672	79894
138	KPNA6	23633
139	INSM2	84684
140	PPP4R1	9989
141	SH3GL3	6457
142	DCPS	28960
143	NOC4L	79050
144	RTTN	25914
145	PRKAB2	5565
146	SCGB2A1	4246
147	COBRA1 / NELFB	25920
148	CDK6	1021
149	MCL1	4170
150	NMUR2	56923
151	CORO2A	7464
152	MRPL46	26589
153	LILRA3	11026
154	MRPS23	51649
155	RAB6B	51560

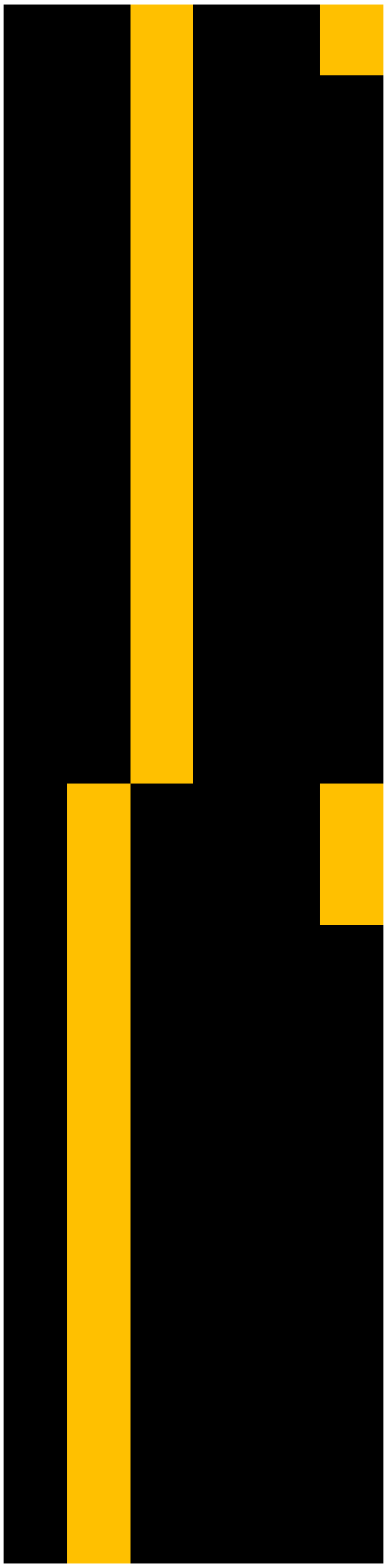

156	DGKG	1608
157	MAP3K3	4215
158	GOLT1A	127845
159	GOT1L1	137362
160	SP100	6672
161	LRWD1	222229
162	CPA6	57094
163	KIF9	64147
164	MED14	9282
165	BFSP1	631
166	UQCRC2	7385
167	ANGPTL5	253935
168	ARHGAP15	55843
169	SIN3A	25942
170	CYC1	1537
171	MRPL21	219927
172	DHX8	1659
173	ZNF645	158506
174	FAM72A	729533
175	GPR19	2842
176	TUBA1B	10376
177	C6orf173	387103
178	PTTG1	9232
179	NUSAP1	51203
180	RAD54L	8438
181	BUB1	699
182	C15orf42 / TICRR	90381
183	MCM5	4174
184	NUF2	83540
185	TUBB	203068
186	TACC3	10460
187	AURKA	6790
188	RCC1	1104
189	BUB1B	701
190	SGOL1	151648
191	TOP2A	7153
192	EME1	146956
193	MCM7	4176
194	NEK2	4751
195	NCAPG	64151
196	PLK1	5347
197	CDC20	991
198	RRM2	6241
199	ORC1L / ORC1	4998

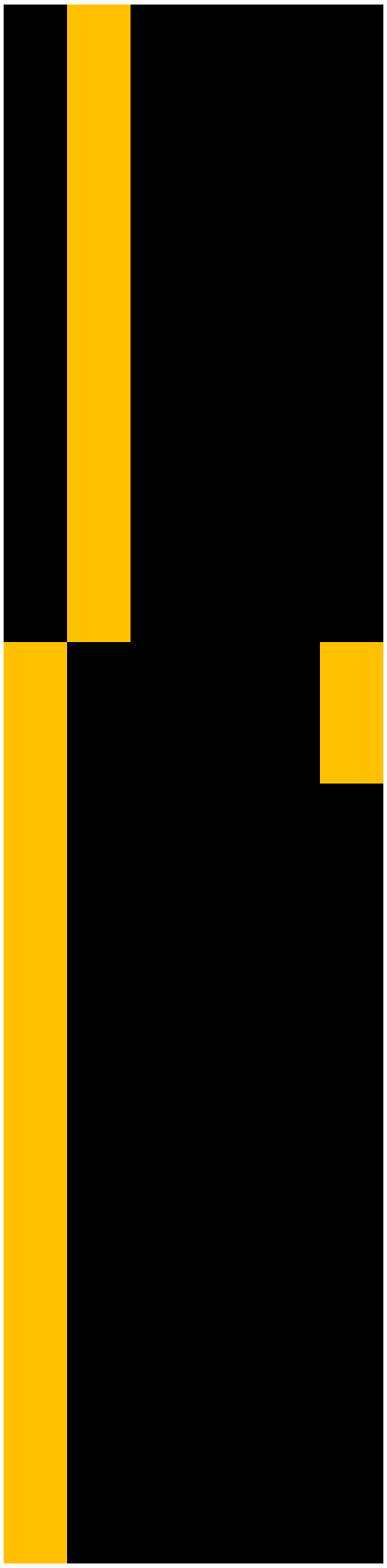

200	GINS4	84296	
201	KIF20A	10112	
202	ZWINT	11130	
203	PLK4	10733	
204	TYMS	7298	
205	RNASEH2A	10535	
206	RAD51AP1	10635	
207	SNRPC	6631	
208	STMN1	3925	
209	SPAG5	10615	
210	GTSE1	51512	
211	TRIP13	9319	
212	FAM54A / MTFR2	113115